

# **Mechanistic investigation on methylation of metal(loid)s by methylcobalamin**

## **Dissertation**

zur Erlangung des  
Doktors der Naturwissenschaften  
(Dr. rer. nat.)

vorgelegt von Oliver Würfel

geboren am 10.02.1981 in Gelsenkirchen

Fakultät Chemie der Universität Duisburg-Essen

September 2012

Die vorliegende Arbeit wurde im Zeitraum von November 2008 bis September 2012 im Arbeitskreis von Prof. Dr. Torsten C. Schmidt (Instrumentelle Analytische Chemie) sowie im Arbeitskreis von Prof. Dr. Reinhard Hensel (Mikrobiologie I) der Universität Duisburg-Essen durchgeführt.

Tag der Disputation: 21.12.2012

Vorsitzender: Prof. Dr. Thomas Schrader

1. Gutachter: Prof. Dr. Torsten C. Schmidt
2. Gutachter: Prof. Dr. Reinhard Hensel
3. Gutachter: Prof. Dr. José A.C. Broekaert

**ACKNOWLEDGMENTS**

In general, I would like to thank Prof. Dr. Torsten C. Schmidt and Prof. Dr. Reinhard Hensel for the warm welcome to their working groups, for giving me the opportunity to carry out my dissertation in this interesting field of research as well as for their constructive help and discussions during the PhD thesis and critical reading of this work. Furthermore, I like to thank José A.C. Broekaert for the review.

A special thank goes to Dr. Roland A. Diaz-Bone for his great help, ideas, endurance, motivation, and sharing his knowledge on Analytical Chemistry. In addition, I want to thank him for a good cooperation, enjoyable trips to various conferences, all his support, and overall a nice time while his supervision, where I learned a lot. In addition, I thank him for critical reading.

Furthermore, I have to thank Dr. Maik Jochmann for his help and support in respect to the IRMS analysis, discussions, a good cooperation, and critical reading some of the chapters of this work.

At last, I would like to thank all my nice colleagues, in particular all the members of the isotope lab, the members of the working group 'microbiology I', especially Frank Thomas, and of the Institute for Environmental Analytical Chemistry: Thanks for an enjoyable time!

**Chapter 2:**

I like to thank Dr. Frank Thomas for his contribution, the purification of recombinant MtaA as well as for critical reading of this chapter. My gratitude also goes to Marcel Schulte for his conduction of some of the experiments under my supervision during his Master's thesis.

**Chapter 3:**

My thanks to Dr. Frank Thomas, for the productive and enjoyable cooperation regarding the investigation of arsenic methylation by methylcobalamin using the oxidation-state specific hydride generation as well as for the purification of recombinant MtaA, discussions and critical reading. Furthermore, I would like to thank Alfred V. Hirner for providing access to the Agilent ICP-MS.

## Chapter 4:

I would like to thank Manuel Stephan for technical support regarding the GC-IRMS. Furthermore, I thank Dirk Steinmann for supporting the FIA-IRMS measurements and Sasan Rabieh for synthesis of the TMAO standard. In addition, I thank Roland Diaz-Bone for providing of the compost sample. For the EA-IRMS measurements of the compost, I sincerely thank Heinrich Taubald and Bernd Steinhilber from the geochemistry department at the University of Tübingen. For providing access to the GC-EI-MS-ICP-MS system, I thank Alfred V. Hirner of the Institute for Environmental Analytical Chemistry. Additionally, I thank Harald Lowag and Martin Elsner from the Institute for Groundwater Ecology at the Helmholtz Center Munich - National Research Center for Environmental Health for referencing the CO<sub>2</sub> gas.

## Chapter 5:

I want to thank Frank Keppler and Markus Greule from the Max Planck Institute in Mainz for the position-specific determination of the methyl-group of CH<sub>3</sub>Cob and SAM using HI. In addition, I have to thank Jörg Hippler of the Institute for Environmental Analytical Chemistry for providing the used arsenicals. Furthermore, I thank David Widory of the BGRM (Orleans, France) for measurement of our reference CO<sub>2</sub> gas and the ZWU of the University of Duisburg-Essen for financial support.

*„Überall geht ein früheres Ahnen dem späteren Wissen voraus.“*

Alexander von Humboldt

**ABSTRACT**

The methylation of metal(loid)s is a widespread phenomenon in the environment which occurs by abiotic as well as enzymatically catalyzed transfer of a methyl group. While S-adenosyl methionine is the main methyl-donor in many bacteria and mammals, methylcobalamin ( $\text{CH}_3\text{Cob}$ ) can be the methyl-donor for the methylation of metal(loid)s by anaerobic microorganisms, such as methanoarchaea. Several reaction mechanisms have been proposed for the enzyme-catalyzed as well as the abiotic methylation, but have not really been proven yet. Since the methylation alters both biomobility and toxicity of the precursory metal(loid)s, the full comprehension of the underlying reaction mechanisms is of high importance for a conclusive risk assessment. Hence, in this thesis new approaches and techniques were developed, validated, and applied to foster the understanding of the methylation of the group 15 and 16 metal(loid)s arsenic, selenium, antimony, tellurium, and bismuth by  $\text{CH}_3\text{Cob}$ . Here, particular emphasis was put on the toxicologically highly relevant element arsenic, which is a widespread contaminant in drinking water.

In terms of methylation of metal(loid)s by methanoarchaea, the role cob(I)alamin (Cob(I)) regarding this process was reinvestigated, since a catalytic role of the former was suggested for the methylation of metal(loid)s by  $\text{CH}_3\text{Cob}$  in the literature – Cob(I) is intermediary formed by enzyme-catalyzed (MtaA) transfer of the methyl group from  $\text{CH}_3\text{Cob}$  to coenzyme M (CoM) in the course of methylotrophic methanogenesis. UV/Vis spectroscopic and purge and trap (P&T) gas chromatography (GC) inductively coupled plasma mass spectrometry (ICP-MS) analyses revealed that Cob(I) induces the transfer of the methyl group from  $\text{CH}_3\text{Cob}$  to the metal(loid)s. Since this indicates that biological electron carriers are important factors for the methylation capability of methanoarchaea, the efficiency of abiotic methylation of As, Bi, Sb, Se, and Te by  $\text{CH}_3\text{Cob}$  was studied in the presence of glutathione (GSH) as cofactor in many bacteria and eucaryotes. In comparison, the methylation by  $\text{CH}_3\text{Cob}$  in presence of CoM and by titanium citrate that is often used in biochemical assays as well as photolytic induced methylation was investigated exemplarily for arsenic. As all of the investigated biological “reducing agents” induced the methylation of metal(loid)s, different biological reducing agents apparently might contribute to the multi-element methylation *in vivo* in dependency of their availability.

For a more detailed mechanistic investigation of the MtaA-mediated methylation of arsenic, a new oxidation-state specific hydride generation technique was developed,

which is also an alternative to common high performance liquid chromatography for analysis of environmental samples. Here, the efficient methylation of trivalent arsenic species without a change in oxidation state indicated, that the methyl transfer does proceed *via* a non-oxidative methylation. In addition, thorough UV/Vis and P&T-GC-ICP-MS analyses pointed towards a similar mechanism for antimony, bismuth, selenium, and tellurium and indicated that the methyl group transfer proceeds either *via* a concerted nucleophilic substitution or *via* a caged radical mechanism.

Another approach to investigate the biomethylation and elucidate the proposed reaction mechanisms, is the investigation of the carbon isotopic fractionation due to the transfer of the methyl group to the metal(loid). For example, the extent of the kinetic isotope effect (*KIE*) allows the differentiation between different reaction types, such as concerted ( $S_N2$ ) or stepwise ( $S_N1$ ) nucleophilic substitution. Hence, the first method for determination of the carbon isotopic composition of metal(loid) compounds in complex matrices was developed. It involves selective hydride generation of the organometal(loid)s followed by P&T enrichment, heart-cut gaschromatography and isotope ratio mass spectrometry (IRMS). The applicability was demonstrated for biogenically formed trimethylarsine oxide in a compost sample. Afterwards, the method was extended and optimized to the analysis of partly methylated arsenicals.

For an investigation of the occurring *KIE* due to the methyl transfer, a prerequisite is the determination of initial  $\delta^{13}C$  of the transferred methyl group. Because of the high importance of this  $\delta^{13}C$ -value, different independent approaches for methyl group abstraction were applied, including reaction with platinum (II/IV) couples or HI, light irradiation as well as thermolytic cleavage. Subsequently, the products were analyzed by GC-IRMS or by flow injection analysis (FIA)-IRMS in the case of Pt.

By use of the developed IRMS techniques, the *KIE* of the abiotic GSH-induced methylation of arsenic by  $CH_3Cob$  was determined and pointed to a concerted reaction mechanism.

Overall, the results of this thesis advance the field of biomethylation and the developed techniques offer new opportunities to investigate methylation of metal(loid)s in the environment.

**KURZFASSUNG**

Die Methylierung von Metall(oid)en ist in der Umwelt ein weit verbreitetes Phänomen und erfolgt durch den abiotischen als auch enzymkatalysierten Transfer einer Methylgruppe. Während in vielen Bakterien und Säugetieren S-Adenosylmethionin (SAM) die Hauptquelle für diese Methylgruppen darstellt, kann bei anaeroben Mikroorganismen, wie den Methanoarchaeen, Methylcobalamin ( $\text{CH}_3\text{Cob}$ ) als Methylendonoren dienen. Verschiedene Reaktionsmechanismen wurden bereits postuliert, jedoch noch nicht schlüssig bewiesen. Da die Methylierung sowohl die Bioverfügbarkeit als auch die Toxizität der anorganischen Ausgangsstoffe stark verändert, ist ein komplettes Verständnis der zu Grunde liegenden Mechanismen von hoher Wichtigkeit für eine schlüssige Risikoabschätzung. Daher wurden neue Ansätze und Analysetechniken entwickelt, validiert und verwendet, um ein besseres Verständnis des Methylierungsprozesses von As, Sb, Te, Se und Bi durch  $\text{CH}_3\text{Cob}$  zu ermöglichen. Besonders Augenmerk lag dabei auf dem toxikologisch hoch relevanten As, welches ein weit verbreiteter Umweltschadstoff im Trinkwasser ist.

Bezüglich der Methylierung von Metall(oid)en durch Methanoarchaeen, wurde die Rolle von Cob(I)alamin (Cob(I)) in diesem Prozess genauer untersucht, da in der Literatur dessen katalytische Rolle in Betracht gezogen wurde – Cob(I) wird intermediär durch den MtaA-katalysierten Transfer der Methylgruppe von  $\text{CH}_3\text{Cob}$  zu Coenzym M (CoM) im Laufe der methylo trophen Methanogenese gebildet. Untersuchungen mittels UV/Vis-Spektroskopie sowie Gaschromatographie (GC) nach Purge&Trap (P&T) in Verbindung mit induktiv gekoppeltem Plasma Massenspektrometrie (ICP-MS) führten zu dem Erkenntnis, dass Cob(I) den Transfer der Methylgruppe von  $\text{CH}_3\text{Cob}$  zu den Metall(oid)en induziert. Da dies belegt, dass biologische Elektronenüberträger bedeutende Faktoren für die Befähigung zur Methylierung der Methanoarchaeen sind, wurde die Effizienz der abiotischen Methylierung von As, Sb, Se, Te und Bi durch  $\text{CH}_3\text{Cob}$  in Gegenwart von Glutathion (GSH) als wichtigem Kofaktor in vielen Bakterien und Eucaryoten untersucht. Zum Vergleich wurde die Methylierung in Gegenwart von CoM oder Titancitrat, das oft in biochemischen Assays eingesetzt wird, sowie die Photomethylierung exemplarisch an As untersucht. Da alle untersuchten „Bioreduktionsmittel“ den Transfer der Methylgruppe von  $\text{CH}_3\text{Cob}$  zu As induzieren konnten, legt dies nahe, dass verschiedene Bioreduktionsmittel in Abhängigkeit von ihrer Verfügbarkeit zur Methylierung *in vivo* beitragen können. Zur detaillierteren Untersuchung des Reaktionsmechanismus der MtaA-vermittelten Methylier-

nung von As durch  $\text{CH}_3\text{Cob}$  wurde eine neue Oxidationsstufenspezifische Hydridgenerierung (HG) in Verbindung mit Analyse *via* GC-ICP-MS entwickelt. Die effiziente Methylierung nur der dreiwertigen Arsenspezies ohne Änderung der Oxidationsstufe deutete darauf hin, dass der Transfer der Methylgruppe über eine nicht-oxidative Methylierung erfolgt. Des Weiteren zeigten detaillierte UV/Vis und P&T-GC-ICP-MS Analysen, dass es sich wahrscheinlich um einen ähnlichen Mechanismus für Se, Sb, Te und Bi handelt und dass der Methyltransfer mittels einer konzertierten nukleophilen Substitution oder in einem „caged“ Radikalmechanismus erfolgen muss.

Ein anderer Ansatz zur Untersuchung der Biomethylierung und Aufklärung der Reaktionsmechanismen ist die Analyse der Kohlenstoff-Isotopenfraktionierung während des Transfers der Methylgruppe zum Metall(oid). Anhand der Größe des auftretenden kinetischen Isotopeneffektes (*KIE*) lassen sich beispielsweise eine konzertierte und eine schrittweise nukleophile Substitution voneinander unterscheiden. Daher wurde die erste Methode entwickelt, um das Kohlenstoffisotopenverhältnis von metall(oid)organischen Verbindungen in einer komplexen Matrix bestimmen zu können. Die Methode nutzt die selektive HG der Organometall(oid)e zur Volatilisierung und Matrixabtrennung gefolgt von P&T-Anreicherung, Heart-Cut Gaschromatographie und Isotopenverhältnis-Massenspektrometrie (IRMS). Die Anwendbarkeit der Methode wurde anhand der Analyse eines mit Trimethylarsenoxid belasteten Kompostes gezeigt. In einem weiteren Schritt wurde die Methode für die Analyse der niedrig siedenden teilmethylierten Arsenverbindungen erweitert und optimiert.

Um letztendlich den *KIE* untersuchen zu können, muss der Startwert, das Isotopenverhältnis der zu transferierenden Methylgruppe, bestimmt werden. Aufgrund der hohen Bedeutung des Isotopenwertes wurden mehrere voneinander unabhängige Verfahren für die positions-spezifische Isotopenanalyse von  $\text{CH}_3\text{Cob}$  angewendet – Abstraktion der Methylgruppe mittels HI, Licht, erhöhter Temperatur sowie Pt (II/IV) und anschließende Analyse der Reaktionsprodukte mittels GC-IRMS oder Fließinjektionsanalyse (FIA)-IRMS im Falle von Pt.

Mittels der entwickelten IRMS Techniken wurde schließlich die abiotische Methylierung von Arsenit in Gegenwart von GSH durch  $\text{CH}_3\text{Cob}$  untersucht. Der ermittelte *KIE* deutet dabei auf eine konzertierte Reaktion hin.

Insgesamt liefert diese Doktorarbeit neue Erkenntnisse auf dem Gebiet der Biomethylierung und darüber hinaus bieten die entwickelten Techniken neue Möglichkeiten die Methylierung von Metall(oid)en in der Umwelt zu untersuchen.

**TABLE OF CONTENTS**

<b>Chapter 1. General Introduction .....</b>	<b>1</b>
1.1. Selected properties of the investigated elements .....	1
1.2. Arsenic distribution in the environment .....	1
1.3. Toxicity of arsenic .....	3
1.4. Transformation of arsenic in the human body .....	5
1.5. Transformation of antimony, bismuth, selenium, and tellurium in the human body .....	6
1.6. Transformation of metal(loid)s by microorganisms.....	7
1.7. Methanogenic Archaea .....	8
1.8. Methylcobalamin and its derivatives and its role for the methylation of metal(loid)s.....	8
1.9. Metal speciation by hyphenation of inductively coupled plasma mass spectrometry .....	13
1.9.1. Quantification of volatile organometal(loid) compounds .....	14
1.9.2. Hydride generation of metal(loid)s .....	15
1.10. Compound-specific stable isotope analysis.....	16
1.10.1. Instrumental details for CSIA.....	18
1.11. Elemental Analyzer IRMS bulk analysis for referencing.....	19
1.12. SCOPE OF THE THESIS .....	20
1.13. REFERENCES .....	22
<b>Chapter 2. Investigation on the role of biological “reducing agents” for the         methylation of metal(loid)s by methylcobalamin.....</b>	<b>27</b>
2.1. ABSTRACT .....	27
2.2. INTRODUCTION.....	28
2.3. EXPERIMENTAL SECTION.....	29
2.3.1. Electrochemical preparation of Cob(I).....	30
2.3.2. Investigations on the role of Cob(I) .....	30
2.3.3. Headspace P&T-GC-ICP-MS analysis.....	31
2.3.4. Investigation of the methylation capability and efficiency of different “bioreducing agents” .....	31

---

2.3.5. Hydride generation P&T-GC-ICP-MS method.....	32
2.4. RESULTS AND DISCUSSION .....	33
2.4.1. The role of cob(I)alamin for the multi-metal(loid) methylation .....	33
2.4.2. Abiotic methylation of As, Sb, Se, Te, and Bi by CH <sub>3</sub> Cob in presence of GSH .....	38
2.4.3. Investigation of the methylation of As by CH <sub>3</sub> Cob in presence of GSH under various reaction conditions .....	39
2.4.4. Investigation of the methylation of As by CH <sub>3</sub> Cob in the presence of CoM, TiCit, and Cob(I), or under irradiation with UV-light .....	41
2.5. CONCLUSION .....	44
2.6. REFERENCES.....	45
<b>Chapter 3. Investigation of the mechanism of multi-metal(loid) methylation and hydride generation by methylcobalamin and cob(I)alamin.....</b>	<b>47</b>
3.1. ABSTRACT .....	47
3.2. INTRODUCTION.....	48
3.3. EXPERIMENTAL SECTION.....	50
3.3.1. <i>In vitro</i> protein assays. ....	50
3.3.2. Oxidation state specific HG/P&T/GC-ICP-MS procedure.....	51
3.3.3. P&T/GC-ICP-MS procedure.....	52
3.4. UV/VIS EXPERIMENTS.....	53
3.5. RESULTS AND DISCUSSION .....	54
3.5.1. Development and validation of pH-specific hydride generation derivatization for redox-specific speciation of methylated arsenic species .....	54
3.5.2. Investigation of methylation and hydride generation of arsenic.....	57
3.5.3. Investigation of methylation and hydride generation of antimony, bismuth, selenium, and tellurium.....	65
3.5.4. Possible mechanisms for multi-element methylation.....	67
3.5.5. Possible mechanisms for hydride generation as exemplified on arsenite .....	69
3.6. CONCLUSION .....	70

---

3.7. REFERENCES.....	71
<b>Chapter 4. Determination of <math>^{13}\text{C}/^{12}\text{C}</math> isotopic ratios of biogenic organometal(loid) compounds in complex matrices.....</b>	<b>73</b>
4.1. ABSTRACT .....	73
4.2. INTRODUCTION.....	74
4.3. EXPERIMENTAL SECTION.....	77
4.3.1. Chemicals for hydride generation.....	77
4.3.2. Description of the compost sample .....	77
4.3.3. HG-P&T-hcGC procedure .....	78
4.3.4. Control of the purity of the heart-cut fractions by HG-P&T-hcGC-GC-MS .....	79
4.3.5. HG-P&T-hcGC-GC-IRMS procedure .....	79
4.3.6. Flow-injection analysis-IRMS .....	81
4.3.7. Elemental Analyzer-IRMS measurement of the compost sample .....	81
4.4. RESULTS AND DISCUSSION .....	81
4.4.1. Optimization of matrix separation by HG-P&T-hcGC-ICP-MS .....	81
4.4.2. Control of purity of heart-cut fraction by GC-MS .....	83
4.4.3. HG-P&T-hcGC-GC-IRMS for carbon isotope ratio analysis of TMAOs .....	85
4.5. CONCLUSION .....	88
4.6. REFERENCES.....	90
<b>Chapter 5. Position specific isotope analysis of the methyl group carbon in methylcobalamin for the investigation of biomethylation processes and mechanistic investigation of the abiotic methyl transfer from <math>\text{CH}_3\text{Cob}</math> to arsenic induced by glutathione .....</b>	<b>92</b>
5.1. ABSTRACT .....	92
5.2. INTRODUCTION.....	93
5.3. EXPERIMENTAL SECTION.....	98
5.3.1. Position specific determination of the methyl group of $\text{CH}_3\text{Cob}$ using photolytic or thermolytic cleavage .....	98
5.3.2. Position specific determination of the methyl group of $\text{CH}_3\text{Cob}$ using platinum(II)/platinum(IV).....	100

5.3.3. Position specific determination of the methyl group of CH <sub>3</sub> Cob using HI . .....	100
5.3.4. Modifications of the hydride generation method.....	101
5.3.5. Validation of the heartcut-window using HG-P&T-hcGC-GC-EI-MS detection .....	102
5.3.6. Extended method for determination of carbon isotope ratios of organometal(loid)s in complex matrices.....	102
5.3.7. Elemental analysis (EA-IRMS) measurement of the arsenic standard compounds .....	103
5.3.8. Abiotic methylation of arsenic by methylcobalamin in presence of GSH.. .....	103
<b>5.4. RESULTS AND DISCUSSION .....</b>	<b>104</b>
5.4.1. Position-specific determination of the methyl-group of methylcobalamin .....	104
5.4.3. Investigation of the carbon fractionation due to the abiotic methyl group transfer from methylcobalamin to arsenic induced by GSH .....	114
5.5. CONCLUSION .....	116
5.6. REFERENCES.....	118
<b>Chapter 6. General Conclusion and Outlook.....</b>	<b>120</b>
6.1. GENERAL CONCLUSION .....	120
6.2. OUTLOOK.....	122
<b>Chapter 7. Appendix .....</b>	<b>123</b>
7.1. ABBREVIATIONS .....	123
7.2. LIST OF TABLES .....	125
7.3. LIST OF FIGURES.....	127
7.4. ORIGIN 8.5 SCRIPT FOR SEMI-AUTOMATED EVALUATION OF GC-ICP- MS MEASUREMENTS.....	132
7.5. CONVERTER FOR ELAN 6000 ICP-MS DATA BASED ON MICROSOFT WORD (.XL to .CSV).....	138
7.6. CV .....	142
7.7. DECLARATION.....	147

## Chapter 1. General Introduction

### 1.1. Selected properties of the investigated elements

As this study focuses on the mechanistic investigation of the methylation of antimony, tellurium, selenium, bismuth, and especially of the toxicologically highly relevant element arsenic by methylcobalamin, at first, some details on these elements are given in Table 1-1.

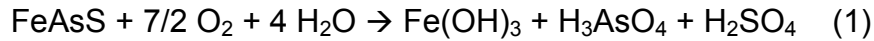
**Table 1-1.**Elemental properties (combined from<sup>[1]</sup>)

Element	Group, atomic number	Electro-negativity (Pauling)	Electron configuration	Mass numbers of stable isotopes	Common oxidation states	Abundance in the earth's crust [mg kg <sup>-1</sup> ]
As	15, 33	2.18	[Ar] 3d <sup>10</sup> 4s <sup>2</sup> 4p <sup>3</sup>	75	5, 3, 0, -3	1.8
Sb	15, 51	2.05	[Kr] 4d <sup>10</sup> 5s <sup>2</sup> 5p <sup>3</sup>	121,123	5, 3, 0, -3	2*10 <sup>-1</sup>
Bi	15, 83	2.02	[Xe] 4f <sup>14</sup> 5d <sup>10</sup> 6s <sup>2</sup> 6p <sup>3</sup>	209	5, 3	0.5*10 <sup>-3</sup>
Se	16, 34	2.55	[Ar] 3d <sup>10</sup> 4s <sup>2</sup> 4p <sup>4</sup>	74, 76, 77, 78, 80	6, 4, -2	5*10 <sup>-2</sup>
Te	16, 52	2.1	[Kr] 4d <sup>10</sup> 5s <sup>2</sup> 5p <sup>4</sup>	122, 124, 125, 126	6, 4, -2	1*10 <sup>-3</sup>

### 1.2. Arsenic distribution in the environment

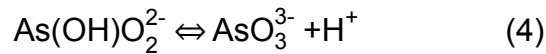
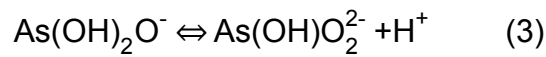
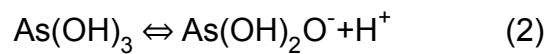
Arsenic belongs to the 21 mononuclidic elements. Its only stable isotope has an atomic mass of 74.92.<sup>[2]</sup> Pure arsenic is very rare as it is often mixed with sulfur, copper, nickel, antimony, silver, iron, lead, and cobalt in more than 200 arsenic containing minerals.<sup>[3]</sup>

Due to mining activities, weathering of rocks, application of pesticides, or drilling of tube wells, arsenic can enter the drinking water cycle. For example, minerals such as arsenopyrite (FeAsS) can be mobilized in oxygen rich water according to equation 1:<sup>[4]</sup>

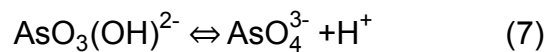
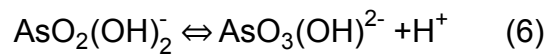
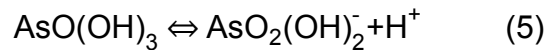


The German guideline for the arsenic content in drinking water is  $0.01 \text{ mg L}^{-1}$ . In the water, arsenic is mostly present in soluble form as  $\text{As}^{\text{III}}$  or  $\text{As}^{\text{V}}$ .

Both arsenite as well as arsenate are amphoteric and can be successively deprotonated with rising  $pH$  according to equation (2-4) and (5-7), respectively.<sup>[5]</sup>



At a neutral  $pH$ ,  $\text{As}(\text{OH})_3$  is the dominant species ( $pK_{a1}=9.2$ ;  $pK_{a2}=12.1$ ;  $pK_{a3}=12.7$ ), while arsenate exists as a mixture of  $\text{AsO}_2(\text{OH})_2^-$  and  $\text{AsO}_3(\text{OH})_2^-$ . ( $pK_{a1}=2.3$ ;  $pK_{a2}=6.8$ ;  $pK_{a3}=11.6$ ).



In many countries around the world people suffer from elevated arsenic concentration in the groundwater (up to  $>5 \text{ mg L}^{-1}$ ).<sup>[5]</sup> Table 1-2 shows a summary of countries, where elevated arsenic concentrations have been found. In the Asian countries alone, at least 60 million people were affected according to a World Bank report in 2005.<sup>[6]</sup>

**Table 1-2.** Countries with elevated arsenic concentration found in the groundwater. (reproduced from B. Petrushevski *et al.*)<sup>[7]</sup>

Asia	Bangladesh, Cambodia, China (including provinces of Taiwan and Inner Mongolia), India, Iran, Japan, Myanmar, Nepal, Pakistan, Thailand, Vietnam
America	Alaska, Argentina, Chile, Dominica, El Salvador, Honduras, Mexico, Nicaragua, Peru, USA
Europe	Austria, Croatia, Finland, France, Germany, Greece, Hungary, Italy, Romania, Russia, Serbia, UK
Africa	Ghana, South Africa, Zimbabwe,
Pacific	Australia, New Zealand

In Asian countries, mostly rice is a major source of food. Due to the rice farming process in wet cultures, the arsenic is absorbed by the plant mostly by phosphate co-transporters and aquaporines.<sup>[8]</sup> By drinking contaminated water, eating those crops or other contaminated foodstuffs, inhalation dust from combustion processes, e.g. produced from coal power plants,<sup>[9]</sup> the arsenic can enter the human body.

### 1.3. Toxicity of arsenic

Beside the acute toxicity of arsenic, the long time exposure to small amounts of arsenic can lead to a lot of diseases or cancer regarding the gastrointestinal tract, respiration tract, skin, liver, cardiovascular system, hematopoietic system, and nervous system.<sup>[10]</sup> 700000 people were affected by arsenicosis in the East and South Asian countries till 2005.<sup>[6]</sup>

The toxicity of arsenic strongly depends on its speciation. The organic arsenic compound arsenobetaine found in sea food is considered as rather harmless, while arsenite is highly toxic and arsenate shows a moderate toxicity in mice (Table 1-3).

**Table 1-3.** Acute toxicity of selected arsenic species. LD<sub>50</sub> refers to the oral administration of mice, if not indicated otherwise.

Species	Formula	Oxidation state	LD <sub>50</sub> [mg kg <sup>-1</sup> ]
Arsenic trioxide (As <sup>III</sup> )	As <sub>2</sub> O <sub>3</sub>	+III	34.5 <sup>[11]</sup>
Monomethylarsonous acid (MMA <sup>III</sup> )	CH <sub>3</sub> As(OH) <sub>2</sub>	+III	a3.6 <sup>[12]</sup>
Dimethylarsinous acid (DMA <sup>III</sup> )	(CH <sub>3</sub> ) <sub>2</sub> AsOH	+III	n.a.
Arsenate (As <sup>V</sup> )	AsO <sub>4</sub> <sup>-3</sup>	+V	b110 <sup>[13]</sup> , c220 <sup>[13]</sup>
Methylarsonic acid (MMA <sup>V</sup> )	CH <sub>3</sub> AsO(OH) <sub>2</sub>	+V	1,800 <sup>[14]</sup>
Dimethylarsinic acid (DMA <sup>V</sup> )	(CH <sub>3</sub> ) <sub>2</sub> AsO(OH)	+V	1,200 <sup>[14]</sup>
Trimethylarsine oxide (TMAO)	(CH <sub>3</sub> ) <sub>3</sub> AsO	+V	10,600 <sup>[14]</sup>
Arsenobetaine	(CH <sub>3</sub> ) <sub>3</sub> As <sup>+</sup> CH <sub>2</sub> COO <sup>-</sup>	+V	>10,000 <sup>[11]</sup>

a: hamster, intraperitoneally

b: rat

c: hamster

n.a. not available

Hughes reviewed in 2002 arsenic toxicity and the potential mode of action. While the pentavalent arsenicals are believed to replace phosphate, many biochemical reactions due to the chemical similarity, trivalent arsenic species interact with critical thiol groups.<sup>[15]</sup> A more recent review by Martinez *et al.* stated that carcinogenicity of arsenic originates from either generation of reactive oxygen species, changes in DNA methylation patterns, histone modification or altered expression of microRNAs.<sup>[16]</sup> Beside of methylated oxo-species, the formation of sulfur,<sup>[17]</sup> and arsenic-selenium species<sup>[18]</sup> by intestinal microorganism has been demonstrated. Formed dimethylmonothioarsenic acid (LC<sub>50</sub>=10.7 μM) was shown to be almost as cytotoxic as As<sup>III</sup> (LC<sub>50</sub>=5.5 μM) and DMA<sup>III</sup> (LC<sub>50</sub>=2.2 μM).<sup>[19]</sup> The toxicity of arsenic-selenium species is widely unknown.

#### 1.4. Transformation of arsenic in the human body

After absorption in respiration or gastrointestinal tract of the body, inorganic arsenic can be subject to complex transformation processes. Mainly in the liver, there can be a stepwise methylation by the transfer of a methyl group from S-adenosyl methionine (SAM) to arsenic or another metal(loid) with the involvement of a methyltransferase. SAM (Figure 1-1) is a conjugate of the amino acid methionine as well as the nucleotide adenosine and an essential metabolic intermediate in every cellular life form<sup>[20]</sup>.

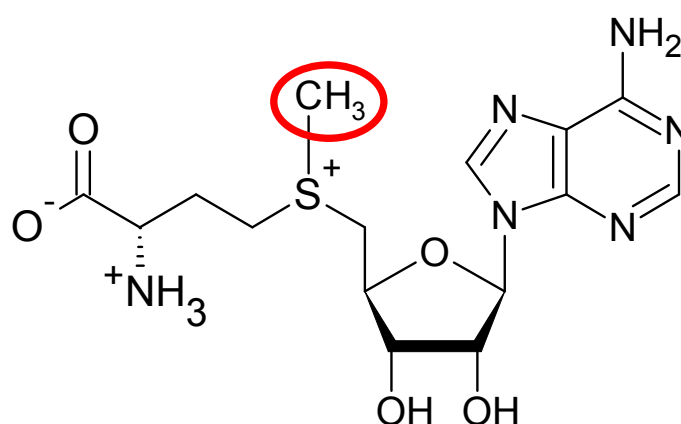


**Figure 1-1.** Chemical structure of SAM. The transferable methyl group is highlighted.

For the methylation of arsenic by SAM two important mechanisms have been proposed (Figure 1-2). In the 1940s, Challenger proposed a stepwise methylation mechanism starting from arsenate.<sup>[21]</sup> The pentavalent arsenicals are reduced by glutathione (GSH), followed by oxidative methylation till trimethylarsine oxide (TMAO) is formed. More recently, an alternative pathway of methylation was suggested by Hayakawa *et al.*<sup>[22]</sup> Prior to a enzyme-catalyzed methylation with SAM by the human methyltransferase Cyt 19, an arsenic-GSH (As(GS)<sub>3</sub>) complex is formed. Afterwards, the methyl group of SAM and the glutathionyl moiety of As(GS)<sub>3</sub> are exchanged. In contrast to the former mechanism, no change of the oxidation state of arsenic is observed.

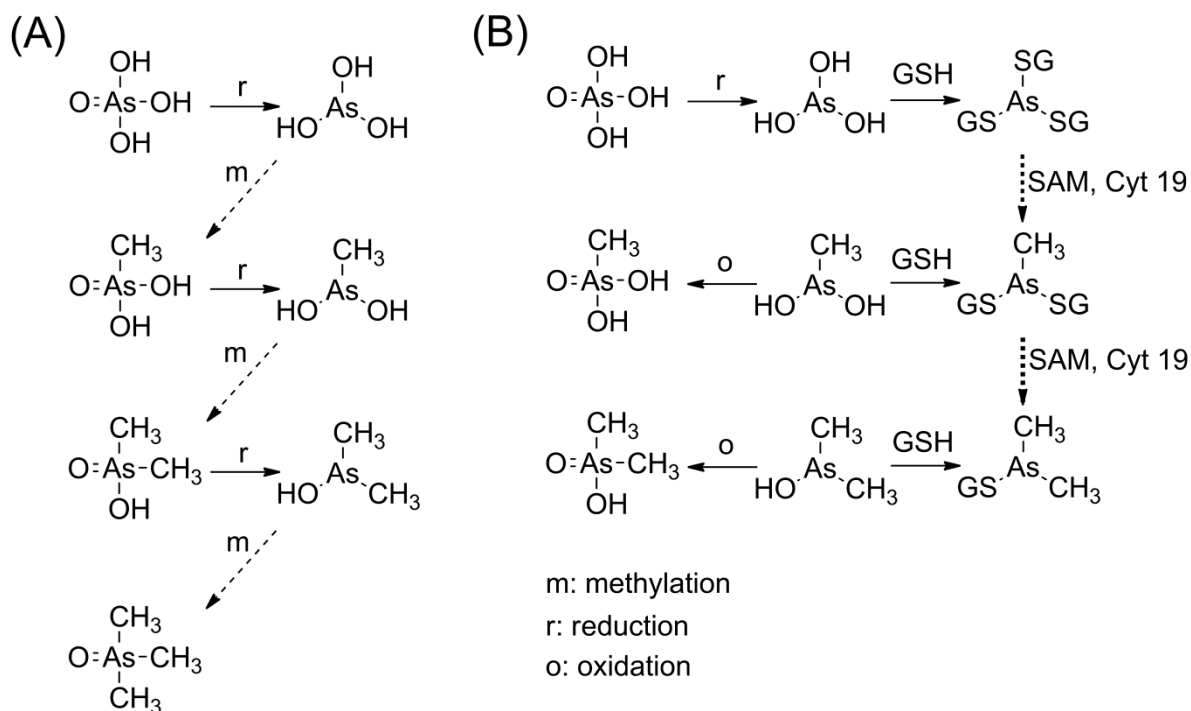


**Figure 1-2.** Methylation mechanisms according to Challenger (A) and Hayakawa *et al.* (B).

After metabolism, the arsenicals enter the kidney and are excreted via the urine. Besides, 20-25% of the ingested inorganic arsenic is excreted unmethylated.<sup>[23]</sup> The resting time of the ingested arsenic is about several days depending on the speciation, the biological half life is 30-40 h.<sup>[24]</sup>

Initially, this methylation process of arsenic has been characterized as a detoxification due to the less toxic pentavalent methylated arsenicals,<sup>[25]</sup> but the metabolites MMA<sup>III</sup> and DMA<sup>III</sup> are even more potent toxics than As<sup>III</sup> (Table 1-3).<sup>[26-27]</sup> The order regarding the toxic potential is: MMA<sup>III</sup>>DMA<sup>III</sup>>As<sup>III</sup>>As<sup>V</sup>>MMA<sup>V</sup>>DMA<sup>V</sup>.<sup>[28]</sup> In general, the methylation of metal(loid)s has a great influence on the bioavailability<sup>[29]</sup> and the toxicity. For example, the highly toxic methylmercury (CH<sub>3</sub>Hg<sup>+</sup>) which is responsible for much of the mercury poisoning at Minimata Bay in Japan and can penetrate the blood-brain barrier.<sup>[30]</sup>

### 1.5. Transformation of antimony, bismuth, selenium, and tellurium in the human body

In contrast to arsenic, there is little evidence for methylation of antimony in the human body.<sup>[31]</sup> However, the production of methylated antimony compounds in

presence of GSH was demonstrated and a formation of antimony-GSH complexes was shown.<sup>[32]</sup> Additionally, a toxicological interesting fact is that  $\text{SbCl}_3$  was shown to inhibited the methylation of arsenic *in vitro*.<sup>[31]</sup>

After ingestion of colloidal bismuth subcitrate, trimethylbismuth was found in the breath of volunteers.<sup>[33]</sup> Furthermore, Hollmann *et al.* observed formation of trimethylbismuth by hepatic cells.<sup>[34]</sup> Von Recklinghausen *et al.* found that methylbismuth was better taken up by the cells than Bi-Cit and Bi-GS.<sup>[35]</sup> Dopp *et al.* stated elevated cytotoxicity and genotoxicity of trimethylbismuth in comparison to inorganic bismuth.<sup>[36]</sup>

For the essential metal(loid) selenium, Kremer *et al.* found volatile dimethylselenide (DMSe) in breath of healthy male volunteers after oral administration of sub-toxic amounts of selenite.<sup>[37]</sup>

For tellurium, at least transformation in rats has been demonstrated. The ingested tellurium was methylated in the organs forming dimethylated tellurium, transported in the blood and finally excreted in urine as trimethyltelluronium and dimethyltelluride, respectively.<sup>[38]</sup>

Beside these methylation processes, Diaz-Bone and Van de Wiele reviewed on the Biotransformation of metal(loid)s by intestinal microorganisms.<sup>[39]</sup>

### 1.6. Transformation of metal(loid)s by microorganisms

Beside the methylation of metal(loid)s in the body of mammals, there are different other sources of these compounds: (i) anthropogenic sources, e.g. organotin compounds that were used as anti-fouling agents or the dimethyl arsenic acid solution called “agent blue” used for defoliation during the Vietnam war<sup>[40]</sup>, (ii) abiotic methylation, (iii) transmethylation,<sup>[41]</sup> (iv) and methylation by microorganisms.

Microbial methylation has been demonstrated for a wide variety of metal(loid)s, including Ge, As, Se, Cd, In, Sn, Sb, Te, Hg, Tl, Pb, Bi, and Po.<sup>[42]</sup> In anerobic habitats, including fresh-water sediments, hydrothermal vents, rice paddies, sewage digestors, landfills, the rumen, and the intestinal tract<sup>[43]</sup>, methanoarchaea are mainly involved in the formation process of organometal(loid) compounds. Furthermore, their capability to methylate multiple elements (As, Sb, Se, Te, Bi) was demonstrated.<sup>[44]</sup>

### 1.7. Methanogenic Archaea

Archaea are one out of the three primary lineages (Eucarya, Bacteria, Archaea). They resemble Bacteria in morphology and genomic organization and lack in eucaryotic cell nuclei, but the molecular organization of their cells is similar to eucaryotes.<sup>[45-46]</sup> Within the Archaea, the methanogenic microorganisms represent the largest and most diverse group<sup>[43]</sup> containing the five orders Methanopyrales, Methanococcales, Methanobacteriales, Methanomicrobiales and Methanosarcinales.<sup>[47]</sup> The characteristics of Methanosarcinales are the existence of cytochromes and methanophenazine as well as a wide substrate spectrum. Most can use acetate, methanol, methylamines and some CO<sub>2</sub> and H<sub>2</sub> for their energy metabolism by methane formation, which is called methanogenesis.<sup>[47]</sup> Different enzymes and cofactors are involved in this multi-step process. An enzyme system composed of three polypeptides, MtaA, MtaB and MtaC, has been identified for the utilization of methanol in *Methanosarcina bakeri*.<sup>[48]</sup> The methyl group of methanol is transferred by the methyltransferase MtaB to the corrinoid-binding protein MtaC, forming CH<sub>3</sub>-MtaC. Next, the methyltransferase MtaA catalyzes the transfer to coenzyme M (CoM, 2-mercaptoethane sulfonate) yielding methylated CoM and regenerating MtaC, which has been shown to be replaceable by free cob(I)alamin (Cob(I)) in *in vitro* experiments.<sup>[48]</sup> The final step is the methane formation of methane by a methyl-coenzyme M reductase with the cofactor F430 and coenzyme B.<sup>[49]</sup>

### 1.8. Methylcobalamin and its derivatives and its role for the methylation of metal(loid)s

The intermediary formed CH<sub>3</sub>Cob (Figure. 1-3) is a derivative of cyanocobalamin, also known as vitamin B12. Butler and Greutler, for instance, published a detailed review on the B12 biochemistry.<sup>[50]</sup> Typical for the cobalamins is a cobalt central atom which is coordinated by corrin ligand, a 5,6-dimethyl benzimidazole moiety, and a further functional group, which in the case of methylcobalamin is a methyl group. B12-coenzymes are important biological cofactors that only can be formed by microorganisms.<sup>[50]</sup>

There are a lot of B12-dependent biological methyl transfer reactions, such as in the methanogenesis, in the acetyl-coenzyme A pathway of the carbon-dioxide fixation, or in the methionine synthesis.<sup>[51]</sup>

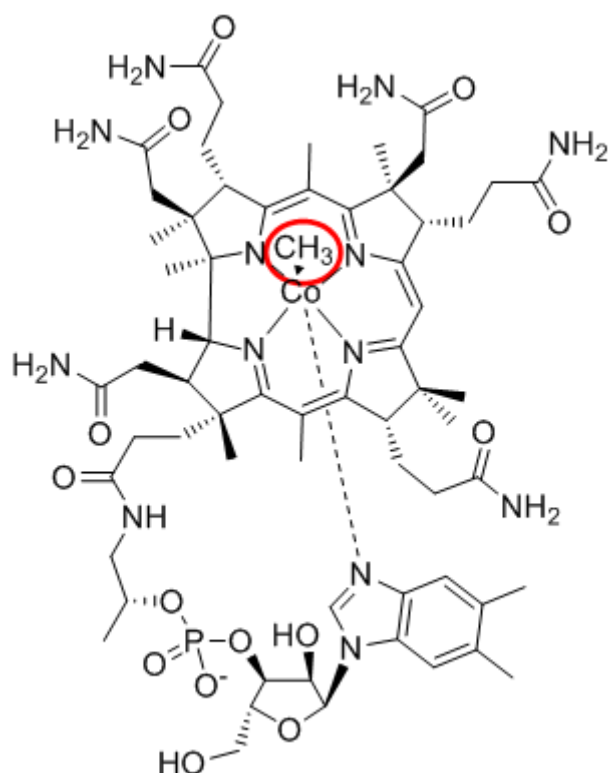


**Figure 1-3.** Chemical structure of CH<sub>3</sub>Cob. The transferable methyl group is highlighted.

With decreasing  $pH$  the nitrogen of the benzimidazole moiety is protonated converting the CH<sub>3</sub>Cob from the “base on” to its “base off” configuration (Figure 1-4), in which the benzimidazole moiety is not coordinated to the central atom ( $pK_a=2.7$ ).<sup>[52]</sup>

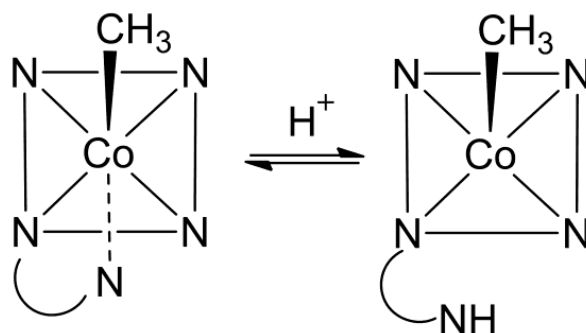


**Figure 1-4.** Simplified methylcobalamin in “base on” (left) and “base off” (right) configuration.

Furthermore, Pignatello and Fanchiang observed a concentration-dependent shift in the 279-Mhz  $^1\text{H-NMR}$  spectrum of methylcobalamin indicating a dimer formation due to  $\pi$ - $\pi$  bonding between adjacent corrin rings.<sup>[53]</sup>

$\text{CH}_3\text{Cob}$  has been considered as donor of the methyl group instead of SAM for the methylation of metal(loid)s by anaerobic microorganisms. The methyl group of  $\text{CH}_3\text{Cob}$  can be transferred either as carbocation, carboanion, or methyl radical (Figure 1-5) depending on the reaction conditions and the metal(loid) itself.

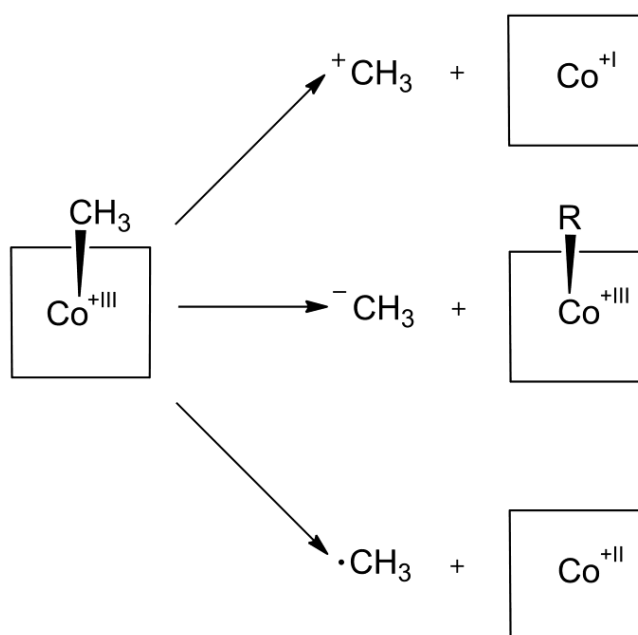
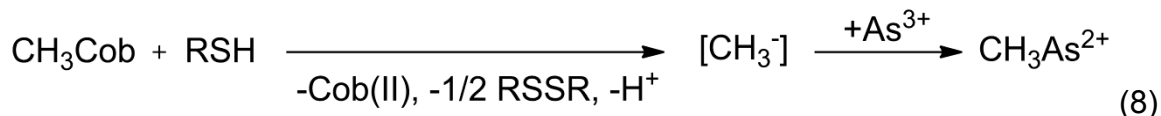


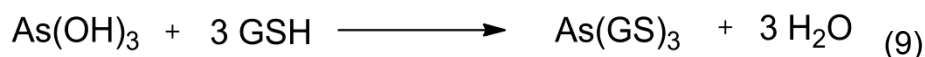
**Figure 1-5.** Possible ways transferring the methyl group of  $\text{CH}_3\text{Cob}$ .  $\text{CH}_3\text{Cob}$  is drawn simplified. R represents a ligand, such as  $\text{H}_2\text{O}$  or  $^-\text{CN}$ , which replaces the methyl group.

An example for an abstraction of the methyl group as carbocation is the enzyme-catalyzed reaction of CoM with  $\text{CH}_3\text{Cob}$  during the methanogenesis.<sup>[54]</sup> A transfer as carbanion is described for mercury, lead, and palladium.<sup>[55]</sup> In addition, different mechanisms for radical methyl transfer to heavy elements have been proposed.<sup>[56]</sup> As the methyl-cobalt bonding of  $\text{CH}_3\text{Cob}$  can be cleaved homolytically either by photo- or thermolysis<sup>[57]</sup> (see below) the metal(loid) can thereupon function as a radical trap as reported for arsenic.<sup>[55]</sup> Moreover, radical abstraction has been proposed in the case of tin and a free radical formation due to a one-electron transfer has been described for hexachloroiridate.<sup>[56]</sup> Besides, the non-enzymatical

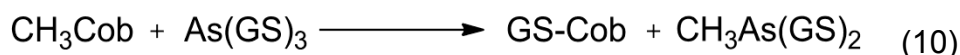
methylation by methylcobalamin has been demonstrated for arsenic in presence of thiols. For the reaction mechanism in presence of a thiol Schrauzer proposed the formation of a crypto carbanion followed by arsenic methylation:<sup>[58]</sup>



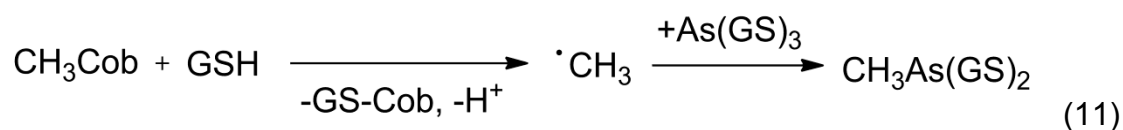
Zakharian and Aposhian showed the methylation of arsenic in presence of GSH. They proposed the formation of a glutathione-arsenic complex (equation 9) followed by nucleophilic attack of the arsenic-GSH complex on  $\text{CH}_3\text{Cob}$ .<sup>[59]</sup>



Hayakawa *et al.* showed the formation of the  $\text{As(GS)}_3$  complex and drafted a concerted group exchange mechanism according to equation (10).<sup>[22]</sup>



Finally, Nakamura *et al.* assumed a radical mechanism (equation 11). By transaxial coordination of  $\text{CH}_3\text{Cob}$  a Co-GSH complex and a methyl radical is formed which reacts with  $\text{As(GS)}_3$ .<sup>[55]</sup>



As shown in Figure 1-5 Cobalt can exist in three oxidation states in this complex. The enzyme-catalyzed demethylation by CoM produces black-green Cob(I), which can be easily oxidized yielding yellow Cob (II). Cob(II) again can be oxidized producing Cob(III), which is coordinated with a ligand such as  $\text{H}_2\text{O}$  or  $\text{CN}^-$ .<sup>[60]</sup>

Starting from aquocobalamin (Cob(III)), a reduction via Cob(II) to Cob(I) is possible, either by electrochemical reduction (equation 12), chemical reduction, or not in a pure state by catalytic hydrogenation after reoxidation.<sup>[61-62]</sup>

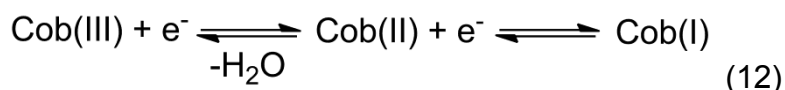
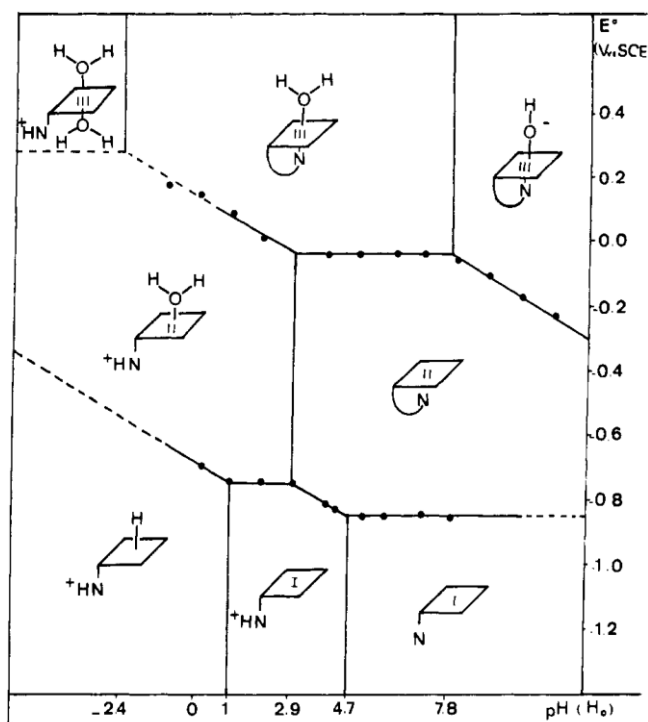


Figure 1-6 shows the Pourbaix diagram for the different cobalamin species.



**Figure 1-6.** Pourbaix diagram of cobalamin<sup>[63]</sup>

Cob(I) acting as cofactor in the methanogenesis is a strong reducing agent due to negative standard reduction potential (-610 mV)<sup>[64]</sup> and has been considered to be involved in methylation and hydrogenation processes as intermediate compound by Schrauzer *et al.*<sup>[58]</sup> In addition, in organic chemistry cob(I)alamin has been used as reduction catalyst.<sup>[65-68]</sup>

The carbon-cobalt bonding, which has a dissociation enthalpy of  $32 \pm 2 \text{ kcal mol}^{-1}$ ,<sup>[69]</sup> can be cleaved homolytically by temperatures  $> 210^\circ\text{C}$  by or by light irradiation.<sup>[57]</sup> Anaerobic photolysis yielded a methane/ethane ratio of about 1:2 and the observed reaction was very slow. However, the methane ratio could be increased by increasing the *pH*. By adding KCN, a thiol or methanol the ethane production due to methyl radical combination could be completely suppressed. By adding an alcohol, the reaction rate could be significantly increased (isopropyl alcohol  $> n$ -

propanol>ethanol>methanol>*tert.*-butanol).<sup>[70]</sup> Here, the alcohol functions as H-donor. The formed methyl radical is capable to abstract hydrogen in the alpha position. This was verified by the formation of pinacol in an extract of an anaerobically photolyzed solution of methylcobalamin in isopropyl alcohol. Methane from methylcobalamin can also be formed by hydrogenation in the presence of platinum with a yield of about 75%.<sup>[71]</sup>

### 1.9. Metal speciation by hyphenation of inductively coupled plasma mass spectrometry

As metal speciation is important for risk assessment as well for the investigation of environmental processes, such as the biomethylation of metal(loid)s, highly sensitive analytical techniques for trace element analysis in environmental samples are a requirement.

For element speciation inductively coupled plasma (ICP) mass spectrometry (MS) is a widely used and highly sensitive technique in hyphenation to gas chromatography (GC) or liquid chromatography (LC). A wide range of elements can be analyzed with a high dynamic range of 6-9 orders of magnitude and detection limits in the ppt range.

As ICP-MS breaks down analyte molecules to its elements, identification of the analytes can be achieved either by comparison of the retention times with standard compounds or due to a coupling with electron impact (EI)-MS and electrospray ionization (ESI)-MS, that allows parallel molecule specific detection.

An ICP-MS system mainly consists of the sample introduction, the plasma, the interface, ion optics, a quadrupole mass filter and the detector (Figure 1-7).

The liquid sample or the internal standard solution is introduced in the plasma using a pneumatic nebulizer, where an aerosol is produced. Afterwards, a cooled spray chamber is used for removing droplets >10  $\mu\text{m}$  from the gas stream of about 1 l  $\text{min}^{-1}$ , which enters the argon plasma. For gaseous sample introduction a T-joint is placed between spray chamber and plasma torch. The plasma torch is centered between the plasma coil and consists of three concentric quartz tubes. The sample enters the middle tube. Between the outer and the middle tubes 12–17 l  $\text{min}^{-1}$  of argon is used to form the plasma. In the plasma at a temperature of about 7000-10000 K, first the sample is dried, decomposed, evaporated, atomized and finally

ionized. In the interface, the pressure is reduced in three steps from atmospheric pressure in plasma to below  $10^{-3}$  Pa in the mass spectrometer. The ions, that are produced in the plasma, pass a photon stop and then reach the ion optics. The ion optics consists of a number of cylinders and discs, electromagnetic lenses, and serve to focus the ion beam on the entrance of the quadrupole mass spectrometer, which acts as a mass filter. Finally, a secondary electron multiplier (SEM) is used as detector.

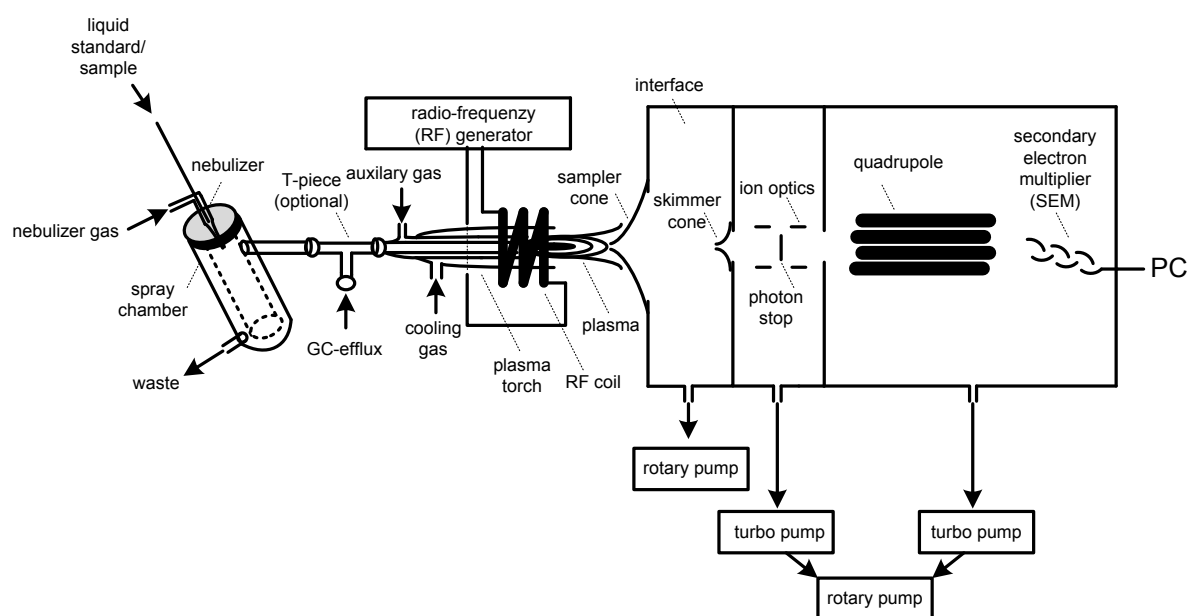


**Figure 1-7.** Schematic overview of an ICP-MS

### 1.9.1. Quantification of volatile organometal(loid) compounds

Volatile organometal(loid) compounds can be quantified using a modified interelement interaggregate calibration method developed by Feldmann *et al.*<sup>[72]</sup> with an error within the range of  $\pm 35\%$ . At first, a factor (relative standard factor,  $RSF_A$ ) is determined (equation 13) using an internal standard solution with a known concentration of an internal standard ( $c_{Ist}$ ) and the analyte ( $c_A$ ) which reflects the sensitivity of an analyte in relation to the sensitivity of an internal standard. The used internal standard should have a similar mass and ionization energy, for example  $^{71}\text{Ga}$  in the case of  $^{75}\text{As}$ . The mean intensities of the analyte ( $I_A$ ) and the internal standard ( $I_{Ist}$ ) are corrected by subtraction of the blank level ( $I_{A,bl}$  resp.  $I_{Ist,bl}$ ).

$$RSF_A = \frac{c_A \times (I_A - I_{A,b})}{c_{Ist} \times (I_{Ist} - I_{Ist,b})} \quad (13)$$

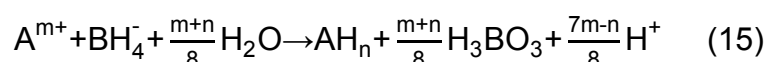
While measuring of the volatile compounds, a liquid internal standard solution is continuously added. With the corresponding peak area of  $A_A$ , the intensity of the internal standard at the same time, the mass of the analyte  $m_A$  can be determined under inclusion of the nebulizer flow rate  $v$ , the efficiency of the nebulizer  $z$  and the concentration of the internal standard solution:

$$m_A = \frac{c_{Ist} \times A_A \times v \times z}{I_{Ist} \times RSF_A} \quad (14)$$

### 1.9.2. Hydride generation of metal(loid)s

Beside the analysis of volatile compounds, a derivatization by sodium tetrahydroborate ( $\text{NaBH}_4$ ) allows the speciation of non-volatile organometal(loid)s *via* purge and trap (P&T)-GC-ICP-MS with low limits of detection.

Kumar and Riyazuddin reviewed on the mechanism of hydride generation. Two important theories for the mechanism of hydride generation have been proposed. The first was based on the formation of nascent hydrogen.<sup>[73]</sup> According to Laborda *et al.*,<sup>[74]</sup> the reaction of an analyte  $A$  with the oxidation state  $m$  ( $A^{m+}$ ) with  $\text{NaBH}_4$  can be expressed as in equation 15, with the coordination number of the hydride  $n$ .



The second is a non-nascent-mechanism, which was finally proved by experiments with deuterated chemicals. Hydrolysis experiments of  $\text{KBH}_4$  in acidified  $\text{D}_2\text{O}$  resulted in HD formation as main product. Furthermore, the hydride generation of  $\text{As}^{\text{III}}$  and  $\text{As}^{\text{V}}$  using  $\text{NaBD}_4$  in acidified  $\text{H}_2\text{O}$  yielded  $\text{AsD}_3$  as main product indicating that there has to be a direct transfer of the hydrogen.<sup>[73]</sup>

As hydride generation is *pH* specific,<sup>[73]</sup> this can be utilized for differentiation between different oxidation states of the precursing metal(loid) compounds yielding the same volatile compound after reduction using  $\text{NaBH}_4$ .<sup>[75-76]</sup> In the optimal *pH* range, the arsenic species are fully protonated.<sup>[77]</sup> For the derivatization of the different arsenic

species follows that TMAO is derivatized at alkaline/neutral conditions. Then, with decreasing  $pH$ , follow the ideal  $pH$  ranges for hydride generation of  $DMA^{III}$ ,  $MMA^{III}$ ,  $As^{III}$ ,  $DMA^V$ ,  $MMA^V$ , and finally  $As^V$  at a strongly acidic  $pH$ .

### 1.10. Compound-specific stable isotope analysis.

Despite intensive research many questions in the field of biomethylation remain unanswered, e.g. the methylation pathways. As the compound-specific stable isotope analysis (CSIA) allows the differentiation between different reaction mechanisms, such as a concerted ( $S_N2$ ) or a stepwise nucleophilic substitution ( $S_N1$ ),<sup>[78]</sup> by studying the extent of the isotopic fractionation during a reaction, the application of CSIA could clearly advance this field of investigation.

Because of slightly different properties of isotopologues, which are molecules of the same chemical structure, but a different isotopic composition, there can be depletion or enrichment during a physical process or a chemical reaction.

During a unidirectional process, such as the most biogeochemical reactions or evaporation in an open system, which means that there's no equilibrium, the fractionation is called kinetic fractionation. Due to differences in the zero point energy of the isotopologues leading to different activation energies (Figure 1-8), the lighter isotopologue normally reacts faster and becomes enriched in the product.

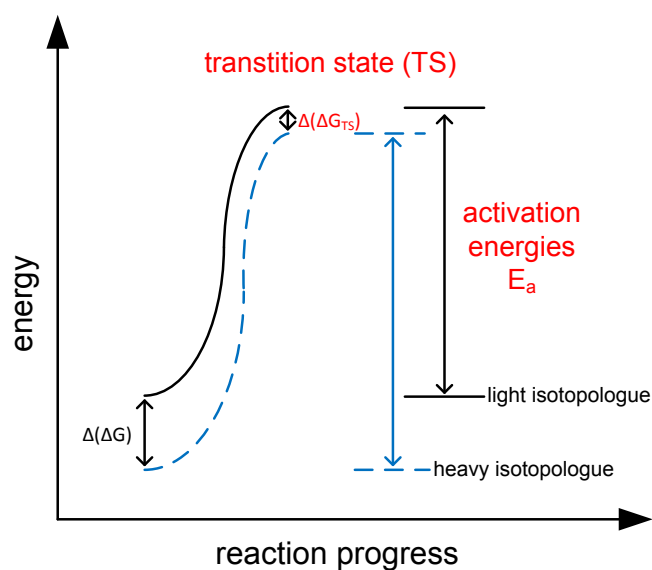


**Figure 1-8.** Differences in energies of isotopologues during an unidirectional process.  $G$  represents the Gibbs free energy. (modified from<sup>[78]</sup>).

Isotopic fractionation originating from kinetic isotope effects can be used to distinguish between different types of reaction even if the same final product is obtained like in the case of  $S_N1$  and  $S_N2$ -reactions, which leads to markedly different kinetic isotope effects due to the different transition states. [79]

The relation between the reaction rates yields the kinetic isotope effect (*KIE*) (equation 16).

$$KIE = \frac{k_{light}}{k_{heavy}} \quad (16)$$

For the determination of the *KIE* the ratio *R* of the heavy to the light isotope according to equation 17 regarding to carbon is determined for a sample by IRMS.

$$R = \frac{^{13}\text{C}}{^{12}\text{C}} \quad (17)$$

Due to the small differences of the isotopic ratios resulting in small values, the delta notation is used. The delta value for  $^{13}\text{C}$  is defined as following:

$$\delta^{13}\text{C} = \frac{R_{sample} - R_{VPDB}}{R_{VPDB}} \quad (18)$$

$R_{sample}$  represents the ratio of the light to the heavy isotope of the sample.  $R_{VPDB}$  is the ratio of the internal standard Vienne PeeDee Belemnite (VPDB) which is used for referencing. VPDB replaced the original standard Pee Dee Belemnite PDB, a primeval carbonate with a  $^{13}\text{C}/^{12}\text{C}$  ratio of 0.0112372. [80]

The isotopic fractionation between a reactant and a product can be described according to equation 19 using the fractionation factor  $\alpha$  which is related to the *KIE* and the enrichment factor  $\epsilon$  that is used, because  $\alpha$  is close to 1.

$$\alpha = \frac{\delta^{13}\text{C}_{product} + 1}{\delta^{13}\text{C}_{reactant} + 1} = \frac{1}{KIE} = \epsilon + 1 \quad (19)$$

### 1.10.1. Instrumental details for CSIA

Before compound-specific analysis by isotopic ratio mass spectrometry (IRMS), the compounds are separated by either gas chromatography (GC)<sup>[81-82]</sup> or high performance liquid chromatography (HPLC). Figure 1-9 shows the schematic structure of a GC-IRMS system. GC-IRMS was demonstrated first in 1978 by Matthews and Hayes.<sup>[83]</sup> and allows to determine ratios of stable Isotopes ( $^{13}\text{C}/^{12}\text{C}$ ,  $^{15}\text{N}/^{14}\text{N}$ ,  $^2\text{H}/^1\text{H}$ )

After separation of the organic compounds by gas chromatography, helium as carrier gas transfers the efflux through a combustion oven. The combustion oven is a tube of alumina oxide filled with wires of Pt, NiO and CuO in the inside. These oxides provide the required oxygen for the combustion of organic compounds at a temperature of 940°C yielding  $\text{CO}_2$ ,  $\text{H}_2\text{O}$  and small amounts of nitrogen oxides.

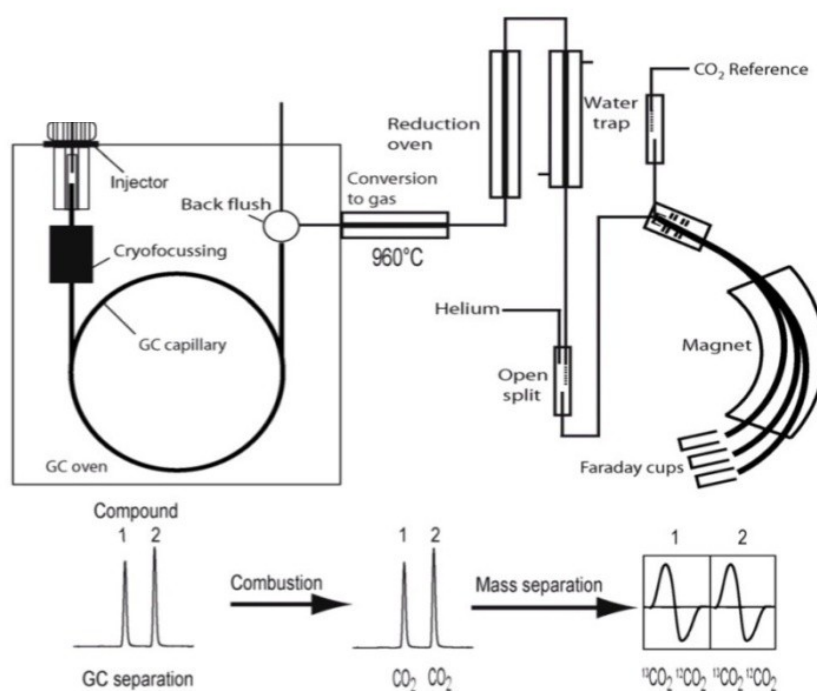


**Figure 1-9.** Schematic view of a GC-IRMS system.

Afterwards, the compounds enter a reduction furnace, where the remaining nitrogen oxides are reduced to  $\text{N}_2$  using Cu at 640 °C. For the analysis of  $\text{CO}_2$ , this step is skipped.

Using a Nafion membrane (a sulfonated tetrafluorethylene polymer), the water originating from the combustion process is removed, because ions produced in the ion source like to react with hydrogen-bearing molecules to form protonated ions. Thus, an isobaric interference from  $^{12}\text{C}^{16}\text{O}_2\text{H}^+$  could be formed interfering with  $^{13}\text{C}^{16}\text{O}_2$ .<sup>[84]</sup>

Finally, the  $\text{CO}_2$  enters a sector field mass spectrometer with three Faraday cups *via* an open split. To ensure the required precision for the measurement of  $\text{CO}_2$ , the ions with the mass-charge ratios 44 ( $^{12}\text{C}^{16}\text{O}_2$ ), 45 ( $^{13}\text{C}^{16}\text{O}_2$ ) and 46 ( $^{12}\text{C}^{18}\text{O}^{16}\text{O}$ ) for correction purposes are monitored.

The obtained  $^{13}\text{C}/^{12}\text{C}$  ratios  $R$  are usually related to a reference  $\text{CO}_2$  gas which is normalized to the international standard Vienna Pee Dee Belemnite (VPDB).

The compounds containing  $^{13}\text{C}$  show weaker interactions with stationary phase of a non-polar column which results in the so called isotopic swing in a plot of the ratio of mass-charge relation ( $m/z$ ) 45 to 44 vs. the retention time (Figure 1-10).

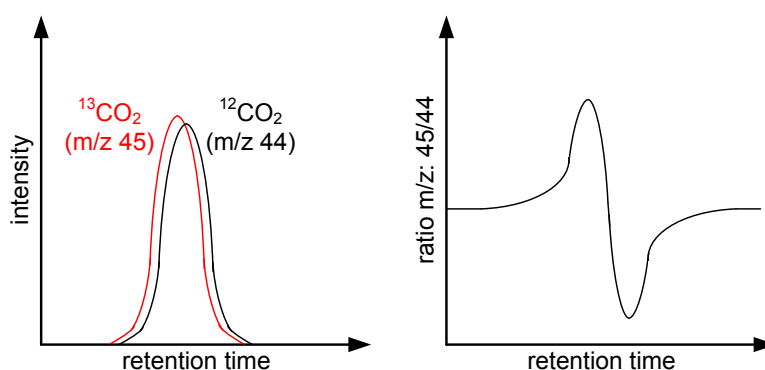


**Figure 1-10.** Origin of isotopic swing in ratio  $m/z$ : 45/44 (right) due to slight differences in the retention times of the isotopologues (left). (redrawn from<sup>[85]</sup>)

### 1.11. Elemental Analyzer IRMS bulk analysis for referencing

For referencing, a bulk analysis of a compound is usually achieved by coupling of an Elemental Analyzer (EA) to the IRMS. In the EA, the compound in a tin capsule is abruptly combusted at a temperature up to  $1800^\circ\text{C}$  while adding oxygen. Afterwards,  $\text{H}_2\text{O}$  is removed and eventually formed nitrous oxides are reduced by Cu to  $\text{N}_2$ . The formed gases  $\text{CO}_2$ ,  $\text{N}_2$ , and  $\text{SO}_2$ , if the compounds contain nitrogen or sulfur, are isothermally separated on a GC column and the isotope ratios  $^{13}\text{C}/^{12}\text{C}$ ,  $^{15}\text{N}/^{14}\text{N}$ , and  $^{34}\text{S}/^{32}\text{S}$  are sequentially measured.

### 1.12. SCOPE OF THE THESIS

Microorganisms have been shown to be capable to methylate various metal(loid)s, including arsenic antimony, selenium, tellurium, and bismuth. Besides, enzyme-catalyzed methylation in mammals as well as abiotic methylation has been demonstrated. In the long history of research in this field, several reaction mechanisms have been proposed for the enzyme-catalyzed as well as the abiotic methylation, but have not really been proven yet. Since the methylation alters both biomobility and toxicity of the precursory metal(loid)s, the full comprehension of the underlying reaction mechanism is of high relevance for a conclusive risk assessment. Hence, the scope of this study is to foster the mechanistic understanding of the methylation by  $\text{CH}_3\text{Cob}$  of the group 15, and group 16 elements As, Se, Te, Sb, and Bi by development, validation, and application of new approaches and analytical techniques. Particular emphasis is put on the toxicologically highly relevant arsenic which is a widespread contaminant in the drinking water.

**Chapter 2** deals with the role of biological "reducing agents" for the methylation of metal(loid)s by methylcobalamin. The role of the strong reducing agent cob(I)alamin during MtaA-mediated methylation of group 15 and group 16 elements by methylcobalamin as a side reaction of the methanogenesis of methanobacteria is investigated. Furthermore, different biotic as well as abiotic "reducing agents" are tested with regard to their methylation capability and efficiency.

In **Chapter 3**, for a differentiation of an oxidative and a non-oxidative methylation mechanism for the MtaA-mediated methylation of arsenic by methylcobalamin, a new oxidation-state specific hydride generation technique is developed and used. Furthermore, a series of detailed UV/Vis and P&T-GC-ICP-MS studies on the methylation as well as the hydrogenation of arsenic and the other group 15 and 16 elements by methylcobalamin is conducted to elucidate the underlying reaction mechanisms.

As the investigation of a change in the isotopic signature in the course of a reaction can be a promising tool to investigate the underlying reaction mechanism, in **Chapter 4**, the first method for the determination of the carbon isotopic values of organometal(loid)s in complex matrices is developed and validated. The applicability

---

of this method is shown for biogenically formed trimethylarsine oxide in a compost matrix.

For an investigation of the occurring kinetic isotope effect, the initial value, which is the carbon isotopic signature of the methyl group from the methyl donor methylcobalamin, has to be determined. Therefore, five different independent approaches, including abstraction of the methyl group with HI, light irradiation, thermolytic cleavage, and platinum (II/IV) couples and subsequent measurement of the products by GC-IRMS or by flow injection analysis (FIA)-IRMS in the case of Pt, are tested in **Chapter 5**. Additionally, the technique for determination of the carbon isotopic values of organometal(loid)s in complex matrices from Chapter 4 is extended to the partly methylated arsenicals. With this methodology, the abiotic methylation of arsenic by methylcobalamin in presence of GSH is investigated.

**Chapter 6** provides the general conclusions that can be drawn from this thesis and gives an outlook to future studies and opportunities of the developed techniques.

1.13. REFERENCES

- [1] D. Lide, *CRC Handbook of Chemistry and Physics, 90th Edition*, CRC Press, **2010**.
- [2] M. Berglund, M. E. Wieser, *Pure Appl. Chem.* **2011**, *83*, 397.
- [3] P. L. Smedley, D. G. Kinniburgh, *Appl. Geochem.* **2002**, *17*, 517.
- [4] A. H. Welch, D. B. Westjohn, D. R. Helsel, R. B. Wanty, *Ground Water* **2000**, *38*, 589.
- [5] V. K. Sharma, M. Sohn, *Environ. Int.* **2009**, *35*, 743.
- [6] K. M. K. Kemper, *The World Bank* **2005**, *Volume I policy report*.
- [7] S. S. B. Petrushevski, J. C. Schippers, K. Shordt, *Thematic Overview Paper 17, IRC* **2007**.
- [8] A. A. Meharg, *Trends Plant Sci.* **2004**, *9*, 415.
- [9] D. F. S. Natusch, J. R. Wallace, C. A. Evans, *Science* **1974**, *183*, 202.
- [10] B. K. Mandal, K. T. Suzuki, *Talanta* **2002**, *58*, 201.
- [11] T. Kaise, S. Watanabe, K. Itoh, *Chemosphere* **1985**, *14*, 1327.
- [12] J. S. Petrick, B. Jagadish, E. A. Mash, H. V. Aposhian, *Chem. Res. Toxicol.* **2001**, *14*, 651.
- [13] S. G. Schäfer, R. L. F. Dawes, B. Elsenhans, W. Forth, K. Schümann, in *Toxicology* (Eds.: M. Hans, G. S. Siegfried, M. Roger, S. G. S. R. M. Frank WelschA2 - Hans Marquardt, W. Frank), Academic Press, San Diego, **1999**, pp. 755.
- [14] T. Kaise, H. Yamauchi, Y. Horiguchi, T. Tani, S. Watanabe, T. Hirayama, S. Fukui, *Appl. Organomet. Chem.* **1989**, *3*, 273.
- [15] M. F. Hughes, *Toxicol. Lett.* **2002**, *133*, 1.
- [16] V. D. Martinez, E. A. Vucic, D. D. Becker-Santos, L. Gil, W. L. Lam, *J. Toxicol.* **2011**, *2011*, 431287.
- [17] H. R. Hansen, R. Pickford, J. Thomas-Oates, M. Jaspars, J. Feldmann, *Angew. Chem. Int. Ed. Engl.* **2004**, *43*, 337.

- [18] R. A. Diaz-Bone, M. Hollmann, O. Wuerfel, D. Pieper, *J. Anal. At. Spectrom.* **2009**, *24*, 808.
- [19] H. Naranmandura, K. Ibata, K. T. Suzuki, *Chem. Res. Toxicol.* **2007**, *20*, 1120.
- [20] P. Kozbial, A. Mushegian, *BMC Struct. Biol.* **2005**, *5*, 19.
- [21] F. Challenger, *Chem. Rev.* **1945**, *36*, 315.
- [22] T. Hayakawa, Y. Kobayashi, X. Cui, S. Hirano, *Arch. Toxicol.* **2005**, *79*, 183.
- [23] C. Hopfenhaynrich, A. H. Smith, H. M. Goeden, *Environ. Res.* **1993**, *60*, 161.
- [24] T. Gebel, *Chem. Biol. Interact.* **1997**, *107*, 131.
- [25] T. Sakurai, *J. Health Sci.* **2003**, *49*, 171.
- [26] J. S. Petrick, F. Ayala-Fierro, W. R. Cullen, D. E. Carter, H. V. Aposhian, *Toxicol. Appl. Pharmacol.* **2000**, *163*, 203.
- [27] M. Styblo, L. M. Del Razo, L. Vega, D. R. Germolec, E. L. LeCluyse, G. A. Hamilton, W. Reed, C. Wang, W. R. Cullen, D. J. Thomas, *Arch. Toxicol.* **2000**, *74*, 289.
- [28] R. A. Yokel, S. M. Lasley, D. C. Dorman, *J. Toxicol. Environ. Health B Crit. Rev.* **2006**, *9*, 63.
- [29] J. S. Thayer, *Abstr. Pap. Am. Chem. Soc.* **1988**, *195*, 79.
- [30] I. Wagner-Dobler, *Appl. Microbiol. Biotechnol.* **2003**, *62*, 124.
- [31] T. Gebel, *Chem.-Biol. Interact.* **1997**, *107*, 131.
- [32] S. Wehmeier, A. Raab, J. Feldmann, *Appl. Organomet. Chem.* **2004**, *18*, 631.
- [33] J. Boertz, L. M. Hartmann, M. Sulkowski, J. Hippler, F. Mosel, R. A. Diaz-Bone, K. Michalke, A. W. Rettenmeier, A. V. Hirner, *Drug Metab. Dispos.* **2009**, *37*, 352.
- [34] M. Hollmann, J. Boertz, E. Dopp, J. Hippler, A. V. Hirner, *Metallomics* **2010**, *2*, 52.
- [35] U. von Recklinghausen, L. M. Hartmann, S. Rabieh, J. Hippler, A. V. Hirner, A. W. Rettenmeier, E. Dopp, *Chem. Res. Toxicol.* **2008**, *21*, 1219.

- [36] E. Dopp, U. von Recklinghausen, J. Hippler, R. A. Diaz-Bone, J. Richard, U. Zimmermann, A. W. Rettenmeier, A. V. Hirner, *J. Toxicol.* **2011**, 2011, 503576.
- [37] D. Kremer, G. Ilgen, J. Feldmann, *Anal. Bioanal. Chem.* **2005**, 383, 509.
- [38] Y. Ogra, R. Kobayashi, K. Ishiwata, K. T. Suzuki, *J. Inorg. Biochem.* **2008**, 102, 1507.
- [39] R. A. Diaz-Bone, T. Van de Wiele, *Pure Appl. Chem.* **2010**, 82, 409.
- [40] J. M. Stellman, S. D. Stellman, R. Christian, T. Weber, C. Tomasallo, *Nature* **2003**, 422, 681.
- [41] E. Dopp, L. M. Hartmann, A.-M. Florea, A. W. Rettenmeier, A. V. Hirner, *Crit. Rev. Toxicol.* **2004**, 34, 301.
- [42] J. S. Thayer, *Appl. Organomet. Chem.* **2002**, 16, 677.
- [43] J. G. Ferry, *Crit. Rev. Biochem. Mol. Biol.* **1992**, 27, 473.
- [44] K. M. Michalke, J. Meyer, R. Hensel, R. Garrett, H. P. Klenk, in *Archaea-Evolution, Physiology, and Molecular Biology*, Blackwell Publishing Ltd, **2007**, pp. 285.
- [45] U. Deppenmeier, *Progress in Nucleic Acid Research and Molecular Biology, Vol 71* **2002**, 71, 223.
- [46] P. Baumann, S. A. Qureshi, S. P. Jackson, *Trends Genet.* **1995**, 11, 279.
- [47] R. K. Thauer, A.-K. Kaster, H. Seedorf, W. Buckel, R. Hedderich, *Nat Rev Micro* **2008**, 6, 579.
- [48] K. Sauer, R. K. Thauer, *Eur. J. Biochem.* **1999**, 261, 674.
- [49] R. K. Thauer, *Microbiology-Sgm* **1998**, 144, 2377.
- [50] P. Butler, B. Kräutler, *Top. Organomet. Chem.* **2006**, 17, 1.
- [51] K. Gruber, B. Puffer, B. Krautler, *Chem. Soc. Rev.* **2011**, 40.
- [52] Y. T. Fanchiang, G. T. Bratt, H. P. C. Hogenkamp, *Proc. Natl. Acad. Sci.* **1984**, 81, 2698.
- [53] J. J. Pignatello, Y.-T. Fanchiang, *J. Chem. Soc., Dalton Trans.* **1985**.

- [54] S. Gencic, G. M. LeClerc, N. Gorlatova, K. Peariso, J. E. Penner-Hahn, D. A. Grahame, *Biochemistry (Mosc.)* **2001**, *40*, 13068.
- [55] K. Nakamura, Y. Hisaeda, L. Pan, H. Yamauchi, *J. Organomet. Chem.* **2009**, *694*, 916.
- [56] P. J. Craig, F. Glockling, *The biological alkylation of heavy elements*, Royal Society Of Chemistry, London, **1988**.
- [57] G. N. Schrauzer, J. W. Sibert, R. J. Windgassen, *J. Am. Chem. Soc.* **1968**, *90*, 6681.
- [58] G. N. Schrauzer, J. A. Seck, R. J. Holland, T. M. Beckham, E. M. Rubin, J. W. Sibert, *Bioinorg. Chem.* **1973**, *2*, 93.
- [59] R. A. Zakharyan, H. V. Aposhian, *Toxicol. Appl. Pharmacol.* **1999**, *154*, 287.
- [60] G. N. Schrauzer, *Angew. Chem. Int. Edit* **1976**, *15*, 417.
- [61] T. M. Kenyhercz, H. B. Mark, *J. Electrochem. Soc.* **1976**, *123*, 1656.
- [62] G. H. Beaven, E. A. Johnson, *Nature* **1955**, *176*, 1264.
- [63] D. Lexa, J. M. Saveant, *Acc. Chem. Res.* **1983**, *16*, 235.
- [64] J. U. Kreft, B. Schink, *Eur. J. Biochem.* **1994**, *226*, 945.
- [65] A. Fischli, *Helv. Chim. Acta* **1978**, *61*, 2560.
- [66] Y. Chen, X. P. Zhang, *J. Org. Chem.* **2004**, *69*, 2431.
- [67] S. K. Ghosh, P. N. Balasubramanian, G. C. Pillai, E. S. Gould, *Inorg. Chem.* **1991**, *30*, 487.
- [68] J. Shey, C. M. McGinley, K. M. McCauley, A. S. Dearth, B. T. Young, W. A. van der Donk, *J. Org. Chem.* **2002**, *67*, 837.
- [69] R. L. Birke, Q. Huang, T. Spataru, D. K. Gosser, *J. Am. Chem. Soc.* **2006**, *128*, 1922.
- [70] R. H. Yamada, S. Shimizu, S. Fukui, *Biochim. Biophys. Acta* **1966**, *124*, 195.
- [71] D. Dolphin, A. W. Johnson, R. Rodrigo, *J. Chem. Soc.* **1964**.
- [72] J. Feldmann, *J. Anal. At. Spectrom.* **1997**, *12*.
- [73] A. R. Kumar, P. Riyazuddin, *Anal. Sci.* **2005**, *21*, 1401.

- 
- [74] F. Laborda, E. Bolea, M. T. Baranguan, J. R. Castillo, *Spectrochim. Acta B* **2002**, 57, 797.
- [75] L. M. Del Razo, M. Styblo, W. R. Cullen, D. J. Thomas, *Toxicol. Appl. Pharmacol.* **2001**, 174, 282.
- [76] V. Devesa, L. M. Del Razo, B. Adair, Z. Drobna, S. B. Waters, M. F. Hughes, M. Styblo, D. J. Thomas, *J. Anal. At. Spectrom.* **2004**, 19, 1460.
- [77] A. G. Howard, *J. Anal. At. Spectrom.* **1997**, 12, 267.
- [78] M. Elsner, *J. Environ. Monit.* **2010**, 12, 2005.
- [79] L. Melander, W. H. Saunders, *Reaction rates of isotopic molecules*, John Wiley, New York, **1980**.
- [80] H. Craig, *Geochim. Cosmochim. Acta* **1957**, 12, 133.
- [81] D. E. Matthews, J. M. Hayes, *Anal. Chem.* **1978**, 50, 1465.
- [82] A. L. Sessions, *J. Sep. Sci.* **2006**, 29, 1946.
- [83] D. E. Matthews, J. M. Hayes, *Anal. Chem.* **1978**, 50, 1465.
- [84] W. A. Brand, in *Handbook of Stable Isotope Analytical Techniques* (Ed.: A. d. G. Pier), Elsevier, Amsterdam, **2004**.
- [85] W. Meier-Augenstein, *J. Chromatogr. A* **1999**, 842, 351.

## **Chapter 2. Investigation on the role of biological “reducing agents” for the methylation of metal(loid)s by methylcobalamin**

*\*Partly redrafted from “Frank Thomas, Roland A. Diaz-Bone, Oliver Wuerfel, Britta Huber, Katrin Weidenbach, Ruth A. Schmitz, Reinhard Hensel, Connection between multi-metal(loid) methylation in methanoarchaea and central intermediates of methanogenesis, Appl. Environ. Microbiol. 2011, 77(24), 8669-75”*

### **2.1. ABSTRACT**

Though the methylation of metal(loid)s has a significant impact on the toxicity as well as the bioavailability of metals and metalloids in the environment, the process is not fully understood. However, microorganisms in anaerobic habitats play an important role in this methylation process in the environment. Methanoarchaea, for instance, are capable of methylating a large number of different elements. A methylation pathway, which is different from the known element-specific methyltransferase systems, is responsible for the multi-element methylation observed.

We demonstrate that the same metal(loid)s (arsenic, selenium, antimony, tellurium, and bismuth) that are methylated and hydrogenated by the methanoarchaeum *Methanosarcina mazei in vivo* as well as by purified recombinant methyltransferase MtaA, are methylated in the presence of electrochemically produced cob(I)alamin (Cob(I)). Cob(I), which is also formed by MtaA-catalyzed demethylation of CH<sub>3</sub>Cob in the course of methylotrophic methanogenesis, is identified as the causative agent inducing the methyl transfer from CH<sub>3</sub>Cob to the metal(loid)s. This indicates that biological electron carriers are important factors for the multi-metal(loid) methylation capability of methanoarchaea.

To confirm this assumption, the efficiency of abiotic methylation of As, Bi, Sb, Se and Te by CH<sub>3</sub>Cob was studied in the presence of electrochemically produced Cob(I), glutathione (GSH), CoM, and titanium citrate (TiCit) in comparison to photolytic methylation. As all of the investigated biological “reducing agents” induce the methylation of metal(loid)s, different biological reducing agents apparently contribute to the multi-element methylation *in vivo* in dependency of their availability.

## 2.2. INTRODUCTION

In the environment, especially in anaerobic habitats, the methylation and hydride generation of metal(loid)s like arsenic, selenium, tellurium, antimony and bismuth are common and important processes. These transformation processes have a significant impact on the bioavailability as well as the toxicity of metals and metalloids by enhancing the lipophilicity<sup>[1]</sup> and thus the membrane permeability. However, the underlying formation processes are not completely elucidated. Various reaction mechanisms have been proposed for the methylation of heavy elements by the main methyl group donors in biotic systems, methylcobalamin ( $\text{CH}_3\text{Cob}$ )<sup>[2-4]</sup> and S-adenosyl methionine (SAM).<sup>[3, 5-6]</sup> Beside the methyl group donor, these depend strongly on the reaction conditions and the reacting metal(loid).

Both abiotic as well as enzyme-catalyzed methylation can occur, but sulfate reducing bacteria and methane producing microorganisms, called methanoarchaea, are mainly involved in the formation process of organometal(loid) compounds in anaerobic habitats. Methanoarchaea, which are found in e.g. fresh-water sediments, hydrothermal vents, rice paddies, sewage sludge digestors, landfills, the rumen, and the intestinal tract of some mammals<sup>[7]</sup> are shown to be capable of methylating multiple elements resulting in formation of volatile as well as non-volatile methylated compounds<sup>[8]</sup>. This process seems to be coupled to the methanogenesis, their central energy metabolism.

The term "methanogenesis" refers to the biogenic and anaerobic formation of methane for energy generation by methanogenic microorganisms. The carbon which is reduced to methane is derived from either from methanol, acetate, methylated amines, or carbon dioxide. The aforementioned substrates are converted to methane in a series of reactions catalyzed by different enzymes. An enzyme system composed of three polypeptides, MtaA, MtaB and MtaC, has been identified for the utilization of methanol in *Methanosarcina bakeri*.<sup>[9]</sup> The methyl group of methanol is transferred by the methyltransferase MtaB to the corrinoid-binding protein MtaC, forming  $\text{CH}_3\text{-MtaC}$ . Next, the methyltransferase MtaA catalyzes the transfer to coenzyme M (CoM, 2-mercaptoethane sulfonate) yielding methylated CoM and regenerating MtaC. It has been shown in *in vitro* experiments that the corrinoid-binding protein MtaC can be substituted with free cob(I)alamin (Cob(I)).<sup>[9]</sup> Finally,

methane is formed by a methyl-coenzyme M reductase with the cofactor F430 and coenzyme B.<sup>[10]</sup>

An arsenic element specific methyltransferase ArsM has been identified in *Rhodospseudomonas palustris*.<sup>[11]</sup> Though, homologue genes have been identified in other organisms including methanoarchaea, this does not explain the multi-element methylation capability observed in the environment. The question arises if there are various element-specific methyltransferases, or whether an alternative way of methylation without involvement of element-specific enzymes exists.

“Bioreducing agents” are usually involved in abiotic and enzyme-catalyzed methylation processes: Cob(I) has been considered to play a catalytic role for metal(loid) methylation by Schrauzer<sup>[4]</sup> and it is also involved in the methanogenesis as mentioned before. The bioreduction equivalent CoM is also involved in the methanogenesis as already mentioned. Glutathione (GSH) which is present in many cells at millimolar concentrations<sup>[12]</sup>, has been shown to be an important factor for methylation of arsenic by S-adenosyl methione (SAM).<sup>[3, 5, 13]</sup> Various studies even showed the abiotic methylation of arsenic<sup>[2, 4, 14-16]</sup> by methylcobalamin induced by GSH. Furthermore, for antimony Feldmann *et al.* demonstrated the abiotic methylation in the presence of GSH involving selenite.<sup>[17]</sup> Additionally, Schrauzer showed the formation of dimethylselenium from CH<sub>3</sub>Cob and selenite in the presence of a thiol (dithioerythritol (DTE)).<sup>[4]</sup>

In this Chapter, the role of biological “reducing agents” for the multi-metal(loid) methylation including As, Se, Sb, Te, and Bi of methanoarchaea was reinvestigated by the use of UV/Vis spectroscopy as well as purge and trap gas chromatography-inductively coupled plasma mass spectrometry (P&T-GC-ICP-MS). Therefore, Cob(I), formed enzymatically or electrochemically, CoM and GSH, at different *pH* values, were investigated regarding the methylation of the aforementioned elements.

Additionally, titanium citrate (TiCit) was applied for mechanistic investigation of the reaction, as it is a one electron donor and is used as a redox buffer in anaerobic systems and cultures.<sup>[18]</sup> In comparison, photocatalytic methylation of arsenic was conducted.

### 2.3. EXPERIMENTAL SECTION

For all experiments deionized water (Seralpur Pro 90 CN system, Elga Berkefeld GmbH, Celle, Germany) has been used. In the case of anaerobic experiments the

water has been freed from oxygen by bubbling with nitrogen for at least 20 min with a flow rate  $>500 \text{ mL min}^{-1}$ . The chemicals had analytical grade or better.

### 2.3.1. Electrochemical preparation of Cob(I).

Cob(I) was formed by electrochemical reduction of aquocob(III)alamin as reported previously<sup>[19]</sup>. A total of 250 mg of aquocob(III)alamin (Sigma-Aldrich, St. Louis, MO) solved in 20 mL of oxygen-free 50 mM phosphate buffer at *pH* 7.2 was reduced in a magnetically stirred standard three-compartment electrochemical cell with a gold foil working electrode and platinum counter electrode in an anaerobic glove box ( $\text{H}_2/\text{N}_2$ , 2%/98%). Output voltage was set to 3.0 V (Model 4005, Voltcraft; Conrad Electronics, Hirschau, Germany). The final concentration of Cob(I) was determined via UV/Vis spectroscopy (Specord 200, Analytic Jena, Jena, Germany).

### 2.3.2. Investigations on the role of Cob(I)

The cultivation of *M. mazei* with methanol and purification of recombinant MtaA (MM\_1070) by Frank Thomas has been described elsewhere.<sup>[20]</sup>

For the investigation on the role of Cob(I) MtaA at a concentration of  $10 \mu\text{g mL}^{-1}$  was added to assay mixtures containing  $0.1 \mu\text{M}$  arsenite,  $0.1 \text{ mM}$   $\text{CH}_3\text{Cob}$  (Sigma-Aldrich, St. Louis, MO) and either  $0.05 \text{ mM}$  CoM or  $0.14 \text{ mM}$  CoM ( $\text{HSCH}_2\text{CH}_2\text{SO}_3\text{Na}$ , Sigma-Aldrich, St. Louis, MO). The reaction was allowed to proceed until no further demethylation of  $\text{CH}_3\text{Cob}$  was observed by UV/Vis spectrometry. Afterwards, assays were analyzed by P&T-GC-ICP-MS.

Furthermore, assays containing  $0.1 \text{ mM}$  electrochemical produced Cob(I) only, or  $0.05 \text{ mM}$  and  $0.05 \text{ mM}$   $\text{CH}_3\text{Cob}$  were analyzed as above.

All reactions were conducted under strict anaerobic conditions in  $50 \text{ mM}$  HEPES ( $\text{C}_{16}\text{H}_{35}\text{N}_4\text{NaO}_8\text{S}_2$ , AppliChem GmbH, Gatersleben, Germany) at *pH* 7 at  $30^\circ\text{C}$  in septum sealed UV/Vis cuvettes. Total volumes were adjusted to  $1 \text{ mL}$ . UV/Vis spectra were measured in 1-min intervals for 10 min. Afterwards, the cuvettes were wrapped with alumina foil under dim red light and the headspace was analyzed by purge and trap gas chromatography inductively coupled plasma mass spectrometry (P&T-GC-ICP-MS) as described below.

For the analysis of the volatile species pattern,  $1 \text{ mM}$   $\text{CH}_3\text{Cob}$  and  $1 \text{ mM}$  CoM in  $50 \text{ mM}$  HEPES *pH* 7 were incubated with  $10 \mu\text{g mL}^{-1}$  purified recombinant MtaA in the presence of  $0.1 \mu\text{M}$  As ( $\text{AsNaO}_2$ , Fluka, Buchs, Switzerland),  $10 \mu\text{M}$  Se ( $\text{H}_2\text{SeO}_3$ ),

0.1  $\mu\text{M}$  Sb ( $\text{SbCl}_3$ ), 10  $\mu\text{M}$  Te ( $\text{Na}_2\text{TeO}_3$ ) and 0.1  $\mu\text{M}$  Bi ( $\text{C}_3\text{H}_5\text{O}(\text{COO})_3\text{Bi}$ ), all Sigma-Aldrich, St. Louis, MO) at 30 °C for 10 min prior to headspace analyses.

For comparison, 5 mL of 0.5 mM  $\text{CH}_3\text{Cob}$  in 50 mM phosphate-buffer *pH* 7 were incubated with 0.25 mM electrochemically produced Cob(I) and either 0.25 mM As, Sb, Bi, Se or Te at 37 °C for 30 min prior to headspace analyses by P&T-GC-ICP-MS. Septum sealed 20 mL vials wrapped with alumina foil were used.

### 2.3.3. Headspace P&T-GC-ICP-MS analysis

For ICP-MS analysis a modified semi-automated purge and trap system was used that has been coupled to an ELAN 6000 (PerkinElmer, Rodgau, Germany) ICP-MS system as described elsewhere.<sup>[21]</sup> The vials/cuvettes were tempered at 37°C using a water bath. The reaction solution and headspace of the reaction vials were purged with a constant helium flow ( $200 \text{ mL min}^{-1}$ ) for 10 min and the efflux trapped on a packed column cooled by liquid nitrogen. For the investigation of the methylation capability of reducing agents static headspace analysis was conducted. Aliquots of 100  $\mu\text{L}$  of the headspace were analyzed. For gaschromatographic separation a helium 5.0 flow rate of  $88 \text{ mL min}^{-1}$  (Air Liquide, Düsseldorf, Germany) was used. After removal of the liquid nitrogen filled dewar the trap was warmed by the ambient air for 150 s to room temperature and subsequently heated with a linear ramp to 180°C within 570 s. The GC efflux was introduced into ICP-MS *via* a T-piece between the plasma torch and the nebulizer. For quantification, an internal standard solution ( $10 \mu\text{g L}^{-1}$  Li, Ga, Y, Rb, Rh, Ce, Tl,  $100 \mu\text{g L}^{-1}$  In, in 1% subboiled  $\text{HNO}_3$  (v/v), 5% propanol (both Merck, Darmstadt, Germany) was added continuously. Propanol was added to provide a constant carbon background and thus to minimize the effect of carbon eluting from the column on the plasma conditions. Argon of 4.6 quality (Air Liquide, Düsseldorf, Germany) was used for ICP-MS.

### 2.3.4. Investigation of the methylation capability and efficiency of different “bio-reducing agents”

The capability and efficiency of GSH, to methylate the metal(loid)s arsenic, antimony, selenium, tellurium, and bismuth was investigated. Therefore, 0.25 mM of the different elements and 0.5 mM  $\text{CH}_3\text{Cob}$  were incubated in the presence of 2.5 mM or 25 mM GSH for 24 h and 7 days in 50 mM phosphate buffer at *pH* 7 at 37°C. The reaction mixtures had a total volume of 5 mL and were prepared under strict

anaerobic conditions in septum sealed 20 mL vials wrapped with alumina foil under dim red light.

Exemplarily for arsenic, GSH was replaced by CoM or titanium citrate (prepared from  $\text{TiCl}_3$  (all Sigma-Aldrich, St. Louis, US) and sodium citrate (Applichem, Gatersleben, Germany) according to Zehnder *et al.*)<sup>[18]</sup> at concentrations of 2.5 mM or 25 mM. Additionally, the *pH* and temperature dependency of the methylation of arsenic by methylcobalamin in presence of 2.5 mM and 25 mM GSH was investigated by adjusting the assay to a *pH* of 2, 7, and 12 before incubation and increasing temperature to 86°C, respectively.

Furthermore, the photomethylation of arsenic by methylcobalamin was investigated by irradiation of a mixture containing 0.25 mM arsenite and 0.5 mM  $\text{CH}_3\text{Cob}$  in 50 mM phosphate buffer at *pH* 7 by UV-light (100W, 366 nm, 20 cm distance) for 6 and 15 h, respectively.

The formation of volatile and non-volatile species was investigated by headspace P&T-GC-ICP-MS and hydride generation (HG) followed by P&T-GC-ICP-MS as described below. The methylation yield for the single arsenic species has been calculated as the ratio of the amount *A* of specific species *X* to the total amount of all arsenicals measured by ICP-MS according to the following equation.

$$\text{methylation yield (X)} = \frac{A_X}{A_{\text{AsH}_3} + A_{\text{CH}_3\text{AsH}_2} + A_{(\text{CH}_3)_2\text{AsH}} + A_{(\text{CH}_3)_3\text{As}}}$$

X:  $\text{CH}_3\text{AsH}_2$ ,  $(\text{CH}_3)_2\text{AsH}$ ,  $(\text{CH}_3)_3\text{As}$

### 2.3.5. Hydride generation P&T-GC-ICP-MS method

For the analysis of non-volatile metal(loid) species HG-P&T-GC-ICP-MS was applied. The assays were diluted 1:10 with water and 50  $\mu\text{L}$  aliquots were subsequently analyzed by applying a slightly modified single *pH*-gradient hydride generation technique which overcomes the problem of different *pH* optima for HG of metal(loid) species as described elsewhere.<sup>[22]</sup> In brief, the sample was added to 40 mL citric acid buffer at *pH* 7. Then, 10 mL of 1 M  $\text{NaBH}_4$  and 2 M HCl were added within 7 min while purging the solution with a flow rate of 200  $\text{mL min}^{-1}$  helium and cryfocussing the volatile analytes on a packed chromatography column. For an additional minute

the solution was purged to ensure complete removal of analytes volatilized by hydride generation.

The same semi-automated purge and trap system, GC separation parameters, sample introduction, quantification technique, and ICP-MS as mentioned above have been used.

## 2.4. RESULTS AND DISCUSSION

### 2.4.1. The role of cob(I)alamin for the multi-metal(loid) methylation

Thomas *et al.* showed that the CH<sub>3</sub>Cob dependent methyltransferase MtaA of *M.mazei* is involved in multi-metal(loid) methylation of the elements As, Se, Sb, Te, and Bi. The authors found a 100-10.000-fold increased volatilization efficiency of tested metal(loid) upon amending the purified methyltransferase MtaA to methylation assays containing one of the metal(loid)s, CoM and CH<sub>3</sub>Cob. Column A in Figure 2-1 shows the species pattern produced by enzyme mediated reaction which was obtained by P&T-GC-ICP-MS analysis.

Furthermore, the analysis of transcriptome in the presence of bismuth indicated that multi-metal(loid) methylation by *M.mazei* is not attributed to element-specific methyltransferases, but seems to be coupled to methanogenesis.<sup>[20]</sup> MtaA catalyzes the transfer of the methyl group from CH<sub>3</sub>Cob to CoM via formation of a complex by coordination of the thiol group of CoM to the active-site zinc followed by nucleophilic attack of CH<sub>3</sub>Cob yielding methylated CoM and reduced Cob(I).<sup>[23-24]</sup>

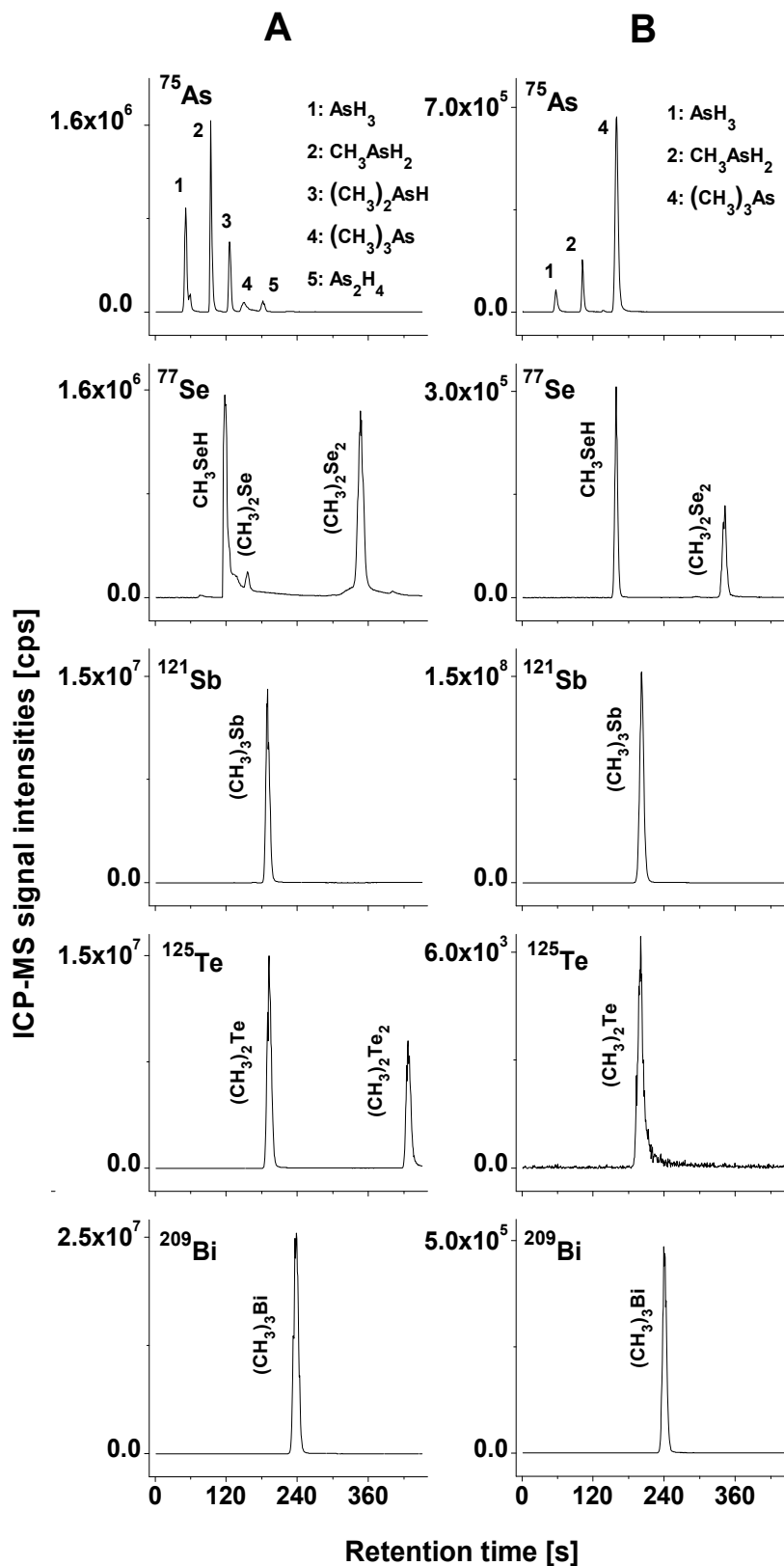


**Figure 2-1.** Comparison of volatile arsenic species patterns produced by methylation assays containing purified MtaA of *M. mazei* (A)<sup>[20]</sup> and electrochemically produced Cob(I) (B) obtained by P&T-GC-ICP-MS analysis.

As Schrauzer *et al.* proposed a contribution of Cob(I) for the methylation of metal(loid)s,<sup>[4]</sup> we reinvestigated this process. Our first step was the formation of Cob(I) by the MtaA catalyzed demethylation of CH<sub>3</sub>Cob in the presence of CoM. As CoM is a limiting reactant, we varied the CoM concentration to achieve a partial conversion by adding CoM at the of the CH<sub>3</sub>Cob concentration (Figure 2-2A), or a nearly quantitative conversion of CH<sub>3</sub>Cob by amending an excess of CoM over CH<sub>3</sub>Cob (Figure 2-2B).

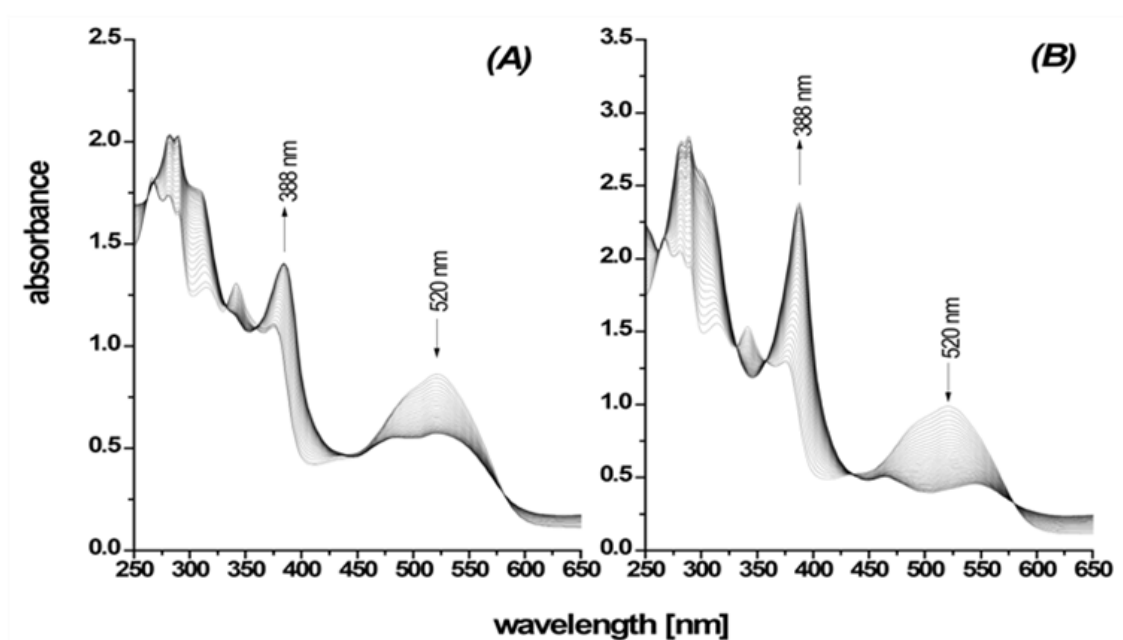


**Figure 2-2.** Formation of Cob(I) due to MtaA catalyzed demethylation of CH<sub>3</sub>Cob in presence of CoM observed by UV/Vis spectrometry. A spectrum of partial (A) and nearly quantitative conversion (B) due to a variation of CoM concentration is shown. Spectra were measured in 1 min intervals for 40 min. The characteristic wavelengths of CH<sub>3</sub>Cob (520 nm) and Cob(I) (388 nm) are indicated.

Upon the addition of arsenite Cob(I) was oxidized to Cob(II) as monitored by UV/Vis spectroscopy as an decrease at 388 nm as well as increases at a wavelength of 312 nm and 476 nm (Figure 2-3, A and B). The assay with partial conversion showed the formation of hydrogenated as well as methylated arsenicals (Figure 2-3, IIA).

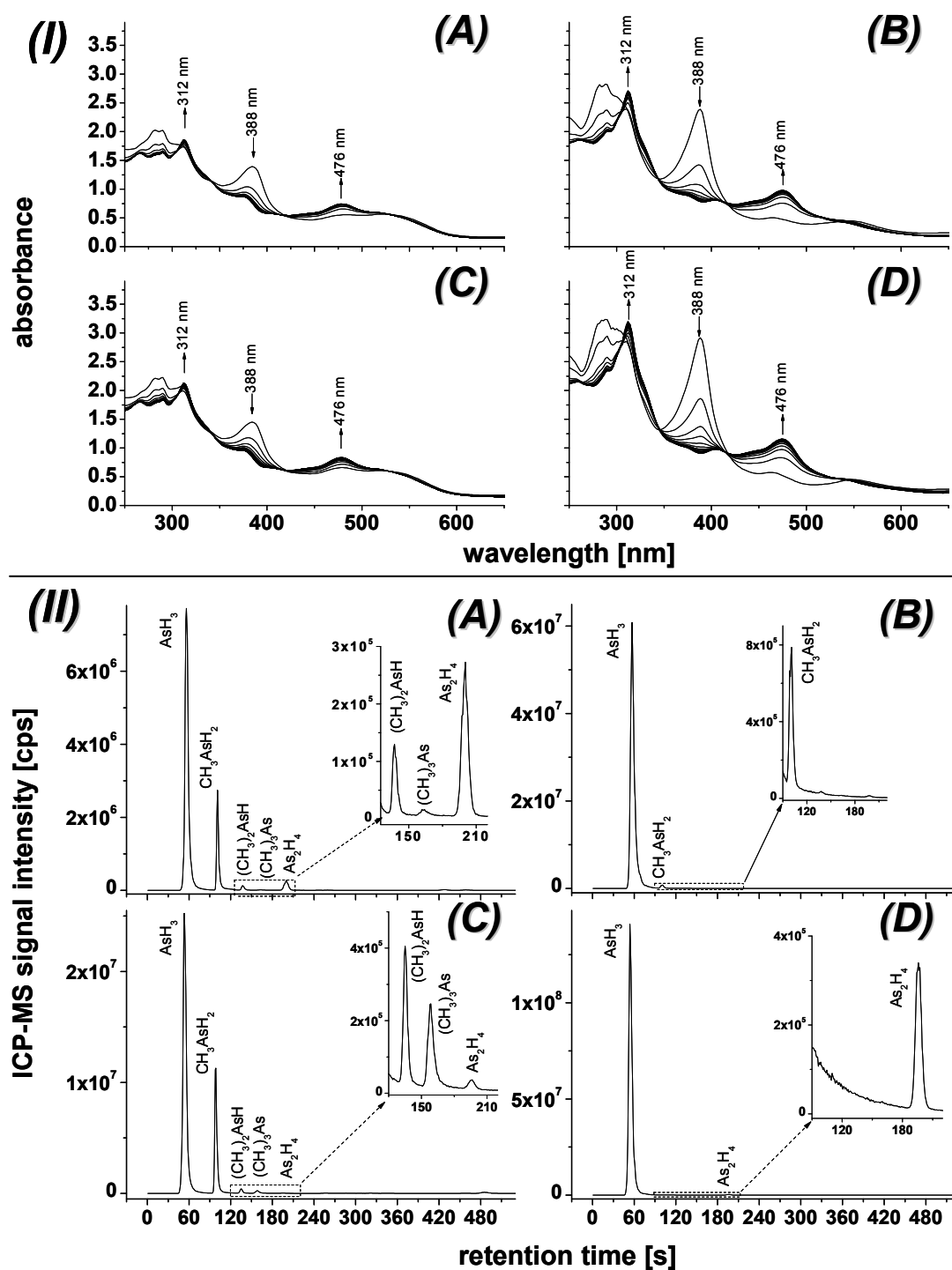


**Figure 2-3.** Reactions of arsenite with equal amounts of  $\text{CH}_3\text{Cob}$  and  $\text{Cob(I)}$  produced by MtaA-catalyzed transfer from  $\text{CH}_3\text{Cob}$  to  $\text{CoM}$  (A), excess of  $\text{Cob(I)}$  produced by MtaA-catalyzed transfer from  $\text{CH}_3\text{Cob}$  to  $\text{CoM}$  (B); equal amounts of electrochemically produced  $\text{Cob(I)}$  and  $\text{CH}_3\text{Cob}$  (C), and electrochemically produced  $\text{Cob(I)}$  only (D). Assays were analyzed by UV/VIS (I) and P&T-GC-ICP-MS (II). The characteristic wavelengths of  $\text{Cob(I)}$  (388 nm) and  $\text{Cob(II)}$  (312, 478 nm) are indicated in (I).

The assay with complete conversion of  $\text{CH}_3\text{Cob}$  to  $\text{Cob(I)}$  produced mainly arsine ( $\text{AsH}_3$ ) with only traces of MMA (Figure 2-3, IIB). This is an indication that on the one hand  $\text{Cob(I)}$  is required for the methylation of arsenite by  $\text{CH}_3\text{Cob}$  and on the other hand  $\text{Cob(I)}$  has the capability of hydride generation. Furthermore,  $\text{CH}_3\text{CoM}$  as an intermediate is not the donor of the methyl group, but  $\text{CH}_3\text{Cob}$ , as no  $\text{CoM}$  is needed in the case of arsenic methylation in presence of  $\text{CH}_3\text{Cob}$  and electrochemically produced  $\text{Cob(I)}$ .

Following these experiments, the enzyme and  $\text{CoM}$  were replaced with electrochemically produced  $\text{Cob(I)}$ . Methylation assays containing  $\text{Cob(I)}$  and  $\text{CH}_3\text{Cob}$  with a ratio of 1:1 and  $\text{Cob(I)}$  alone showed again a fast oxidation of  $\text{Cob(I)}$  to  $\text{Cob(II)}$  after addition of arsenite (Figure 2-3, IC and D, respectively). In absence of  $\text{CH}_3\text{Cob}$  methylation assays produced only  $\text{AsH}_3$  (Figure 2-3, IID), while in the presence of stoichiometric amounts of  $\text{CH}_3\text{Cob}$  methylated arsenic species were formed beside  $\text{AsH}_3$  (Figure 2-3, IIC). These results show that enzymatic reactions are not necessarily needed for arsenic methylation by  $\text{CH}_3\text{Cob}$  and  $\text{Cob(I)}$  as well as hydride generation by  $\text{Cob(I)}$ . Furthermore,  $\text{CoM}$  is not required for the methylation and hydride generation of arsenite.

In addition, the capability of electrochemically generated  $\text{Cob(I)}$  to methylate or hydrogenate the group 15 and 16 elements antimony, selenium, tellurium, and bismuth was investigated. For this purpose, methylation assays containing the elements, methylcobalamin and electrochemically produced  $\text{Cob(I)}$  were analyzed by GC-ICP-MS. The produced species patterns are very similar to those found for the enzymatic assays (Figure 2-1, column B). Only  $(\text{CH}_3)_2\text{Te}_2$  as well as  $(\text{CH}_3)_2\text{AsH}$  were not formed for an unknown reason. Nevertheless, the high analogy indicates that the capability for methylation and hydride generation of multiple elements in *M.mazei* is not attributed to different enzymes catalyzing the methyl transfer, but is rather a side reaction of methanogenesis induced by  $\text{Cob(I)}$ . The assumption is supported by the transcriptome analysis by Frank Thomas *et al.* as already mentioned.<sup>[20]</sup> We observed a dependency of the species pattern on the  $\text{CH}_3\text{Cob}$  to  $\text{Cob(I)}$  ratio. This might explain why no hydride generation of metal(loid)s was found *in vivo* <sup>[8]</sup>, as the local concentration of  $\text{Cob(I)}$  is limited in the cell due to fast remethylation to  $\text{CH}_3\text{Cob}$ .<sup>[9]</sup>

### 2.4.2. Abiotic methylation of As, Sb, Se, Te, and Bi by CH<sub>3</sub>Cob in presence of GSH

As Cob(I) is apparently essential for the multi-element methylation capability of methanoarchaea, other “bio-reducing agents” might also have the ability to induce a methyl transfer from CH<sub>3</sub>Cob to metal(loid)s.

First, experiments with GSH were conducted, as it is present in living cells at millimolar concentrations<sup>[12]</sup> and its contribution to abiotic methylation of arsenic,<sup>[2, 4, 14-16]</sup> and antimony<sup>[17]</sup> has been shown before. Therefore, assays containing CH<sub>3</sub>Cob, GSH and one of the metal(loid)s were incubated for 48 h at 37°C and subsequently analyzed using P&T-GC-ICP-MS (Table 2-1).

**Table 2-1.** Quantitative data of the abiotic multi-element methylation by CH<sub>3</sub>Cob in presence of GSH. P&T-GC-ICP-MS or HG-P&T-GC-ICP-MS was conducted as indicated. In the case of P&T-GC-ICP-MS, the concentration μM refers to the total volume of the liquid phase (5 mL), while in for HG μM refers to a total headspace volume of 15 mL. The recovery of arsenic and antimony exceeding 100% is probably caused by impreciseness of the pipet and the error of quantification method for ICP-MS.<sup>[25]</sup>

metal(loid) added (μM)	type of analysis	metal(loid) species detected (μM)
As (250)	P&T-GC-ICP-MS	n.d.
	HG-P&T-GC-ICP-MS	AsH <sub>3</sub> (294.8±17.2)    CH <sub>3</sub> AsH <sub>2</sub> (89.7±2.9)    (CH <sub>3</sub> ) <sub>2</sub> AsH <sub>2</sub> (4.9±0.3)
Sb (250)	P&T-GC-ICP-MS	n.d.
	HG-P&T-GC-ICP-MS	SbH <sub>3</sub> (170.8±24.9)    CH <sub>3</sub> SbH <sub>2</sub> (130.2±1.1)    (CH <sub>3</sub> ) <sub>2</sub> SbH <sub>2</sub> (2.3±0.9)
Se (250)	P&T-GC-ICP-MS	(CH <sub>3</sub> ) <sub>2</sub> Se (0.4±0.1)    (CH <sub>3</sub> ) <sub>2</sub> Se <sub>2</sub> (*)
Te (250)	P&T-GC-ICP-MS	(CH <sub>3</sub> ) <sub>2</sub> Te (3.8±1.4)
Bi (250)	P&T-GC-ICP-MS	(CH <sub>3</sub> ) <sub>3</sub> Bi (0.01±0.005)

n.d: not detected

\*: <limit of quantification

For selenium, tellurium, and bismuth volatile methylated species were found in the sample headspace. However, in the case of bismuth only very little amounts of trimethylbismuth were detected.

In contrast, no volatile species were detected for arsenic and antimony. Thus, we analyzed the liquid phase of these assays with HG-GC-ICP-MS.

Highest total methylation yield (39%) was found for antimony. In agreement with Feldmann *et al.*<sup>[17]</sup> we found  $(\text{CH}_3\text{SbH}_2)$  and  $(\text{CH}_3)_2\text{SbH}$  after hydride generation as methylated species in the assays containing antimony, but the methylation yield of about 2% in their study was significantly lower, probably due to a shorter incubation time of 30 min.

For arsenic assays, we found  $\text{CH}_3\text{AsH}_2$  as main methylation product and minor amounts of  $(\text{CH}_3)_2\text{AsH}$ . The total methylation yield for arsenic was 24.4% which is in good agreement with the reports of Nakamura *et al.* who found 17.2%  $\text{CH}_3\text{AsH}_2$  and 2.8%  $(\text{CH}_3)_2\text{AsH}$  with similar concentrations in the methylation assay, but aerobic conditions.<sup>[2]</sup>

#### 2.4.3. Investigation of the methylation of As by $\text{CH}_3\text{Cob}$ in presence of GSH under various reaction conditions

Since arsenic is a prominent and toxicologically relevant contaminant, we decided to focus on arsenic, exemplarily for the group 15 and 16 metal(loid)s and investigated the influence of *pH*, concentration of GSH, temperature and incubation time on the efficiency of abiotic methylation of As by  $\text{CH}_3\text{Cob}$  in presence of GSH.

As stated by Hall *et al.* before, the abiotic methylation of arsenic by  $\text{CH}_3\text{Cob}$  in the presence of GSH depends on the *pH*.<sup>[15]</sup> Thus, this issue was reinvestigated. Additionally, the range of *pH* was extended, as assays with a *pH* of 2, 7, and 12 (Figure 2-4) were analyzed. While a total methylation yield of 8.2% for a *pH* of 12 was observed, the yield increased with a factor of 3 to 24.4% for *pH* 7. A further decrease of *pH* to 2 yielded nearly the same methylation yield for  $\text{CH}_3\text{AsH}_2$  but triples the amount of  $(\text{CH}_3)_2\text{AsH}$ . The reason for the increased efficiency due to a decrease of the *pH* is probably caused by a protonation of the benzimidazole moiety in  $\text{CH}_3\text{Cob}$  producing the “base off” conformation of the corrinoid. This conformation may be more prone to demethylation due to a change of the redox potential to a more positive value in comparison to the “base on” conformation, where the benzimidazole moiety is coordinated to cobalt, as suggested by Nakamura *et al.*<sup>[2]</sup> Furthermore, the stability of arsenic glutathione complexes, assumed to be formed before methylation<sup>[2-3, 14]</sup> increases with decreasing *pH*.<sup>[26]</sup> A larger amount of the dimethylated arsenicals are probably formed at acidic *pH* due to the fact that the monomethylarsenic-diglutathione complex  $(\text{CH}_3\text{As}(\text{GS})_2)$  is even less stable than the arsenic triglutathione  $(\text{As}(\text{GS})_3)$  complex at a higher *pH*. Furthermore, with increasing

methylation yield of course more monomethylated arsenic is present in the reaction vessel which can be methylated a second time.

Afterwards, we decided to prolong the incubation times from 48 h to 196 h. We observed a significant increase of the total methylation yield for assays adjusted to *pH* 2 and 12 indicating a slow reaction speed as the reaction is not complete after 48 h. In contrast, for a *pH* 7 no further increase of the methylation yield was observed for 196 h which is in agreement to the kinetic data of previous studies which showed the reaction to be almost finished after 6 h, albeit they have used different molar ratios of the reactant, or  $\text{CH}_3\text{B}_{12}$  ester instead of  $\text{CH}_3\text{Cob}$ , respectively, and aerobic conditions,<sup>[2, 16]</sup>

Next, we varied the concentration of GSH, as it was shown that the concentration of the “bioreducing agent” also influences the yield of methylation.<sup>[16]</sup> According to the Nernst equation the higher concentration of the reducing agent lowers the effective redox potential. As expected, one-tenth of the thiol yielded only about one-tenth of the methylated arsenicals. Furthermore, we increased the incubation temperature from 37°C to 86°C. The higher temperature obviously increases the reaction speed indicating a kinetically controlled reaction.

Overall, we could prove that the methylation yield of As by  $\text{CH}_3\text{Cob}$  in presence of GSH depends on the *pH*, concentration of GSH, the reaction time, as well as the reaction temperature.

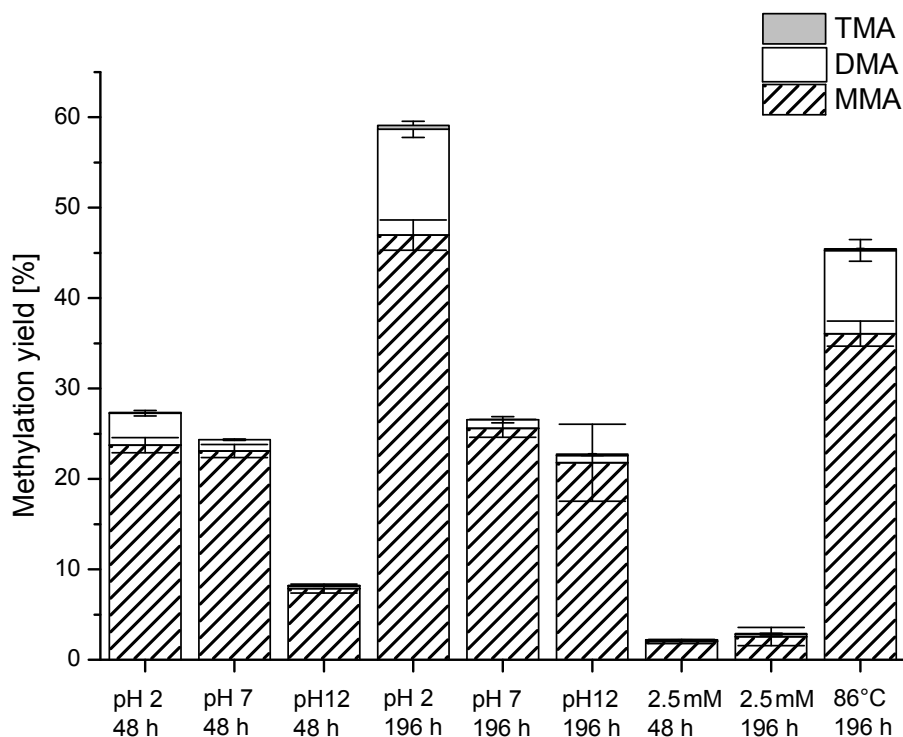


**Figure 2-4.** Dependency of abiotic methylation of arsenic by methylcobalamin in presence of GSH on *pH*, reaction time, concentration as well as on the temperature. Assays have been analyzed by HG-P&T-GC-ICP-MS. If not indicated otherwise, a GSH concentration of 25 mM and an incubation temperature of 37°C, and *pH* 7 were used. MMA:  $\text{CH}_3\text{AsH}_2$ ; DMA:  $(\text{CH}_3)_2\text{AsH}_2$ ; TMA:  $(\text{CH}_3)_3\text{As}$

#### 2.4.4. Investigation of the methylation of As by $\text{CH}_3\text{Cob}$ in the presence of CoM, TiCit, and Cob(I), or under irradiation with UV-light

The methylation yield of CoM and TiCit, both replacing GSH in the methylation assays, as well as photomethylation, was investigated (Figure 2-5).

CoM is known as methyl-group acceptor in methanogenesis. However, in sufficient concentrations CoM is capable to induce the methyl transfer from  $\text{CH}_3\text{Cob}$  to arsenic: The observed reaction yield (12.9%) was significantly lower than that of GSH (24.4%) at the same reaction conditions, namely a concentration of 25 mM, a reaction time of 48 h, and at a *pH* of 7.

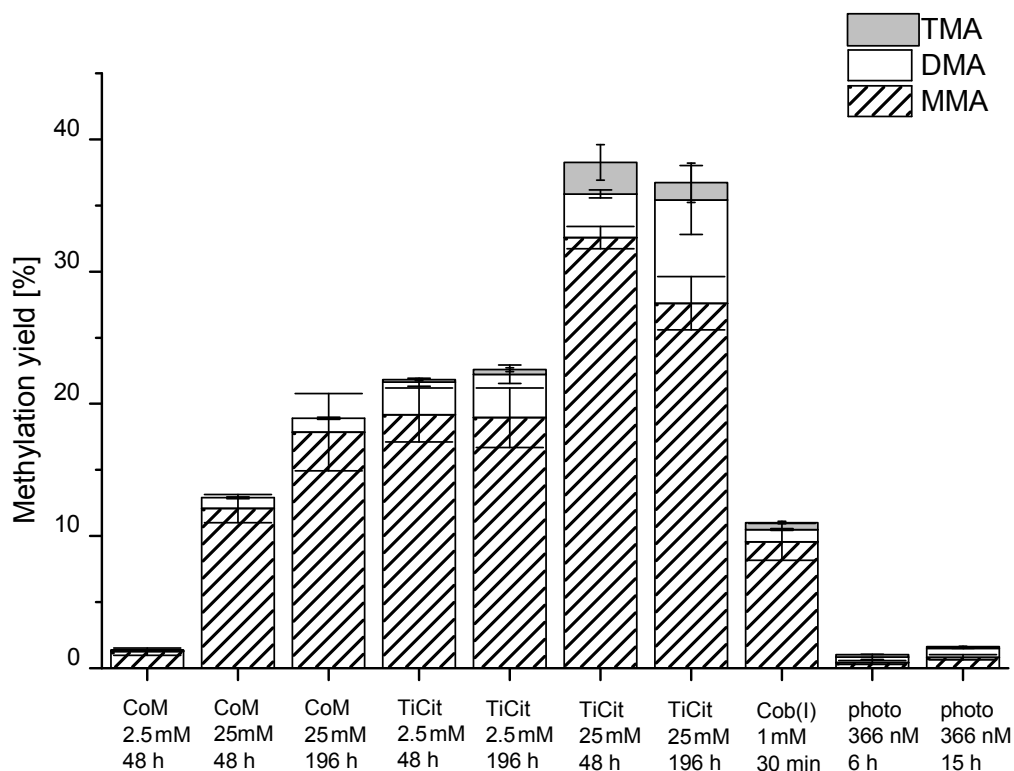


**Figure 2-5.** Comparison of methylation efficiency of arsenic by  $\text{CH}_3\text{Cob}$  in presence of CoM, TiCit, and Cob(I), as well of photomethylation. Concentration and incubation time was varied as indicated. Assays have been analyzed by HG-P&T-GC-ICP-MS. Thus, the methylation yield for Cob(I) regards HS as well as HG. MMA:  $\text{CH}_3\text{AsH}_2$ ; DMA:  $(\text{CH}_3)_2\text{AsH}_2$ ; TMA:  $(\text{CH}_3)_3\text{As}$

Methylation assays with electrochemically produced Cob(I) showed 11% total methylation efficiency at a concentration of 1 mM. A reaction time of 30 min was chosen, because of our previous UV/Vis experiment indicating the high reactivity of Cob(I). In the UV/Vis experiments the analyzed reactions were finished after 10 min even with a lower Cob(I) concentration (0.25 mM). As Cob(I) has the most negative standard potential ( $E_0' = -610 \text{ mV}$ )<sup>[19]</sup> of all the reducing agents we investigated, it was not surprising that Cob(I) is the only one which was capable of producing even low yields of hydrogenated volatile species.

TiCit with a concentration of 2.5 mM showed nearly the same methylation yield as GSH at 25 mM. At 25 mM a very high methylation rate of more than 36% was detected. The reaction is already completed after 48 h as no further increase of the methylation yield at a reaction time of 196 h was found. In contrast to the other

reducing agents significant amounts of trimethylarsine oxide were formed, indicating maybe a different type of reaction mechanism. On the one hand an oxidative methylation and on the other hand fast oxidation of trimethyl arsine is feasible. TiCit is a very strong reducing agent with a highly negative standard potential ( $E_0' = -480$  mV)<sup>[18]</sup> and it is capable of reducing Cob(II) to Cob(I).<sup>[27]</sup> However, the underlying reaction mechanism for the methyl transfer induced by TiCit does not seem to involve this step or at least the local concentration of possibly formed Cob(I) is too low, as no volatile compounds were formed in contrast to assays containing Cob(I) (see above). Overall, all investigated “bioreducing agents” were capable to induce the transfer of the methyl group from  $\text{CH}_3\text{Cob}$  to arsenite at the used concentrations and reaction times, but the species patterns and methylation yields strongly varied. Except for Cob(I), no volatile species were detected in previous P&T-GC-ICP-MS analyses. A very high methylation capability near the physiological  $pH$ , regarding the lowest concentration tested (1 mM), was observed for Cob(I). The highest methylation yield was detected for assays containing 25 mM TiCit, however, exceeding the tested Cob(I) concentration 250-fold. The next highest yield was observed for the assays containing 25 mM GSH ( $E_0' = -240$  mV)<sup>[28]</sup> which were incubated for 196 h. The assays containing CoM, which possesses the most positive redox potential ( $E_0' = -193$  mV)<sup>[29]</sup>, showed the lowest methylation yields out of the used reducing agents. As expected there seems to be a connection between the observed methylation and the redox potential (Cob(I)>TiCit>GSH>CoM). Furthermore, a dependency of concentration of the “reducing agents” is observable.

At last, a photolytically induced methylation of arsenic by methylcobalamin was carried out for comparison. The reaction yield was about 0.8% with a radiation time of 6 h at a wavelength of 366 nm. Equal amounts of  $\text{CH}_3\text{AsH}_2$  and  $(\text{CH}_3)_2\text{AsH}_2$  were found using HG-P&T-ICP-MS. At an increased reaction time of 16 h 1.5% arsenicals (0.8%  $\text{CH}_3\text{AsH}_2$ , 0.7%  $(\text{CH}_3)_2\text{AsH}_2$ ) were produced. Despite a larger methylation yield at a longer reaction time might be observed, the methylation yield is rather low in comparison to the used bioreducing agents except CoM at 2.5 mM. The reason is that also methane and ethane are produced after homolytic cleavage of the cobalt arsenic bond of  $\text{CH}_3\text{Cob}$ .<sup>[30]</sup> Furthermore, a photodegradation of the formed methylated arsenicals by UV-light is possible.<sup>[31]</sup>

## 2.5. CONCLUSION

Cob(I)alamin which is produced by enzyme-catalyzed demethylation of  $\text{CH}_3\text{Cob}$  was shown to be the causative agent during the methylation of arsenic by  $\text{CH}_3\text{Cob}$  in the presence of CoM. Thus, Cob(I) seems to be responsible for the multi-element methylation capability of methanoarchaea and not element specific methyltransferases. This shows the importance of biological reduction agents for methylation processes.

Beside arsenic and antimony the abiotic methylation of selenium, tellurium, and bismuth by  $\text{CH}_3\text{Cob}$  in the presence of GSH was shown. Our studies with CoM, and TiCit showed that these reducing agents are also capable of forming methylated species. The methylation efficiency of the different “bioreducing” agents depends on the reaction conditions, including the concentration, reaction time, *pH*, and especially on the standard potential of the “reducing agent”.

Other biological electron carriers like F420, F430, reduced flavin adenine dinucleotide ( $\text{FADH}_2$ ), reduced nicotinamide adenine dinucleotide (NADH), and ferredoxin could also be capable of methylating metal(loid)s and should be investigated as it seems to be likely that different biological “reducing agents” contribute to the methylation of metal(loid)s *in vivo*.

## 2.6. REFERENCES

- [1] J. S. Thayer, *Abstr. Pap. Am. Chem. S.* **1988**, 195, 79.
- [2] K. Nakamura, Y. Hisaeda, L. Pan, H. Yamauchi, *J. Organomet. Chem.* **2009**, 694, 916.
- [3] T. Hayakawa, Y. Kobayashi, X. Cui, S. Hirano, *Arch. Toxicol.* **2005**, 79, 183.
- [4] G. N. Schrauzer, J. A. Seck, R. J. Holland, T. M. Beckham, E. M. Rubin, J. W. Sibert, *Bioinorg. Chem.* **1973**, 2, 93.
- [5] F. Challenger, *Chem. Rev.* **1945**, 36, 315.
- [6] J. S. Thayer, *Appl. Organomet. Chem.* **2002**, 16, 677.
- [7] J. G. Ferry, *Crit. Rev. Biochem. Mol. Biol.* **1992**, 27, 473.
- [8] J. Meyer, K. Michalke, T. Kouril, R. Hensel, *Syst. Appl. Microbiol.* **2008**, 31, 81.
- [9] K. Sauer, R. K. Thauer, *Eur. J. Biochem.* **1999**, 261, 674.
- [10] R. K. Thauer, *Microbiology-Sgm* **1998**, 144, 2377.
- [11] J. Qin, B. P. Rosen, Y. Zhang, G. J. Wang, S. Franke, C. Rensing, *Proc. Natl. Acad. Sci. U. S. A.* **2006**, 103, 2075.
- [12] A. Meister, *J. Biol. Chem.* **1988**, 263, 17205.
- [13] R. Bentley, T. G. Chasteen, *Microbiol. Mol. Biol. Rev.* **2002**, 66, 250.
- [14] R. A. Zakharyan, H. V. Aposhian, *Toxicol. Appl. Pharmacol.* **1999**, 154, 287.
- [15] M. N. Hall, X. Liu, V. Slavkovich, V. Ilievski, Z. Mi, S. Alam, P. Factor-Litvak, H. Ahsan, J. H. Graziano, M. V. Gamble, *Environ. Health Perspect.* **2009**, 117.
- [16] S. A. Pergantis, M. Miguens-Rodriguez, N. P. Vela, D. T. Heitkemper, *J. Anal. At. Spectrom.* **2004**, 19.
- [17] S. Wehmeier, A. Raab, J. Feldmann, *Appl. Organomet. Chem.* **2004**, 18, 631.
- [18] A. J. B. Zehnder, K. Wuhrmann, *Science* **1976**, 194, 1165.
- [19] J. U. Kreft, B. Schink, *Eur. J. Biochem.* **1994**, 226, 945.
- [20] F. Thomas, R. A. Diaz-Bone, O. Wuerfel, B. Huber, K. Weidenbach, R. A. Schmitz, R. Hensel, *Appl. Environ. Microbiol.* **2011**, 77, 8669.
- [21] O. Wuerfel, R. A. Diaz-Bone, M. Stephan, M. A. Jochmann, *Anal. Chem.* **2009**, 81, 4312.
- [22] R. A. Diaz-Bone, M. Hitzke, *J. Anal. At. Spectrom.* **2008**, 23, 861.
- [23] M. Krüer, M. Haumann, W. Meyer-Klaucke, R. K. Thauer, H. Dau, *Eur. J. Biochem.* **2002**, 269, 2117.

- 
- [24] S. Gencic, G. M. LeClerc, N. Gorlatova, K. Peariso, J. E. Penner-Hahn, D. A. Grahame, *Biochemistry (Mosc.)* **2001**, *40*, 13068.
- [25] J. Feldmann, *J. Anal. At. Spectrom.* **1997**, *12*, 1069.
- [26] A. Raab, A. A. Meharg, M. Jaspars, D. R. Genney, J. Feldmann, *J. Anal. At. Spectrom.* **2004**, *19*, 183.
- [27] T. A. Lewis, M. J. Morra, P. D. Brown, *Environ. Sci. Technol.* **1996**, *30*, 292.
- [28] J. Rost, S. Rapoport, *Nature* **1964**, *201*, 185.
- [29] D. B. Kell, J. G. Morris, *FEBS Lett.* **1979**, *108*, 481.
- [30] G. N. Schrauzer, J. W. Sibert, R. J. Windgassen, *J. Am. Chem. Soc.* **1968**, *90*, 6681.
- [31] C. I. Brockbank, G. E. Batley, G. K. C. Low, *Environmental Technology Letters* **1988**, *9*, 1361.

**Chapter 3. Investigation of the mechanism of multi-metal(loid) methylation and hydride generation by methylcobalamin and cob(I)alamin**

*\*Reproduced from “Oliver Wuerfel, Frank Thomas, Marcel Schulte, Reinhard Hensel, Roland A. Diaz-Bone, Mechanism of multi-metal(loid) methylation and hydride generation by methylcobalamin and Cob(I)alamin – A side reaction of methanogenesis, Appl. Organomet. Chem., 2012, 26, 94-101”*

**3.1. ABSTRACT**

Metal(loid)s are subject to many transformation processes, such as oxidation, reduction, methylation and hydride, predominantly accomplished by prokaryotes. Since these widespread processes affect the bioavailability and toxicity of metal(loid)s to a large extent, the investigation of their formation is of high relevance. Methanoarchaea are capable of methylating and hydrogenating Group 15 and 16 metal(loid)s arsenic, selenium, antimony, tellurium, and bismuth due to side reactions between central methanogenic cofactors, methylcobalamin (CH<sub>3</sub>Cob(III)) and Cob(I)alamin (Cob(I)). Here, we present systematic mechanistic studies on methylation and hydride generation of Group 15 and 16 metal(loid)s by CH<sub>3</sub>Cob(III) and Cob(I). Pentavalent arsenical species showed neither methylation nor reduction as determined by using a newly developed oxidation state specific hydride generation technique, which allows direct determination of tri- and pentavalent arsenic species in a single batch. In contrast, efficient methylation of trivalent species without a change in oxidation state indicated that the methyl transfer does not proceed *via* a Challenger-like oxidative methylation, but *via* a non-oxidative methylation. Our findings also point towards a similar mechanism for antimony, bismuth, selenium, and tellurium. Overall, we suggest that the transfer of a methyl group does not involve a free reactive species, such as a radical, but instead is transferred either in a concerted nucleophilic substitution or in a caged radical mechanism. For hydride generation, we propose the intermediate formation of hydridocobalamin, transferring a hydride ion to the metal(loid)s.

### 3.2. INTRODUCTION

Transformations such as methylation, hydride generation, oxidation, and reduction of metal(loid)s including Ge, As, Se, Cd, In, Sn, Sb, Te, Hg, Tl, Pb, Bi, and Po are a relevant and widespread phenomenon in the environment which is dominated by prokaryotes.<sup>[1]</sup> Due to these processes, the physical and chemical properties of the metal(loid)s are significantly changed resulting in modulated mobility and toxicity. In the case of arsenic for example, which is an important contaminant in large parts of the world, the chemical form of the metal(loid)s, their solubility and oxidation state play an important role.<sup>[2]</sup> The trivalent arsenicals are in general considered as more toxic than pentavalent ones<sup>[3]</sup>. Initially, the biomethylation of arsenic has been characterized as a detoxification process due to the less toxic pentavalent methylated arsenicals,<sup>[4]</sup> but the metabolites monomethylarsinous acid (MMAs<sup>III</sup>) and dimethylarsinous acid (DMAs<sup>III</sup>) are even more potent toxics than arsenite (As<sup>III</sup>).<sup>[2, 5]</sup> Thus, a differentiation of both the oxidation state and the degree of methylation of metal(loid)s in environmental samples is important in order to understand the underlying formation processes and to improve risk assessments.

Several methylation pathways have already been proposed for the methylation of single elements.<sup>[6-11]</sup> In the case of selenium, the methylation is catalyzed by enzymes participating in sulfur amino and selenoamino acid metabolism in numerous pro- and eucaryotic organisms with S-adenosyl methionine (SAM) as the methyl donor. A mechanism involving selenium hydride as an intermediate prior to methylation has been suggested.<sup>[11-12]</sup> For the methylation of arsenic, the arsenite methyltransferase ArsM has been identified which catalyzes the transfer of a methyl group from SAM to trivalent arsenic species.<sup>[13]</sup> Two important methylation mechanisms are discussed for this transfer reaction. On the one hand, the stepwise reduction by glutathione (GSH) of the pentavalent arsenicals followed by an oxidative methylation by the transfer of a carbocation was initially postulated by Frederick Challenger (Figure 3-1: reaction pathway  $R_{+V,0}$ ,  $OM_0$ ,  $R_{+V,1}$ ,  $OM_1$ ,  $R_{+V,2}$ ,  $OM_2$ ),<sup>[6, 11]</sup>. On the other hand, Hayakawa *et al.* suggested a transfer of a methyl group with no formal change of the oxidation state of the methyl group accepting metal(loid) (Figure 3-1: reaction pathway  $Me_{+III,0}$ ,  $Me_{+III,1}$ ,  $Me_{+III,2}$ ).<sup>[7]</sup>

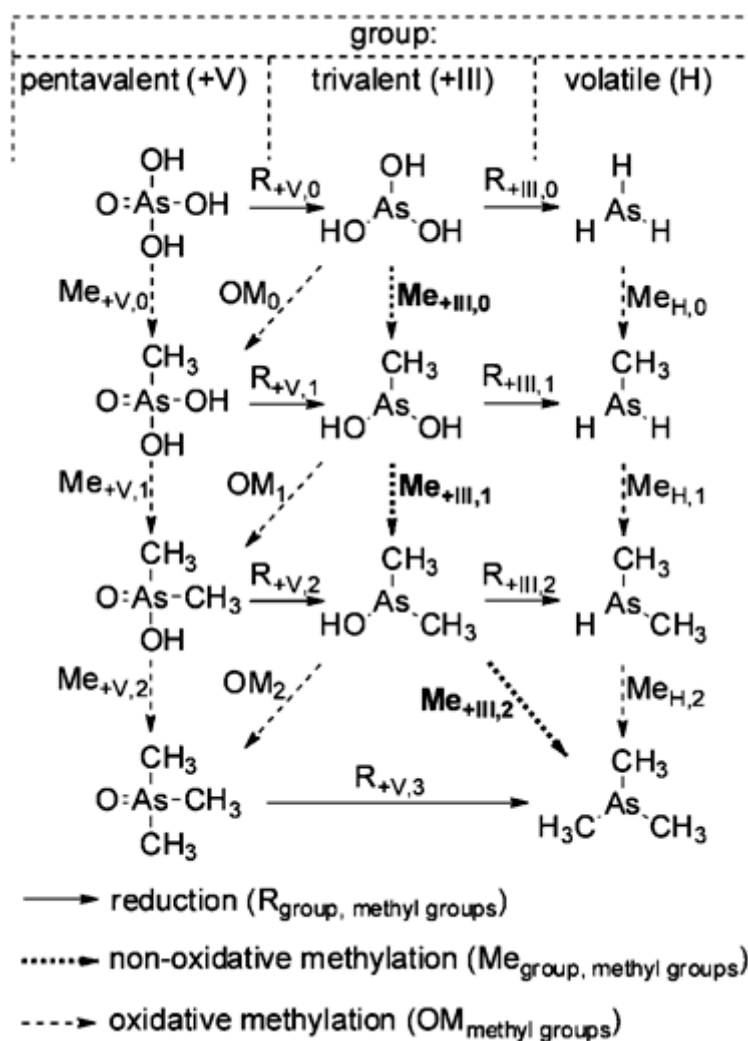


**Figure 3-1.** Overview on possible methylation and reduction pathways. Mechanism proposed for the reaction of arsenite with  $\text{CH}_3\text{Cob(III)}$  and  $\text{Cob(I)}$  is indicated in **bold**.

In contrast to SAM, methylcobalamin ( $\text{CH}_3\text{Cob(III)}$ ) is a more versatile methyl donor for which the transfer of a carbanion, carbocation or methyl radical has been described in dependence of the methyl acceptor and the reaction conditions.<sup>[9]</sup> A transfer as carbanion is described for mercury, lead, and palladium.<sup>[8]</sup> In addition, different mechanisms for radical methyl transfer to heavy elements have been proposed.<sup>[14]</sup> The methyl-cobalt bonding of  $\text{CH}_3\text{Cob(III)}$  can be cleaved homolytically either by photo- or thermolysis<sup>[15]</sup>. The metal(loid) can thereupon function as a radical trap as reported for arsenic.<sup>[8]</sup> Moreover, radical abstraction has been proposed in the case of tin and a free radical formation due to a one-electron transfer has been described for hexachloroiridate.<sup>[14]</sup>

Methanoarchaea, which are found in anaerobic habitats including fresh-water sediments, hydrothermal vents, rice paddies, sewage digestors, landfills, the rumen, and the intestinal tract,<sup>[16]</sup> are capable of producing a broad spectrum of methylated and hydrogenated metal(loid)s.<sup>[17]</sup> This capability is attributed to two central cofactors of methanogenesis, CH<sub>3</sub>Cob(III) and the highly reduced Cob(I)alamin (Cob(I)).<sup>[18]</sup> Cob(I) is a strong reducing agent (standard reduction potential  $E_0 = -610$  mV)<sup>[19]</sup> and can induce the methyl transfer from CH<sub>3</sub>Cob(III) to metal(loid)s.<sup>[18]</sup>

In this work, we carried out mechanistic studies on methylation and hydride generation of Group 15 and 16 metal(loids) As, Sb, Bi, Se, and Te by CH<sub>3</sub>Cob(III) and Cob(I), either produced by enzymatically catalyzed demethylation of CH<sub>3</sub>Cob(III) in presence of 2-mercaptoethanesulfonic acid (CoM) or by electrochemical reduction of aquocobalamin (Cob(III)). The mechanism of this multi-element methylation and hydride generation process has not been elucidated so far. For investigation of redox reactions during methylation, a new oxidation state specific hydride generation technique for non-volatile methylated arsenic species was developed based on pH-dependence of the reaction with sodium borohydride (NaBH<sub>4</sub>).<sup>[20]</sup>

### 3.3. EXPERIMENTAL SECTION

For all experiments, deionized water (Seralpur Pro 90 CN system, Elga Berkefeld GmbH, Celle, Germany) freed from oxygen by purging with nitrogen or helium was used. For strict anaerobic conditions, reaction solutions were assembled in glass vials (10 mL) in an anaerobic glove box (H<sub>2</sub>/N<sub>2</sub> (2%/98%)). The vials were sealed air-tight using silicon-septa prior to handling outside of the anaerobic glove box. All solutions containing CH<sub>3</sub>Cob(III) were handled under dim red light.

#### 3.3.1. *In vitro* protein assays.

*In vitro* assays (1 mL) contained 10 µg mL<sup>-1</sup> recombinant purified protein MtaA (purification has been described elsewhere<sup>[18]</sup>), 1 mM CH<sub>3</sub>Cob(III), CoM (both Sigma-Aldrich, St. Louis, MO), and either 9.3 µM As<sup>III</sup> (AsNaO<sub>2</sub>, Fluka, Buchs, Switzerland), 57.6 µM MMAs<sup>V</sup> (CH<sub>3</sub>AsO(ONa)<sub>2</sub>), 0.9 µM MMAs<sup>III</sup> (CH<sub>3</sub>AsI<sub>2</sub>, both Argus Chemicals, Vernio, Italy) or 1.6 µM DMAs<sup>V</sup> ((CH<sub>3</sub>)<sub>2</sub>AsO(OH), Strem Chemicals, Kehl, Germany) in 50 mM HEPES pH 7 (Applichem, Darmstadt, Germany).

### 3.3.2. Oxidation state specific HG/P&T/GC-ICP-MS procedure.

For oxidation state specific hydride generation (HG), subsequent purge and trap (P&T) enrichment, and gas chromatography, a self-developed semi-automated system was used that has been described elsewhere.<sup>[21]</sup> The introduction of a second trap (Figure 3-2) allowed a new oxidation state specific hydride generation technique, which is a two-step method using the pH-dependence of the formation of volatile hydrides.

Aliquots of the *in vitro* protein assays (50  $\mu$ L) were dissolved in 20 mL of 25 mM TRIS-HCl buffer (Carl Roth GmbH, Karlsruhe, Germany) adjusted to *pH* 8 and purged for 150 s with a helium flow rate of about 230 mL min<sup>-1</sup> for minimization of oxygen. In a first derivatization step, only trivalent arsenic species are derivatized at *pH* 8 by adding 2 mL of 1 M NaBH<sub>4</sub>, stabilized with 0.1 M sodium hydroxide (Carl Roth GmbH, Karlsruhe, Germany), within 300 s. Volatile species were cryo-focused on a packed column using a dewar with liquid nitrogen. To ensure gas-liquid separation of hydride-species the solution was purged for additional 120 s.

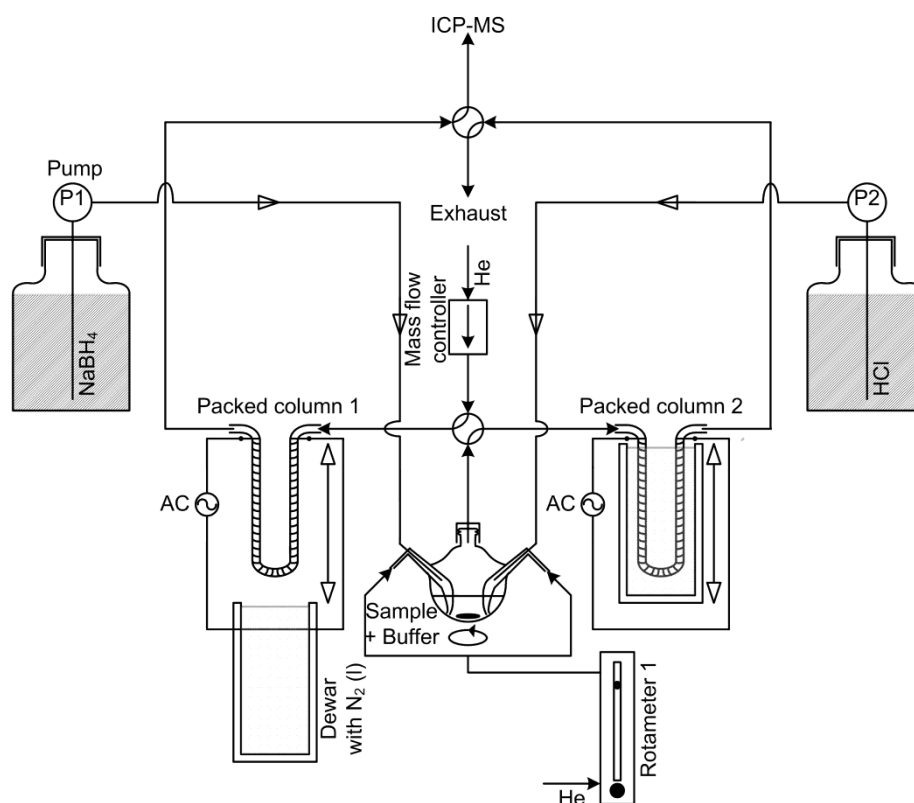


**Figure 3-2.** Schematic view of oxidation state specific HG/P&T/GC-ICP-MS system.

Afterwards, both valves were switched and the GC run for trivalent species was started by removing the dewar. The column was warmed by ambient air for 150 s to 20°C and then heated to 150°C within 450 s using a linear ramp. This temperature was held for 110 s. A flow rate of 65 mL min<sup>-1</sup> He was used for the transfer of the analytes to an Agilent 7500a ICP-MS (Agilent Technologies, Yokogama, Japan) equipped with a microflow nebulizer and a Scott spray chamber. The GC efflux was introduced using an intermediary T-piece between the plasma torch and the nebulizer. For quantification, an internal standard solution (10 µg L<sup>-1</sup> Li, Ga, Y, Rb, Rh, Ce, Tl, 100 µg L<sup>-1</sup> In, in 1% subboiled HNO<sub>3</sub> (v/v), 5% propanol (both Merck, Darmstadt, Germany) was added continuously. Propanol was added to minimize the effect of carbon eluting from the column on the plasma conditions. Helium of 5.0 quality and Argon of 4.6 quality (both Air Liquide, Düsseldorf, Germany) were used for GC and ICP-MS, respectively.

During the GC run, the second trap was cooled with liquid nitrogen and the pentavalent species were derivatized by adding 8 mL of 1 M NaBH<sub>4</sub> and 10 mL of 1 M HCl within 300 s (trace analysis grade, Fisher Scientific, Schwerte, Germany), lowering *pH* below 1 (for a detailed *pH*-course, refer to the electronic supplement, Figure S1). Volatilized arsenicals were trapped on the second column and measured subsequently with the same settings as above.

For method validation, the same arsenic standards as above were applied. Additionally TMA<sub>3</sub>AsO ((CH<sub>3</sub>)<sub>3</sub>AsO), which was synthesized by oxidation of trimethylarsine (Strem Chemicals, Kehl, Germany) with hydrogen peroxide in diethyl ether,<sup>[22]</sup> and As<sup>V</sup> (Na<sub>2</sub>HAsO<sub>4</sub>·7 H<sub>2</sub>O, Fluka, Buchs, Switzerland) were used.

### 3.3.3. P&T/GC-ICP-MS procedure

For headspace measurements, a simplified hand-actuated setup with only one GC column was used. Solutions were purged through for 10 min with a flow rate of about 230 mL min<sup>-1</sup> He controlled by a rotameter (AALBORG, Orangeburg, New York). Volatile analytes were cryo-focussed using liquid nitrogen on a U-shaped packed column made of glass (i.d., 4 mm; length, 40 cm; stationary phase, 1.15 g of 10% SP-2100 on 80/100 mesh Supelcoport (Sigma-Aldrich, St. Louis, MO) kept in position using silanized glass wool (Sigma–Aldrich, Taufkirchen, Germany)). For active heating, the column was wrapped with a 2.1 m resistance wire (3.9 Ω/m; Block, Verden, Germany) connected to a power supply (model 4005, Voltcraft, Conrad

Electronics, Hirschau, Germany). Transfer lines were made of 1/16" fluorinated ethylene. Two 4-port valves coated with PTFE (Hamilton, Bonaduz, Switzerland) were used.

For GC analysis, the two valves were switched and the dewar with liquid nitrogen was removed allowing the column to heat by ambient air for 150 s. Then, the power supply was set to 3 A for 570 s, heating the column to 180 °C. The GC flow rate was set to 65 mL min<sup>-1</sup>, controlled by a mass flow controller (Bronkhorst, Schenkon, The Netherlands). For measurement of the *in vitro* assays, the same introduction and quantification techniques and ICP-MS as above were used.

For all other experiments, an ELAN 6000 ICP-MS (Perkin Elmer, Rodgau, Germany) equipped with a Ryton nebulizer (GemTip Cross-Flow II; PerkinElmer, Rodgau, Germany) and Scott spray chamber (PerkinElmer, Rodgau, Germany) was used. Here, the propanol concentration of internal standard was 1% (v/v) and a GC flow rate of 86 mL min<sup>-1</sup> was adjusted.

For further experimental description, see the figure descriptions in the electronic supplement.

### 3.4. UV/VIS EXPERIMENTS

For UV/Vis measurements, septum-sealed quartz cuvettes heated to 30 °C (Hellma Analytics, Müllheim, Germany) in a Specord 200 spectrometer (Analytik Jena, Jena, Germany) were used. Cob(I) was produced electrochemically from aquocobalamin (Sigma-Aldrich, St. Louis, MO) as described elsewhere.<sup>[18]</sup> The concentration of the B<sub>12</sub>-derivative was 50 µM each in 2 mL of 50 mM phosphate-buffer at a *pH* of 7. The metal(loid) species added - MeSe<sup>IV</sup> (CH<sub>3</sub>SeO(OH)), Sb<sup>III</sup> (SbCl<sub>3</sub>), Sb<sup>V</sup> (K[Sb(OH)<sub>6</sub>]), Se<sup>IV</sup> (H<sub>2</sub>SeO<sub>3</sub>), Se<sup>VI</sup> (H<sub>2</sub>SeO<sub>4</sub>), Te<sup>IV</sup> (Na<sub>2</sub>TeO<sub>3</sub>), Te<sup>VI</sup> (H<sub>6</sub>TeO<sub>6</sub>), and Bi<sup>III</sup> (C<sub>3</sub>H<sub>5</sub>O(COO)<sub>3</sub>Bi) - were obtained from Sigma-Aldrich (St. Louis, MO) and had a final concentration of 1 mM each. The reaction time was 15 min under strict anaerobic conditions.

In order to exclude a methylation pathway involving hydride species for As and Sb, either 30 ng of arsine or stibine, produced by HG of arsenite As<sup>III</sup> and Sb<sup>III</sup> using NaBH<sub>4</sub> in glass vials, were injected through a 2 mL solution of 0.1 mM CH<sub>3</sub>Cob(III) in 50 mM phosphate-buffer *pH* 7 and incubated for 15 min.

For the spin trapping experiment, a solution of 0.1 mM CH<sub>3</sub>Cob(III) and 5 mM  $\alpha$ -(4-Pyridyl N-oxide)-N-tert-butyl nitron (Sigma-Aldrich, St. Louis, MO) was incubated in 50 mM phosphate-buffer at *pH* 7.

### 3.5. RESULTS AND DISCUSSION

#### 3.5.1. Development and validation of pH-specific hydride generation derivatization for redox-specific speciation of methylated arsenic species

For the investigation of redox reactions during methylation, a new oxidation state specific hydride generation technique for non-volatile methylated arsenic species was developed based on the pH-dependency of the reaction with NaBH<sub>4</sub>.<sup>[20]</sup> In previous techniques, two subsamples are derivatized either at two different *pH* values<sup>[23-24]</sup> or with and without a preliminary reduction step.<sup>[25]</sup> The analytes evolving from the different derivatization conditions are measured separately by gas chromatographic analysis, yielding on the one hand the concentration of trivalent arsenic species as well as pentavalent TMA<sub>5</sub>O and on the other hand the sum of tri- and pentavalent arsenic species. The concentration of pentavalent species is then determined from the difference of these two measurements. As the determination of the pentavalent species by subtraction results in an increase of measurement uncertainty due to error propagation, in particular at low relative concentrations of pentavalent species, we chose to conduct the two derivatization steps subsequently in a single batch. Following derivatization of trivalent arsenic species and TMA<sub>5</sub>O by NaBH<sub>4</sub> at *pH* 8 using TRIS-HCl buffer, the *pH* was continuously lowered to 1 (see Figure 3-3) in order to derivatize pentavalent species in accordance to a previous study by Diaz-Bone *et al.*<sup>[26]</sup> The species volatilized under the different reaction conditions were measured separately, thereby allowing the direct analysis of trivalent resp. pentavalent species. By use of two parallel columns, derivatization and GC-ICP-MS analysis of the two reaction conditions can be conducted simultaneously in order to save analysis time. To improve handling and reproducibility, the system was fully automated with exception of the change of reaction vessels and removal of dewars, allowing the computer-controlled addition of reagents, purging, valve switching, as well as column heating.

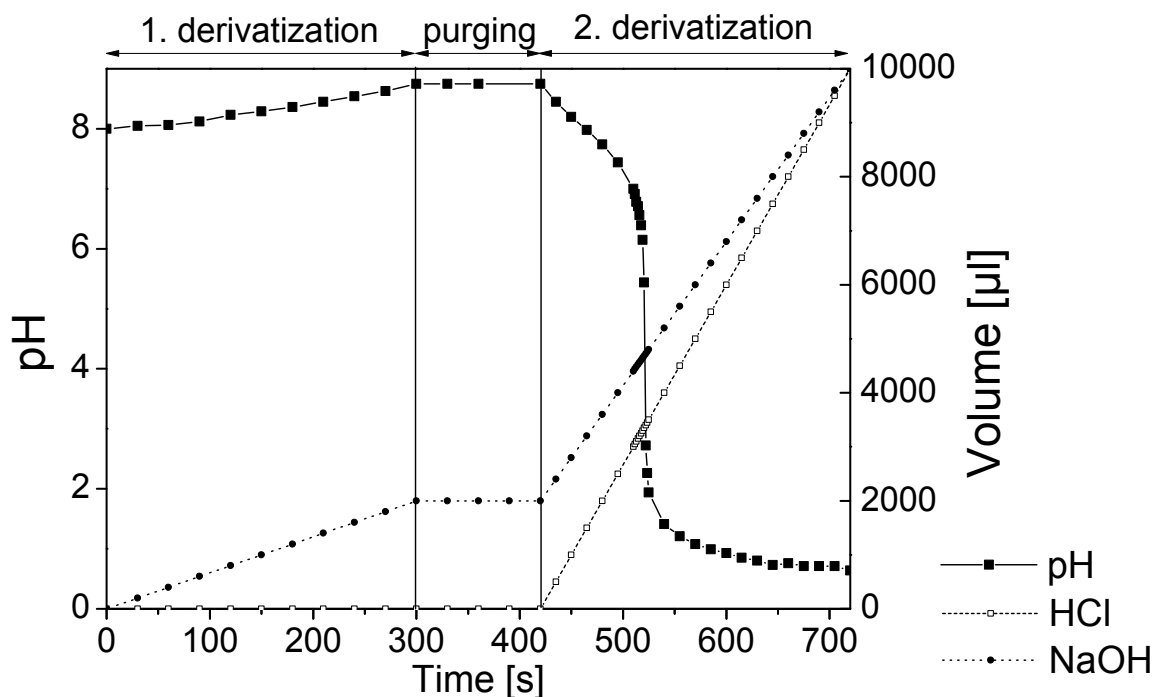


**Figure 3-3.** Simulated pH-course during the two-step oxidation-state-specific HG. For measurement of the pH-course the consumption of protons due to the derivatization using  $\text{NaBH}_4$  was simulated by addition of  $\text{NaOH}$  instead of  $\text{NaBH}_4$  and no sample was added to the buffer-solution.

In detail, 20 mL of 25 mM TRIS-HCl buffer adjusted to  $pH$  8 were purged for 150 s with a helium flow rate of about  $230 \text{ mL min}^{-1}$  for oxygen removal. The pH-course during the first step for the derivatization of the trivalent arsenicals was simulated by adding 2 mL of 1.1 M  $\text{NaOH}$  within 300 s (instead of 1 M  $\text{NaBH}_4$ , stabilized with 0.1 M sodium hydroxide). Afterwards the solution was purged for additional 120 s similar to the real method (experimental section). For simulation of the pH-course during the derivatization of the pentavalent species in the second step 8 mL of 1.1 M  $\text{NaOH}$  (instead of 1 M  $\text{NaBH}_4$ , stabilized with 0.1 M sodium hydroxide) and 10 mL of 1 M  $\text{HCl}$  were added within 300 s, lowering  $pH$  below 1.

For method validation, we analyzed two mixtures of arsenicals containing either  $\text{As}^{\text{III}}$ ,  $\text{MMAs}^{\text{III}}$ , and  $\text{TMAOs}$  or  $\text{As}^{\text{V}}$ ,  $\text{MMAs}^{\text{V}}$ , and  $\text{DMAs}^{\text{V}}$  (Table 3-1, Figure 3-4). The recovery rates for 61-98 ng per arsenic species added varied between 84 to 99%. The redox miss finding rates (percentage of added species that was recovered in the non-predicted derivatization step) of pentavalent arsenicals at  $pH$  8 were below 1% and of the trivalent arsenic species applying the pH-gradient were below 0.5%. In the second derivatization step 7%  $\text{TMAOs}$  were detected, but a differentiation of the redox

state is not necessary for this compound as only one possible precursor exists (TMA<sub>3</sub>O). The detection limits for HG/P&T/GC-ICP-MS were below 50 pg (3 times the standard deviation of blanks).

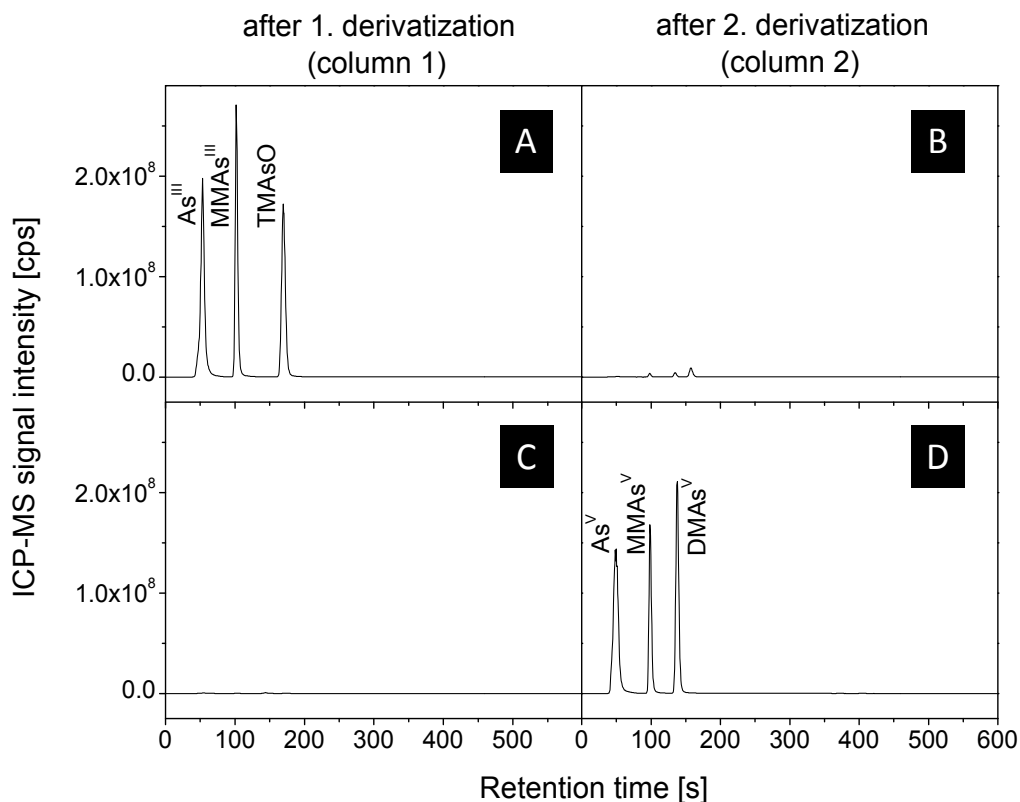


**Figure 3-4.** Sample chromatograms for oxidation-state-specific HG/P&T/GC-ICP-MS. The chromatograms A and B show a two-step oxidation-state-specific HG/P&T/GC-ICP-MS analysis of a standard mixture containing MMA<sup>III</sup>, DMA<sup>III</sup>, TMA<sub>3</sub>O for method validation (for simulated pH-course, refer to Figure 3-3). For C and D a mixture of As<sup>V</sup>, MMA<sup>V</sup>, DMA<sup>5</sup> was used (for quantitative data, refer to Table 3-1). The peaks are labeled with the corresponding starting compounds before derivatization.

**Table 3-1.** Validation of oxidation-state specific hydride generation. Relative recovery as well as percentage of redox miss findings are indicated (n=3) For sample chromatograms refer to Figure 3-4.

	As <sup>III</sup>	MMA <sup>III</sup>	TMA <sub>3</sub> O	As <sup>V</sup>	MMA <sup>V</sup>	DMA <sup>5</sup>
species added [ng]	97.5	84.5	86.1	86.3	60.9	83.7
recovery [%]	85.9±4.2	91±4.6	84±1.3	98.6±4.1	84.8±3.7	92.9±4.2
redox miss finding [%]	0.52±0.12	1.24±0.63	7.36±2.41	0.29±0.05	0.1±0.01	0.41±0.05

### 3.5.2. Investigation of methylation and hydride generation of arsenic

For differentiation between an oxidative and a non-oxidative methylation mechanism, we investigated the formation of volatile as well as non-volatile tri- and pentavalent arsenic species in *in vitro* assay solutions with Cob(I) produced by MtaA catalyzed demethylation of CH<sub>3</sub>Cob(III) in the presence of CoM<sup>[27]</sup> under variation of redox state and degree of methylation of the arsenic reactant species As<sup>III</sup>, MMAs<sup>III</sup>, MMAs<sup>V</sup>, DMAs<sup>V</sup> applied (Table 3-2; Figure 3-5). In parallel, the reaction of the arsenic reactants species with electrochemically produced Cob(I) in presence and absence of CH<sub>3</sub>Cob(III) was followed by UV/Vis spectroscopy in order to eliminate possible interfering influences of the enzyme and CoM on the reaction (Figure 3-7, B-D). The abiotic methylation and hydride generation of arsenicals by CH<sub>3</sub>Cob(III) and CoM in the absence of the methyltransferase MtaA was negligible (Table 3-4).

**Table 3-2.** Formation of volatile and non-volatile arsenic compounds from trivalent and pentavalent arsenic reactants by MtaA containing *in vitro* assays (quantitative data). For calculation of total volatilization, all volatile species detected for each experiment were summarized first (data not shown). Means and relative standard deviations were calculated from these summarized values. Experiments were performed at least in triplicates. See Table 3-3 for a detailed quantitative list of detected species

		AsNaO <sub>2</sub>	CH <sub>3</sub> AsO(ONa) <sub>2</sub>	CH <sub>3</sub> AsI <sub>2</sub>	(CH <sub>3</sub> ) <sub>2</sub> AsO(OH)
reactants added [pmol] (± %RSD)*		9 304 (± 2%)	57 636 (± 5%)	877 (± 2%)	1 616 (± 2%)
methylation and hydrogenation by <i>in vitro</i> assays containing MtaA					
total	[pmol] (± %RSD)	1 302 (±12%)	2.6 (±20%)	307 (±12%)	3.1 (±38%)
volatilized	[%]	14	<0.01	35	0.19
total	[pmol] (± %RSD)	<b>1 201 (±2%)</b>	<b>2.8 (±14%)</b>	<b>159 (±10%)</b>	<b>11 (±26%)</b>
methylation <sup>‡</sup>	[%]	<b>13</b>	<b>&lt;0.01</b>	<b>18</b>	<b>0.7</b>
recovery	[%]	76 ± 8	105 ± 7	69 ± 12	110 ± 10

\*Amounts of reactants added based on the concentrations of reactants determined by HG/P-T/GC-ICP-MS.

<sup>‡</sup>Only derivatives with a higher methylation grade than the added reactants were considered.

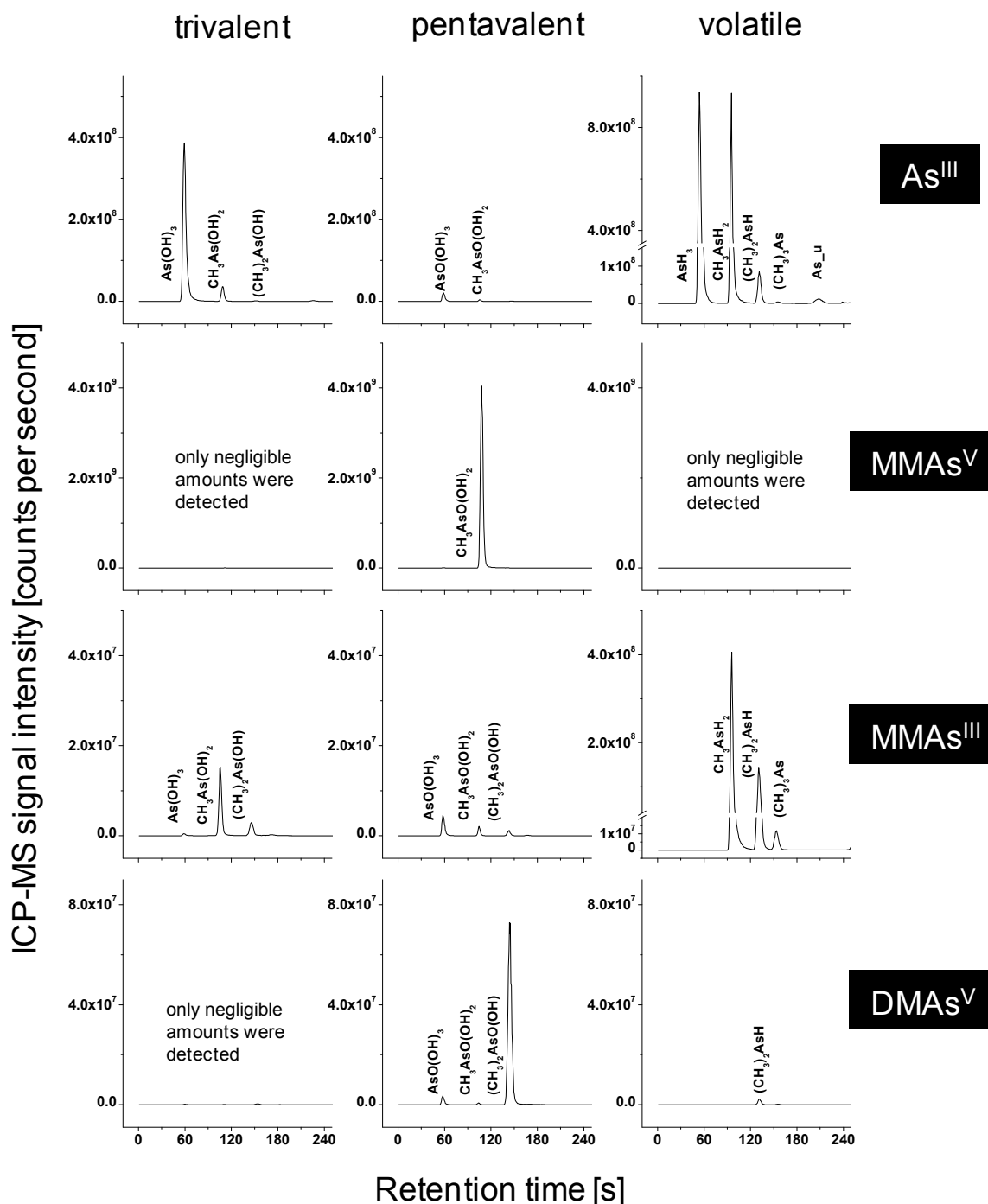


**Figure 3-5.** Investigation of conversion of different arsenic reactants by MtaA containing *in vitro* assays. Trivalent and pentavalent non-volatile arsenicals were analyzed by oxidation-state-specific HG/P&T/GC-ICP-MS after measurement of headspace of the reaction vessels using P&T/GC-ICP-MS. The peaks are labeled with the corresponding starting compounds before derivatization with NaBH<sub>4</sub>. For the arsenic reactants white font on black background is used. See Figure 3-6 for comparison with arsenic standards. As\_u: unidentified volatile arsenical.

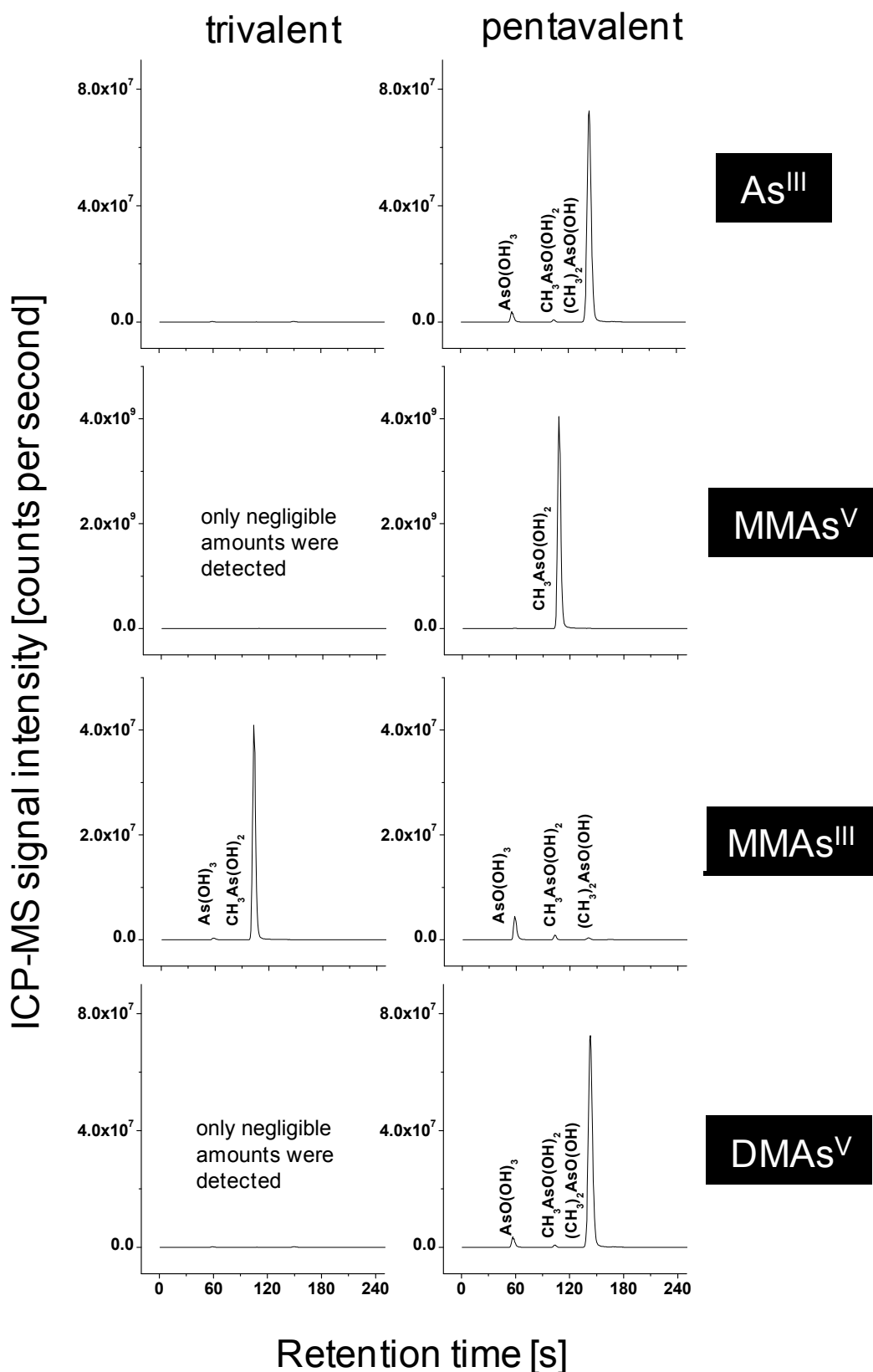


**Figure 3-6.** Measurement of trivalent and pentavalent reactants (white font on black background) *via* oxidation-state-specific HG/P&T/GC-ICP-MS. The peaks are labeled with the corresponding starting compounds before derivatization with  $NaBH_4$ .

**Table 3-3.** Detailed quantitative list of volatile and non-volatile methylated arsenic compounds derived from trivalent and pentavalent arsenic reactants by MtaA containing *in vitro* assays as detected by headspace and HG/P&T/GC-ICP-MS analyses pmol ( $\pm\%$ RSD). Reduced and methylated products are in boldface, reactants not transformed in the MtaA containing *in vitro* assays are in italics. Blank values derived from chemical hydride generation without addition of *in vitro* assays were subtracted.

reactant		AsNaO <sub>2</sub>	CH <sub>3</sub> AsO(ONa) <sub>2</sub>	CH <sub>3</sub> AsI <sub>2</sub>	(CH <sub>3</sub> ) <sub>2</sub> AsO(OH)
trivalent volatile species	AsH <sub>3</sub>	689 ( $\pm 15\%$ )	<DL	<DL	<DL
	CH <sub>3</sub> AsH <sub>2</sub>	<b>514 (<math>\pm 11\%</math>)</b>	2.0 ( $\pm 18\%$ )	205 ( $\pm 14\%$ )	<DL
	(CH <sub>3</sub> ) <sub>2</sub> AsH	<b>68 (<math>\pm 11\%</math>)</b>	<b>0.52 (<math>\pm 27\%</math>)</b>	<b>91 (<math>\pm 10\%</math>)</b>	2.5 ( $\pm 53\%$ )
	(CH <sub>3</sub> ) <sub>3</sub> As	<b>3.8 (<math>\pm 4\%</math>)</b>	<b>0.045 (<math>\pm 36\%</math>)</b>	<b>12.3 (<math>\pm 15\%</math>)</b>	<b>0.36 (<math>\pm 59\%</math>)</b>
	As_u	27 ( $\pm 20\%$ )	<DL	1.3 ( $\pm 0.1\%$ )	<DL
trivalent non-volatile species	As(OH) <sub>3</sub>	<i>4 870 (<math>\pm 10\%</math>)</i>	73 ( $\pm 56\%$ )	6.0 ( $\pm 26\%$ )	7.7 ( $\pm 47\%$ )
	CH <sub>3</sub> As(OH) <sub>2</sub>	<b>521 (<math>\pm 13\%</math>)</b>	103 ( $\pm 1\%$ )	141 ( $\pm 18\%$ )	2.5 ( $\pm 58\%$ )
	(CH <sub>3</sub> ) <sub>2</sub> As(OH)	<b>35 (<math>\pm 21\%</math>)</b>	<b>0.62 (<math>\pm 6\%</math>)</b>	<b>40 (<math>\pm 28\%</math>)</b>	9.4 ( $\pm 10\%$ )
pentavalent non-volatile species	AsO(OH) <sub>3</sub>	288 ( $\pm 12\%$ )	194 ( $\pm 6\%$ )	49 ( $\pm 16\%$ )	64 ( $\pm 37\%$ )
	CH <sub>3</sub> AsO(OH) <sub>2</sub>	<b>45 (<math>\pm 8\%</math>)</b>	<i>60 106 (<math>\pm 6\%</math>)</i>	20 ( $\pm 20\%$ )	9.2 ( $\pm 20\%$ )
	(CH <sub>3</sub> ) <sub>2</sub> AsO(OH)	<b>13 (<math>\pm 6\%</math>)</b>	<DL	<b>22 (<math>\pm 62\%</math>)</b>	1671 ( $\pm 7\%$ )
	(CH <sub>3</sub> ) <sub>3</sub> AsO	<b>2.0 (<math>\pm 15\%</math>)</b>	<DL	<b>1.6 (<math>\pm 10\%</math>)</b>	<b>9.4 (<math>\pm 33\%</math>)</b>

<DL: below detection limit:

detection limit for P-T/GC-ICP-MS was 0.6 fmol s<sup>-1</sup> (3 times the signal-to-noise ratio of the baseline signal; peak widths were in the range of 10-40 s)

detection limits for HG/P-T/GC-ICP-MS were below 680 fmol (3 times the standard deviation of blanks)

As\_u: unknown volatile arsenical

As the pentavalent reactants MMAs<sup>V</sup> and DMAs<sup>V</sup> were almost completely recovered from the *in vitro* assay without being methylated or reduced (Figure 3-5; Table 3-2), the assays are apparently not capable of reducing pentavalent arsenic intermediates into trivalent derivatives (Figure 3-1: reaction pathway R<sub>+V,1</sub>, R<sub>+V,2</sub>). This finding was verified by studying the reaction of electrochemically produced Cob(I) spectroscopically (Figure 3-7 B, C). Here, we could also exclude that Cob(I) despite its redox potential is capable of reducing pentavalent arsenic species (As<sup>V</sup>, MMAs<sup>V</sup>, DMAs<sup>V</sup>, TMAOs) (Figure 3-1: reaction pathway R<sub>+V,1</sub>, R<sub>+V,2</sub>, R<sub>+V,3</sub>) within 15 minutes as no oxidation of Cob(I) could be observed after adding the metal(loid) species in large excess. The absence of pentavalent methylated species as indicated by oxidation-state specific HG shows that there is no transfer of a methyl group to pentavalent arsenicals (Figure 3-1: reaction pathway Me<sub>+V,1</sub>, Me<sub>+V,2</sub>).

When using trivalent arsenical reactants, an at least 100-times higher efficiency of methylation (13-18% of the added reactant within 10 min at 30 °C) as well as hydride generation was observed than of pentavalent arsenic reactants (Table 3-2). 85-96% of the methyl and hydride arsenic species formed from trivalent arsenic reactants were not oxidized in the course of their methylation. The small amounts of pentavalent arsenicals derived from experiments performed with trivalent reactants are likely formed by auto-oxidation or relied on the small miss finding rate (see above).

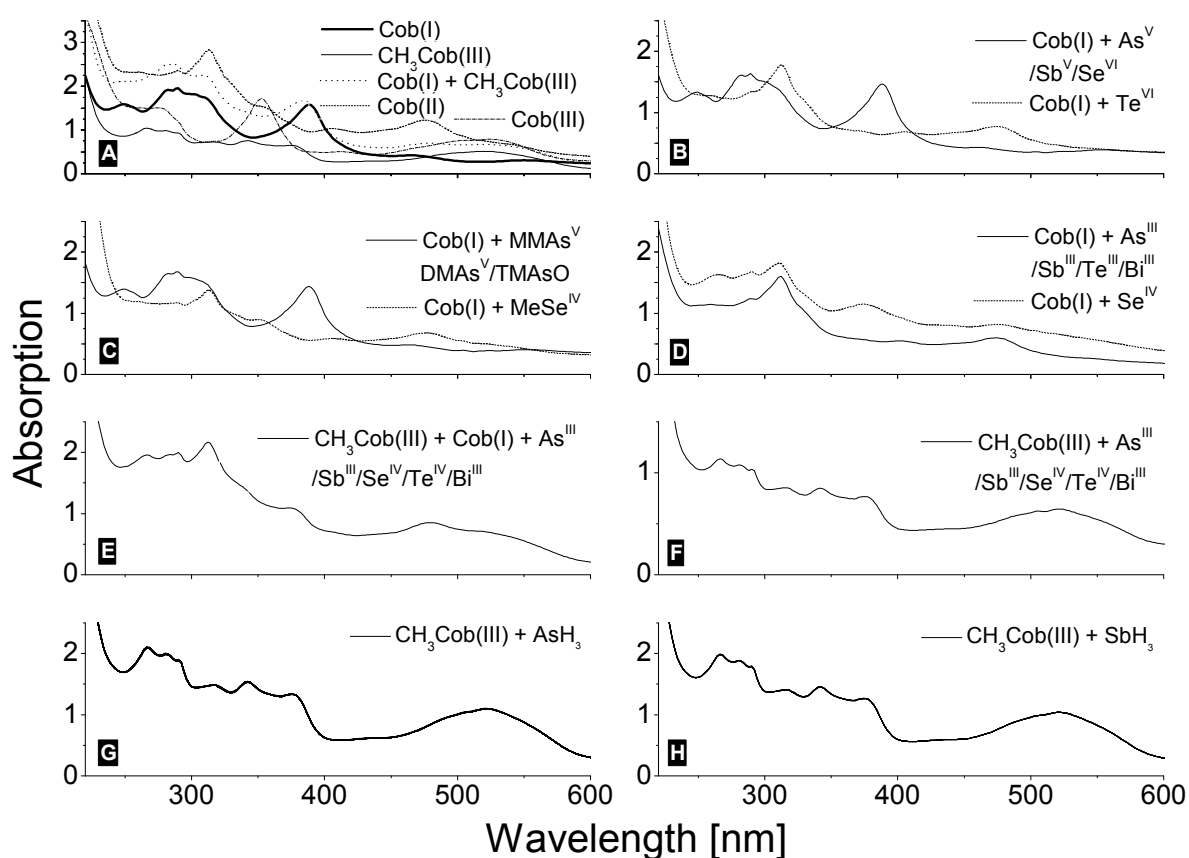


**Figure 3-7.** UV/Vis Analyses of cobalamines in the presence of various reactants. For simplification, only a spectrum for one element is displayed if there were only slight differences in absorbance. Characteristic wavelengths are 520 nm for  $\text{CH}_3\text{Cob(III)}$ , 388 nm for  $\text{Cob(I)}$  and 468 nm for  $\text{Cob(II)}$ . For comparison, see (A).  $\text{Cob(II)}$  was produced by reaction of  $\text{Cob(III)}$  and  $\text{Cob(I)}$ .

**Table 3-4.** Analyses of abiotic volatilization and methylation of trivalent and pentavalent arsenic reactants by CH<sub>3</sub>Cob(III) and CoM. The formation of volatile and non-volatile methylated derivatives from tri- and pentavalent arsenic reactants by *in vitro* assays containing 1 μmol CH<sub>3</sub>Cob(III) and CoM and 1 mL 50 mM HEPES *pH* 7 was investigated. Volatile species were analyzed by headspace P&T-GC-ICP-MS and non-volatile species by HG/P&T/GC-ICP-MS. Chemical hydride generation using NaBH<sub>4</sub> was separately performed at neutral *pH* 8 and during *pH* gradient by continuous addition of 1 M HCl in order to differentiate between trivalent and pentavalent arsenic derivatives. Reduced and methylated products are in boldface, reactants not transformed in the abiotic *in vitro* assays are in italics. Blank values derived from chemical hydride generation without addition of *in vitro* assays were subtracted. Experiments were performed at least in triplicates. For calculation of total volatilization, all volatile species detected for each experiment were summarized first (data not shown). Means and relative standard deviations were calculated from these summarized values.

reactant		AsNaO <sub>2</sub>	CH <sub>3</sub> AsO(ONa) <sub>2</sub>	CH <sub>3</sub> AsI <sub>2</sub>	(CH <sub>3</sub> ) <sub>2</sub> AsO(OH)
[pmol] (± %RSD)*		9 304 (± 2%)	57 636 (± 5%)	877 (± 2%)	1 616 (± 2%)
total methylation and hydrogenation by <i>in vitro</i> assays without enzyme					
total volatilized	[pmol] (± %RSD) [%]	<DL <0.01	<DL <0.01	<DL <0.01	<DL <0.01
total methylation <sup>‡</sup>	[pmol] (± %RSD) [%]	<b>61 (±17%)</b> <b>0.65</b>	<b>0.37 (±13%)</b> <b>&lt;0.01</b>	<b>26 (±38%)</b> <b>2.96</b>	<b>10 (±62%)</b> <b>0.62</b>
recovery	[%]	110	95	109	108
detailed quantitative list of methylated and hydrogenated arsenic derivatives as detected by headspace and HG/P-T/GC-CP-MS analyses [pmol] (±%RSD)					
trivalent volatile species	AsH <sub>3</sub>	<DL	<DL	<DL	<DL
	CH <sub>3</sub> AsH <sub>2</sub>	<DL	<DL	<DL	<DL
	(CH <sub>3</sub> ) <sub>2</sub> AsH	<DL	<DL	<DL	<DL
	(CH <sub>3</sub> ) <sub>3</sub> As	<DL	<DL	<DL	<DL
trivalent non-volatile species	As(OH) <sub>3</sub>	9 917 (±3%)	64 (±9%)	6.5 (±10%)	5.4 (±45%)
	CH <sub>3</sub> As(OH) <sub>2</sub>	<b>38 (±32%)</b>	110 (±15%)	793 (±7%)	2.5 (±52%)
	(CH <sub>3</sub> ) <sub>2</sub> As(OH)	<DL	<b>0.37 (±13%)</b>	<b>19 (±31%)</b>	8.4 (±14%)
pentavalent non-volatile species	AsO(OH) <sub>3</sub>	275 (±25%)	158 (±31%)	58 (±10%)	78 (±45%)
	CH <sub>3</sub> AsO(OH) <sub>2</sub>	<b>14 (±15%)</b>	54 639 (±3%)	44 (±71%)	10 (±24%)
	(CH <sub>3</sub> ) <sub>2</sub> AsO(OH)	<b>7.6 (±22%)</b>	<DL	<b>8.3 (±30%)</b>	1 628 (±9%)
	(CH <sub>3</sub> ) <sub>3</sub> AsO	<b>1.9 (±15%)</b>	<DL	<b>1.6 (±27%)</b>	<b>8.8 (±75%)</b>

<DL: below detection limit:

detection limit for P-T/GC-ICP-MS was 0.6 fmol s<sup>-1</sup> (3 times the signal-to-noise ratio of the baseline signal; peak widths were in the range of 10-40 s)

detection limits for HG/P-T/GC-ICP-MS were below 680 fmol (3 times the standard deviation of blanks)

\*Amounts of reactants added based on the concentrations of reactants determined by HG/P-T/GC-ICP-MS.

<sup>‡</sup>Only derivatives with a higher methylation grade than the added reactants were considered.

We also investigated this process with electrochemically produced Cob(I) *via* UV/Vis spectrometry and P&T/GC-ICP-MS. Upon the addition of trivalent arsenite, a fast oxidation of Cob(I) to Cob(II)alamin (Cob(II)) was observed by UV/Vis spectroscopy (Figure 3-7, D) accompanied by formation of  $\text{AsH}_3$  (Figure 3-8). In the presence of  $\text{CH}_3\text{Cob(III)}$  (Figure 3-7, E), the incubation with an stoichiometric amount of Cob(I) yielded Cob(II) and formation of volatile methylated arsenicals as shown by using P&T/GC-ICP-MS.<sup>[18]</sup> The conversion of  $\text{CH}_3\text{Cob(III)}$  was not quantitative most likely due to the consumption of Cob(I) by parallel hydride generation. Notably, a variation of *pH* changes the ratio of hydrides and methylated arsenicals (Figure 3-9). More arsine is produced in comparison to methylated species at a *pH* of 4-5 than at *pH* 7, indicating the need of protons for hydride generation.

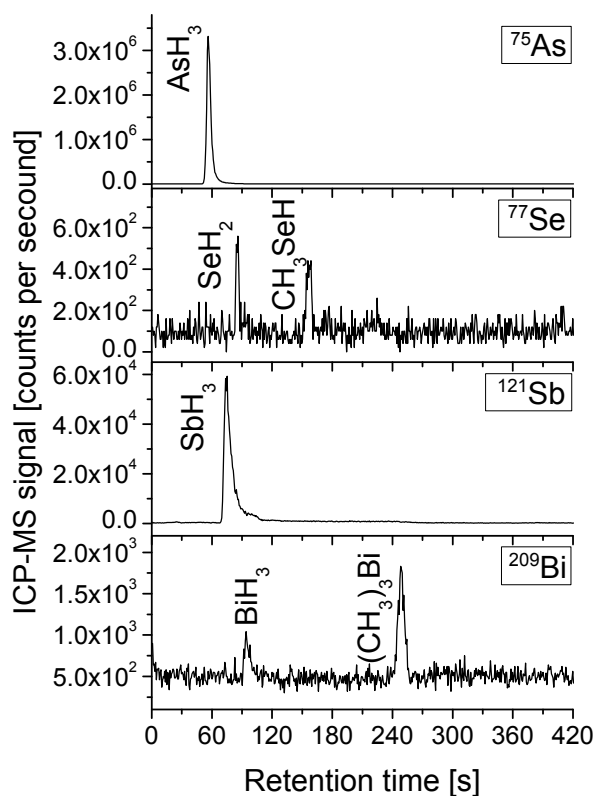


**Figure 3-8.** Hydride generation induced by Cob(I). P&T/GC-ICP-MS chromatograms were produced under the following reaction conditions: 5 mL of 0.5 mM  $\text{CH}_3\text{Cob(III)}$  in 50 mM phosphate-buffer *pH* 7 were incubated with 0.25 mM Cob(I) and either 0.25 mM  $\text{As}^{\text{III}}$ ,  $\text{Sb}^{\text{III}}$ ,  $\text{Bi}^{\text{III}}$ ,  $\text{Se}^{\text{IV}}$  or  $\text{Te}^{\text{IV}}$  (no hydride species were produced (data not shown)) at 37 °C for 30 min prior to headspace analyses. Methylated selenium and bismuth species were properly only detected due to memory effects of the column.

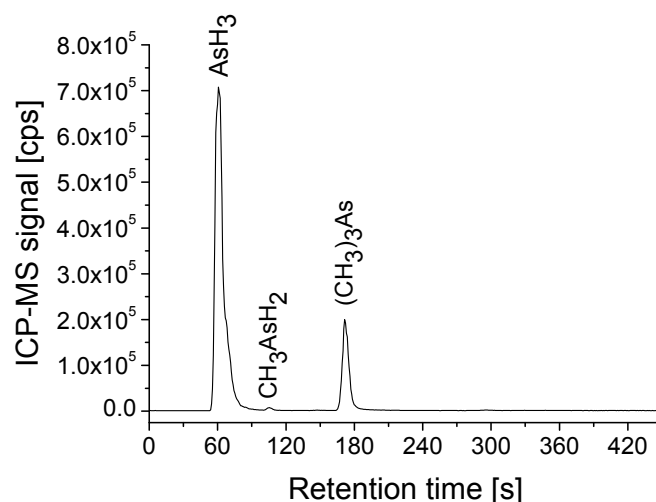


**Figure 3-9.** Arsenic methylation induced by Cob(I) at *pH* 4.5 shows a different hydride to methyl ratio than at *pH* 7 (Figure 3-12). 2 mL of 0.1  $\mu\text{M}$   $\text{As}^{\text{III}}$  in 50 mM phosphate-buffer *pH* 4-5 were incubated with 0.1 mM  $\text{CH}_3\text{Cob}(\text{III})$  and 0.1 mM Cob(I) at 37°C for 30 min prior to P&T/GC-ICP-MS measurement.

To exclude a mechanism proceeding *via* intermediate hydride species analogous to the mechanism proposed for selenium (Figure 3-1: reaction pathway  $\text{R}_{+\text{III},0}$ ,  $\text{Me}_{\text{H},0}$ ),<sup>[11-12]</sup> we used arsine formed by hydride generation for incubation with  $\text{CH}_3\text{Cob}(\text{III})$ . Neither a change in absorbance in the UV/Vis spectrum of  $\text{CH}_3\text{Cob}(\text{III})$  (Figure 3-7, G) nor the formation of methylated volatile arsenic species *via* P&T/GC-ICP-MS could be observed (Figure 3-10), indicating that arsine is not an intermediate of methylation. The detection limit for arsenic for P&T/GC-ICP-MS was 45  $\text{fg s}^{-1}$ , calculated as 3 times the signal-to-noise ratio of the GC-ICP-MS baseline signal. In summary, these experiments contradict a Challenger-like oxidative methylation pathway. Instead methylation of trivalent arsenicals is a non-oxidative reaction either *via* a methyl radical or a carbanion (Figure 3-1: reaction pathway in bold  $\text{Me}_{+\text{III},0}$ ,  $\text{Me}_{+\text{III},1}$ ,  $\text{Me}_{+\text{III},2}$ ). Pentavalent arsenicals must be regarded as side products rather than intermediates of an oxidative methylation mechanism, as they can neither be reduced by Cob(I) nor are methylated in presence of  $\text{CH}_3\text{Cob}(\text{III})$ . The observed hydride generation seems to be a parallel reaction pathway.

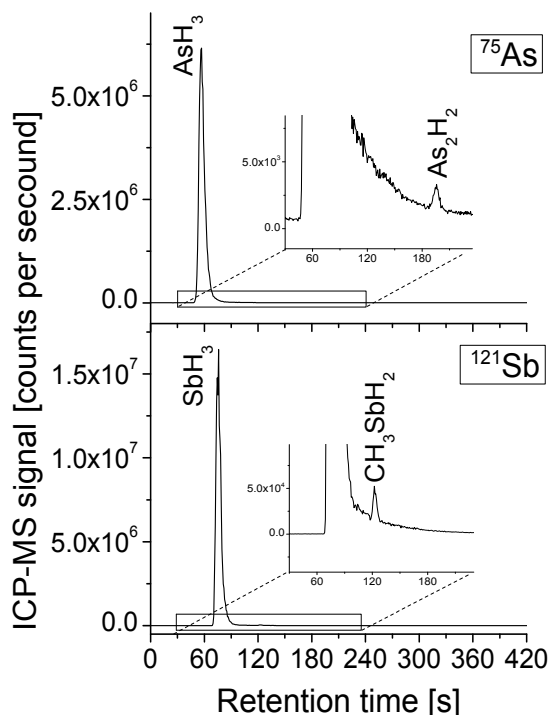


**Figure 3-10.** No significant reaction of arsine and stibine with methylcobalamin. 30 ng arsine and stibine were incubated with 0.1 mM  $\text{CH}_3\text{Cob(III)}$  in 2 mL 50 mM phosphate-buffer  $\text{pH}$  7 at 37 °C for 30 min prior to P&T/GC-ICP-MS measurement.

### 3.5.3. Investigation of methylation and hydride generation of antimony, bismuth, selenium, and tellurium

The next aim was to investigate whether Sb, Bi, Se, and Te are methylated and hydrogenated in similar pathways. In analogy to arsenic, volatile methylated species in presence of  $\text{Cob(I)}$  and  $\text{CH}_3\text{Cob(III)}$  are formed as reported previously.<sup>[18]</sup> In contrast to arsenic, no redox-specific speciation technique was available for the methylated species of these elements. In order to exclude an oxidative methylation pathway for these elements, we executed various incubation experiments with the meta(loid)s species,  $\text{Cob(I)}$  and  $\text{CH}_3\text{Cob(III)}$ .

In agreement with the experiments with  $\text{As}^{\text{V}}$ ,  $\text{Cob(I)}$  showed no change in the UV/Vis spectra in the presence of  $\text{Sb}^{\text{V}}$  (Figure 3-7, B), again contradicting a Challenger-like oxidative-methylation. Due to the instability of pentavalent bismuth species in aqueous solution, an oxidative-methylation can be ruled out in this case, too.  $\text{Sb}^{\text{III}}$  is readily reduced by  $\text{Cob(I)}$  (Figure 3-7, D), like  $\text{As}^{\text{III}}$ , resulting in the formation of  $\text{SbH}_3$  (Figure 3-8). For bismuth, only traces of  $\text{BiH}_3$  were detected presumably due to the

high instability of this compound (Figure 3-7). Likewise for arsine, the incubation of stibine with  $\text{CH}_3\text{Cob(III)}$  shows no change in the UV/Vis spectrum (Figure 3-7, H), but we observed a very low amount of methyl stibine using P&T/GC-ICP-MS (Figure 3-10). In summary, the results for antimony and bismuth point towards a non-oxidative mechanism like in the case of arsenic.

Next, we tried to confer this finding upon Group 16 elements selenium and tellurium.  $\text{Se}^{\text{VI}}$  does not react with Cob(I) (Figure 3-7, B), in parallel to  $\text{As}^{\text{V}}$  and  $\text{Sb}^{\text{V}}$ . In contrast,  $\text{Te}^{\text{VI}}$  oxidized Cob(I) to Cob(II) (Figure 3-7, B), but no volatile species were detected by GC-ICP-MS in the *in vitro* assays with MtaA (data not shown). The addition of  $\text{Se}^{\text{IV}}$  and  $\text{Te}^{\text{IV}}$  led to a fast oxidation of Cob(I) to Cob(II) (Figure 3-7, E) and the formation of trace amounts of  $\text{SeH}_2$  (Figure 3-8), but not of tellurium hydride species presumably due to the instability of tellurium hydrides. Upon the addition of methaneseleninic acid ( $\text{MeSe}^{\text{IV}}$ ) to Cob(I), we observed an oxidation of Cob(I) to Cob(II) (Figure 3-7, C) and the formation of methylselenol and dimethyldiselenide (Figure 3-11). This agrees with the last step of the selenium methylation mechanism proposed by Reamer and Zoller.<sup>[28]</sup> As the reduction of methaneseleninic acid to volatile products is easily achieved by Cob(I), we assume that this is the final step in order to facilitate the volatilization of tetravalent selenium compounds, though we cannot exclude ultimately the formation of hydride species prior to methylation. Overall, the results for Group 16 elements selenium and tellurium are not as conclusive as for the Group 15 elements. An analogous non-oxidative mechanism seems plausible but cannot be differentiated on the basis of the data available.

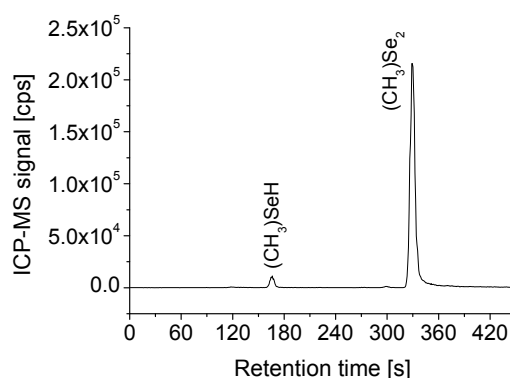


**Figure 3-11.** Transformation of methylseleninic acid induced by Cob(I). A 2 mL solution of 0.1  $\mu\text{M}$  methylseleninic acid and 50  $\mu\text{M}$  electrochemically produced Cob(I) was incubated in 50 mM phosphate-buffer *pH* 7 for 15 min under strict anaerobic conditions prior to P&T/GC-ICP-MS measurement.

#### 3.5.4. Possible mechanisms for multi-element methylation

Our experiments clearly contradict a Challenger-like mechanism, i.e. the oxidation state at least for the Group 15 metal(loid)s arsenic, antimony, and bismuth are not altered in the course of their methylation. The methyl group is transferred either in a nucleophilic substitution as a carbanion or in a radical reaction to tri- (Group15) and tetravalent (Group 16) metal(loid)s, respectively, without noticeably changing the oxidation state of the metal(loid).

In order to check whether the mechanism involves a free methyl radical, we investigated the effect of tert-butanol as a radical trap since methyl radicals from photolysis of methylcobalamin were suggested to abstract a hydrogen of an alcohol.<sup>[29]</sup> In assays with As<sup>III</sup>, CH<sub>3</sub>Cob(III) and electrochemically produced Cob(I), the addition of tert-butanol showed no effect on the methylation efficiency (Figure 3-12) suggesting that the methyl transfer probably does not proceed *via* a radical mechanism. However, we cannot rule out a caged radical mechanism as tert-butanol is not suitable for trapping caged methyl radicals. The use of a spin-trapping agent  $\alpha$ -(4-Pyridyl N-oxide)-N-tert-butyl nitron unfortunately led to the oxidation of Cob(I) (data not shown). Nevertheless, CH<sub>3</sub>Cob(III) and Cob(I) are stable in absence of metal(loid)s in the time range of our UV/Vis experiments (Figure 3-7, A). Thus, the formation of a free reactive species, such as free methyl radical, is unlikely as this would result in changes of the absorbance spectra of the corrinoid containing solutions. In case of a nucleophilic substitution involving a carbanion, a concerted S<sub>N</sub>2-type mechanism has to be assumed. Also a caged radical mechanism could explain that Cob(I) and CH<sub>3</sub>Cob(III) are stable for longer periods due to cage recombination. An interfering metal(loid) could function as a radical trap like in the case of light-induced arsenic methylation.<sup>[8]</sup>

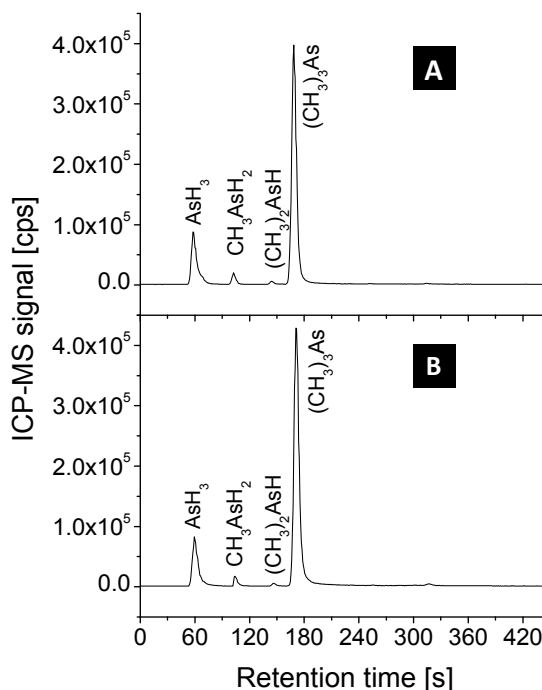


**Figure 3-12.** Tert-butanol shows no effect on arsenic methylation induced by Cob(I). 2 mL of 0.1  $\mu\text{M}$   $\text{As}^{\text{III}}$  in 50 mM phosphate-buffer pH 7 were incubated with 0.1 mM  $\text{CH}_3\text{Cob(III)}$  and 0.1 mM Cob(I) in presence (A) and absence (B) of 50 mM tert-butanol at 37°C for 30 min prior to P&T/GC-ICP-MS measurement.

As the current data do not allow the differentiation between  $\text{S}_{\text{N}}2$  and a caged radical mechanism, we summarize the two possible methylation mechanisms in accordance to our data in Figure 3-13. A one-electron transfer from Cob(I) to  $\text{CH}_3\text{Cob(III)}$  – in analogy to a mechanism for methane formation postulated by Schrauzer *et al.*<sup>[10]</sup> – would result in formation of Cob(II) and a reduced  $\text{CH}_3\text{Cob(III)}$ . Then, the methyl group could be transferred as a carbanion from the reduced  $\text{CH}_3\text{Cob(III)}$  to arsenite or the other metal(loid)s in a  $\text{S}_{\text{N}}2$  reaction, replacing a hydroxyl group (Figure 3-13, pathway 1) despite the fact that  $\text{OH}^-$  is a rather bad leaving group. As an alternative the following radical mechanism is plausible. After one-electron transfer from Cob(I) to  $\text{CH}_3\text{Cob(III)}$  followed by formation of Cob(II) and a reduced  $\text{CH}_3\text{Cob(III)}$ , the cobalt methyl bonding is cleaved homolytically yielding Cob(I) and a methyl radical – in analogy to the mechanism of electrochemical reduction of  $\text{CH}_3\text{Cob(III)}$ <sup>[30]</sup> – that reacts with the metal(loid) (Figure 3-13, pathway 2). However, no mixture of Cob(I) and

Cob(II) is observed presumably due to the consumption of Cob(I) by parallel hydride generation. Thus, both mechanisms are in agreement with our experimental data.

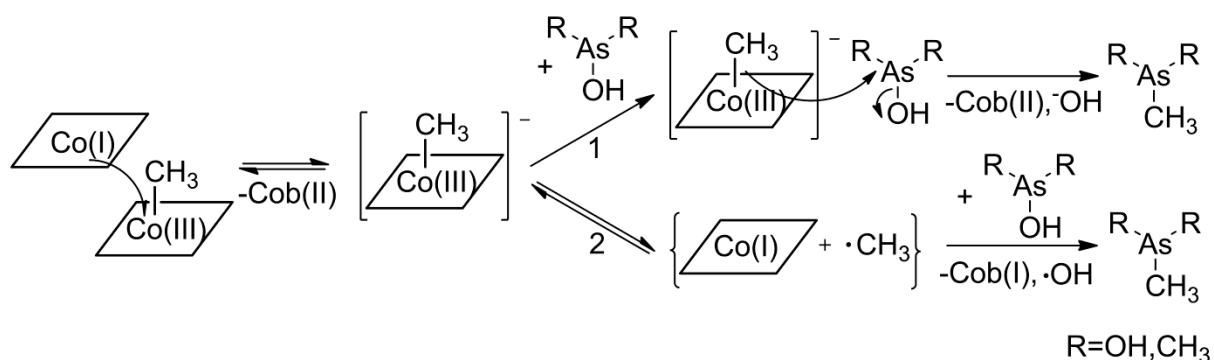
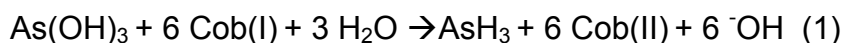


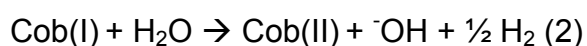
**Figure 3-13.** Proposed reaction schemes for multi-element methylation of trivalent metal(loid)s induced by Cob(I). Exemplarily, arsenic is shown. (1: concerted nucleophilic substitution (S<sub>N</sub>2); 2: caged radical mechanism)

### 3.5.5. Possible mechanisms for hydride generation as exemplified on arsenite

The Cob(I) induced hydride generation for arsenite can be summarized in equation 1:



However, reaction details are unknown yet. At first, Cob(I) could attack H<sub>3</sub>O<sup>+</sup> yielding a free hydride ion and aquocobalamin which would not be observable due to instant comproportionation of aquocobalamin with Cob(I) to Cob(II) (Figure 3-7, F). The formed hydride ion could reduce the metal(loid)s and form the volatile hydride species. Nevertheless, we suggest another mechanism, as Cob(I) decomposes slowly with a half-life time of 22 min at pH 7 in aqueous solution in absence of O<sub>2</sub> according to equation 2.<sup>[31]</sup>



This reaction is substantially slower than the reaction observed.<sup>[18]</sup> Thus, a direct interaction between the metalloid and Cob(I) is more likely as suggested for arsenic by Schrauzer *et al.*<sup>[10]</sup> Despite the low *pK<sub>a</sub>*-value of ca. 1,<sup>[32]</sup> the hydridocobalamin could be intermediately formed. This hydridocobalamin then transfers a hydride ion

directly to the arsenite and the cobalamin accepts the  $\text{H}^-$  in a concerted group exchange yielding an arsenic hydride compound and aquocobalamin.

### 3.6. CONCLUSION

We investigated the multi-element methylation and hydride generation mechanism by Cob(I) and  $\text{CH}_3\text{Cob(III)}$  - both central cofactors of methanogenesis - which are apparently responsible for the capability of methanoarchaea to facilitate multi metal(loid) transformations.

Prior to mechanistic studies, we developed and validated a new oxidation state specific hydride generation technique coupled to detection by GC-ICP-MS which showed acceptable recovery and miss finding rates. Since trivalent arsenicals possess a significantly higher toxicity than pentavalent species, this speciation method is also useful in other fields of application, such as analysis of environmental samples with complex matrices.

By the use of this technique and varying arsenic reactants in enzymatic assays, we clearly pointed out that the underlying reaction mechanism of metal(loid) methylation by  $\text{CH}_3\text{Cob(III)}$  and Cob(I) is not an oxidative one. We underlined this finding and provide further insights into the mechanism by UV/Vis and P&T/GC-ICP-MS investigations using electrochemically produced Cob(I). Our data indicate that the metal(loid)s antimony, selenium, tellurium, and bismuth are methylated in a similar way, even though in the case of Se and Te an additional reduction step is required upon methylation to form volatile species.

Based on our findings, a concerted nucleophilic substitution reaction after formation of a reduced methylcobalamin is likely, but also a caged radical mechanism for the methyl transfer to the metal(loid)s cannot be excluded. For the hydride generation, we assume the formation of hydridocobalamin as an intermediate that transfers a hydride ion directly to the metal(loid)s.

### 3.7. REFERENCES

- [1] J. S. Thayer, *Appl. Organomet. Chem.* **2002**, *16*, 677.
- [2] R. A. Yokel, S. M. Lasley, D. C. Dorman, *J. Toxicol. Environ. Health B Crit. Rev.* **2006**, *9*, 63.
- [3] M. Styblo, L. M. Del Razo, L. Vega, D. R. Germolec, E. L. LeCluyse, G. A. Hamilton, W. Reed, C. Wang, W. R. Cullen, D. J. Thomas, *Arch. Toxicol.* **2000**, *74*, 289.
- [4] T. Sakurai, *J. Health Sci.* **2003**, *49*, 171.
- [5] B. K. Mandal, K. T. Suzuki, *Talanta* **2002**, *58*, 201.
- [6] R. Bentley, T. G. Chasteen, *Microbiol. Mol. Biol. Rev.* **2002**, *66*, 250.
- [7] T. Hayakawa, Y. Kobayashi, X. Cui, S. Hirano, *Arch. Toxicol.* **2005**, *79*, 183.
- [8] K. Nakamura, Y. Hisaeda, L. Pan, H. Yamauchi, *J. Organomet. Chem.* **2009**, *694*, 916.
- [9] W. Ridley, L. Dizikes, J. Wood, *Science* **1977**, *197*, 329.
- [10] G. N. Schrauzer, J. A. Seck, R. J. Holland, T. M. Beckham, E. M. Rubin, J. W. Sibert, *Bioinorg. Chem.* **1973**, *2*, 93.
- [11] T. G. Chasteen, R. Bentley, *Chem. Rev.* **2003**, *103*, 1.
- [12] Y. Ohta, K. T. Suzuki, *Toxicol. Appl. Pharmacol.* **2008**, *226*, 169.
- [13] J. Qin, B. P. Rosen, Y. Zhang, G. J. Wang, S. Franke, C. Rensing, *Proc. Natl. Acad. Sci. U. S. A.* **2006**, *103*, 2075.
- [14] P. J. Craig, F. Glockling, *The biological alkylation of heavy elements*, Royal Society Of Chemistry, London, **1988**.
- [15] G. N. Schrauzer, J. W. Sibert, R. J. Windgassen, *J. Am. Chem. Soc.* **1968**, *90*, 6681.
- [16] J. G. Ferry, *Crit. Rev. Biochem. Mol. Biol.* **1992**, *27*, 473.
- [17] J. Meyer, K. Michalke, T. Kouril, R. Hensel, *Syst. Appl. Microbiol.* **2008**, *31*, 81.
- [18] F. Thomas, R. A. Diaz-Bone, O. Wuerfel, B. Huber, K. Weidenbach, R. A. Schmitz, R. Hensel, *Appl. Environ. Microbiol.* **accepted**
- [19] J. U. Kreft, B. Schink, *Eur. J. Biochem.* **1994**, *226*, 945.
- [20] A. R. Kumar, P. Riyazuddin, *Int. J. Environ. Anal. Chem.* **2007**, *87*, 469.
- [21] O. Wuerfel, R. A. Diaz-Bone, M. Stephan, M. A. Jochmann, *Anal. Chem.* **2009**, *81*, 4312.
- [22] Merijani.A, R. A. Zingaro, *Inorg. Chem.* **1966**, *5*, 187.

- [23] L. M. Del Razo, M. Styblo, W. R. Cullen, D. J. Thomas, *Toxicol. Appl. Pharmacol.* **2001**, 174, 282.
- [24] V. Devesa, L. M. Del Razo, B. Adair, Z. Drobna, S. B. Waters, M. F. Hughes, M. Styblo, D. J. Thomas, *J. Anal. At. Spectrom.* **2004**, 19, 1460.
- [25] T. Matousek, A. Hernandez-Zavala, M. Svoboda, L. Langrova, B. M. Adair, Z. Drobna, D. J. Thomas, M. Styblo, J. Dedina, *Spectrochim. Acta, Part B* **2008**, 63, 396.
- [26] R. A. Diaz-Bone, M. Hitzke, *J. Anal. At. Spectrom.* **2008**, 23, 861.
- [27] G. M. LeClerc, D. A. Grahame, *J. Biol. Chem.* **1996**, 271, 18725.
- [28] D. C. Reamer, W. H. Zoller, *Science* **1980**, 208, 500.
- [29] R. H. Yamada, S. Shimizu, S. Fukui, *Biochim. Biophys. Acta* **1966**, 124, 195.
- [30] R. L. Birke, Q. Huang, T. Spataru, D. K. Gosser, *J. Am. Chem. Soc.* **2006**, 128, 1922.
- [31] S. M. Chemaly, R. A. Hasty, J. M. Pratt, *J. Chem. Soc., Dalton Trans.* **1983**, 2223.
- [32] R. M. Kellett, T. G. Spiro, *Inorg. Chem.* **1985**, 24, 2373.

## **Chapter 4. Determination of $^{13}\text{C}/^{12}\text{C}$ isotopic ratios of biogenic organometal(loid) compounds in complex matrices**

*\*Reproduced from “Oliver Wuerfel, Roland A. Diaz-Bone, Manuel Stephan, Maik A. Jochmann, Determination of  $^{13}\text{C}/^{12}\text{C}$  isotopic ratios of biogenic organometal(loid) compounds in complex matrices, Anal. Chem. **2009**, 81, 4312-4319”*

### **4.1. ABSTRACT**

Methylated metal(loid) compounds are formed in the environment by abiotic as well as enzymatically catalyzed transfer of a methyl group. Due to the increased mobility and toxicity in comparison to the inorganic precursors, the investigation of the formation process is of high relevance. Though the natural abundance carbon isotope ratio can give important insights towards their origin as well as the biochemical methyl transfer process, these species have not been investigated by carbon isotope ratio mass spectrometry (IRMS) so far. This is due to the analytical challenge to precisely determine the natural isotope distribution of trace amounts of metal(loid)-bound carbon in complex organic matrices. To overcome this problem, we tested the concept of selective derivatization of non-volatile organometal(loid)s by hydride generation (HG) followed by purge and trap (P&T) enrichment, heart-cut gaschromatography (hcGC) and subsequent analysis by GC-IRMS. Parameter optimization of HG-P&T-hcGC was conducted using online coupling to element-sensitive ICP-MS (inductively coupled plasma mass spectrometry) detection. The purity of the HG-P&T-hcGC fraction was verified by GC-MS. For the model substance trimethylarsine oxide (TMA<sub>3</sub>O), an excellent agreement of the  $\delta^{13}\text{C}$ -value analyzed by HG-P&T-hcGC-GC-IRMS was achieved in comparison to the bulk  $\delta^{13}\text{C}$ -value, which shows that no significant isotope fractionation occurred during the hydride generation and subsequent separation. The optimized method showed good reproducibility and a satisfying absolute detection limit of 4.5  $\mu\text{g}$  TMA<sub>3</sub>O (1.2  $\mu\text{g}_{\text{carbon}}$ ). This method was applied to the analysis of TMA<sub>3</sub>O in compost. The low  $\delta^{13}\text{C}$ -value of this compound ( $-48.38 \pm 0.41\text{‰}$ ) indicates that biomethylation leads to significant

carbon fractionation. HG-P&T-hcGC-GC-IRMS is a promising tool for investigation of the biomethylation process in the environment.

## 4.2. INTRODUCTION

Compound-specific stable isotope analysis (CSIA) allows tracing of the origin of substances of environmental concern and offers the possibility to investigate isotopic fractionation in chemical and biochemical processes.<sup>[1]</sup> As the natural variability of isotopic abundance is typically in the range of tenth of percent, the  $\delta$ -notation is used. In case of carbon isotope ratios the  $\delta^{13}\text{C}$  value is defined by the following equation,

$$\delta^{13}\text{C} = \frac{R_{\text{sample}} - R_{\text{VPDB}}}{R_{\text{VPDB}}} \quad (1)$$

where  $R_{\text{sample}}$  and  $R_{\text{VPDB}}$  ( $^{13}\text{C}/^{12}\text{C} = 0.0112372$ ) are the ratios of the heavy isotope to the light isotope (here,  $^{13}\text{C}/^{12}\text{C}$ ) in the sample and the international reference standard Vienna Pee-Dee Belemnite.

CSIA requires the hyphenation of either gas or liquid chromatography to isotope ratio mass spectrometry (GC-<sup>[2-3]</sup> or HPLC-IRMS<sup>[4-5]</sup>). In order to achieve the extreme precision required to analyze the natural variability of isotope signatures, in most cases multiple collector mass spectrometry (MC-MS) is applied. In case of light elements such as C, H, O and N, ionization is achieved by electron impact (EI) after chemical conversion into a simple gas, e.g. in the case of carbon by catalyzed oxidation at 960 C to  $\text{CO}_2$ . Ionization of heavy elements can be realized by an inductively coupled plasma (MC-ICP-MS).

The unique ability of CSIA to trace environmental concerning substances by using the isotopic signature is applied in local scale environmental forensics,<sup>[6-7]</sup> source allocation of contaminant hot spots and remediation of contaminants by natural attenuation processes.<sup>[1]</sup> On a global scale, the determination of sinks and sources of substances as well as the elucidation of missing sources is part of research.<sup>[6-7]</sup>

Moreover, CSIA offers the possibility to elucidate reaction pathways of formation and degradation of specific substances by isotopic fractionation processes originating from the slightly different physical and chemical properties of the isotopes.<sup>[8-9]</sup> Isotopic fractionation originating from kinetic isotope effects can be used to distinguish between different types of reaction even if the same final product is

obtained like in the case of  $S_N1$  and  $S_N2$ -reactions, which lead to markedly different primary and secondary kinetic isotope effects.<sup>[10]</sup>

Several rules of thumb allow to estimate the magnitude of kinetic isotope effects.<sup>[11]</sup> In general, fractionations are proportional to differences in the relative isotope masses.<sup>[11]</sup> Therefore, in reactions involving both light and heavy elements, the light element will show significantly higher fractionation. Moreover, another general rule of thumb for kinetic isotope fractionation is that for a given element that is present in covalent bonds of a comparable force constant, isotope effects tend to be greater if the element is bound to heavier atoms.<sup>[11]</sup> Additionally, large carbon isotope effects can be expected for a concerted substitution mechanism such as  $S_N2$  compared to much smaller effects in dissociation-association mechanisms like  $S_N1$ .<sup>[11]</sup>

A particularly interesting and environmentally highly relevant process is the transfer of methyl groups to metal(loid)s, as the addition of methyl groups fundamentally changes physico-chemical properties of the metal(loid). Both abiotic methylation as well as the enzymatically catalyzed transfer of methyl groups (biomethylation) has been demonstrated.<sup>[12]</sup> The fundamental mechanism of biomethylation has been under intensive research since the pioneering work of Challenger in 1945.<sup>[13]</sup> Different methyl donors (methylcobalamin ( $CH_3Cob(III)$ ), S-adenosyl methionine (SAM), tetrahydrofolate (THF)) have been identified.<sup>[12]</sup> A wide range of elements can be methylated in the environment,<sup>[12]</sup> the most prominent examples are mercury and arsenic due to the high toxicological relevance of these elements. In the case of mercury, methylation by prokaryotic cells enhances both toxicity and the tendency for bioaccumulation by orders of magnitude.<sup>[14]</sup> In contrast, the methylation of arsenic has been considered as a detoxification process of eucaryotic cells due to the low toxicity of pentavalent methylated arsenic species. Due to the recent discovery of highly toxic metabolites, the role of methylation is currently under intensive debate.<sup>[15]</sup> Different mechanisms of arsenic methylation including oxidative and reductive methylation have been proposed for arsenic.<sup>[16]</sup>

For organometal(loid) compounds, only the isotopic pattern of the metal(loid) has been analyzed so far.<sup>[17-19]</sup> Isotopic fractionation of antimony during methylation towards volatile trimethylstibine has been investigated by Wehmeyer *et al.*, who found an enrichment of  $^{123}Sb$  in comparison to  $^{121}Sb$ .<sup>[19]</sup>

However, to the best of our knowledge, isotopic ratio mass spectrometry has not been used for investigation of the carbon isotope abundance in biogenic

organometal(loid) compounds nor the fractionation of carbon in the methylation process of metal(loid)s yet. This can be explained by the challenge to precisely analyze the carbon isotopic pattern, as organometal(loid)s occur only at trace or ultratrace concentrations in the environment in presence of complex organic matrices.

Carbon isotope value determination necessitates the quantitative separation of all coeluting organic matrix compounds to prevent a distortion of the measured isotopic signatures. Furthermore, IRMS instruments have a relatively low sensitivity, requiring between 0.1 and 5 nmol carbon in order to obtain the required isotopic precision.<sup>[3]</sup> A preservation of the isotopic signature during the entire analytical process is necessary. Hence, only carbon-free derivatization agents can be used. Moreover, all processes that could lead to fractionation have to be avoided, in particular incomplete derivatization or losses during the extraction process. Finally, GC-IRMS is relatively sensitive to matrix components such as CO<sub>2</sub> and water, which deteriorate the precision of isotopic measurement.<sup>[20]</sup>

The aim of this work was to develop a method to determine the <sup>13</sup>C/<sup>12</sup>C isotopic ratio of biogenically formed organometal(loid) compounds in complex matrices. The approach to achieve both efficient matrix separation and enrichment was selective derivatization of non-volatile organometal(loid) species by hydride generation and enrichment of the volatile derivatives by purge & trap (P&T). Hydride generation was chosen out of several reasons, (i) no additional carbon is introduced into the molecule, (ii) quantitative derivatization of a wide range of organometal(loid) compounds can be achieved even in complex matrices such as compost samples,<sup>[21]</sup> (iii) the derivatization agent reacts directly with the metal(loid), thus, no isotopic fractionation is expected for carbon, (iv) the derivatives are highly volatile and can easily be purged from the reaction solution. Hydride generation has been also used for isotope ratio measurements of antimony<sup>[22]</sup> and selenium.<sup>[23]</sup>

The applicability of the method to organometal(loid)s formed by biomethylation was tested using compost from a laboratory-scale composting experiment. Sodium arsenate was amended at the beginning of the composting process, which was mainly methylated to trimethylarsine oxide (TMA<sub>3</sub>O) by microorganisms. TMA<sub>3</sub>O reacts with the hydride generation agent sodium borohydride to the volatile trimethylarsine (TMA<sub>3</sub>) according to the reaction:



In spite of the high selectivity of hydride generation, the removal of CO<sub>2</sub>, water as well as trace amounts of volatile matrix compounds, was necessary. Chemical separation by sorbents such as NaOH, was unfavorable, as significant loss of organometal(loid), which could lead to isotopic fractionation, has been reported.<sup>[24]</sup> Therefore, pre-separation of volatile matrix compounds after hydride generation was applied by heart-cut gas chromatography (hcGC) prior to the GC-IRMS measurement.

### 4.3. EXPERIMENTAL SECTION

#### 4.3.1. Chemicals for hydride generation

Sodium tetrahydroborate solution (1 M) was prepared by dissolving sodium borohydride (purity >99%, Acros Organics, Geel, Belgium) in 0.1 M sodium hydroxide (Carl Roth GmbH, Karlsruhe, Germany). 2 M hydrochloric acid was obtained by dilution of 37% hydrochloric acid (trace analysis grade, Fisher Scientific, Schwerte, Germany) in deionized water (Seralpur Pro 90 CN system, Elga Berkefeld GmbH, Celle, Germany). 0.04 M citric acid/citrate buffer solution (*pH* 7) was prepared using trisodiumcitrate dihydrate (Merck, Darmstadt, Germany) and citric acid (Fluka, Buchs, Switzerland). 10 mL/L of 1:100 diluted anti-foaming agent (antifoam 289, Sigma-Aldrich, Taufkirchen, Germany) was added to the buffer solution. TMAAsO standard was synthesized by oxidation of TMAAs (99% purity, Strem Chemicals, Kehl, Germany) with hydrogen peroxide in diethyl ether.<sup>[25]</sup> MMAAs<sup>V</sup> (CH<sub>3</sub>AsO(ONa)<sub>2</sub>) was purchased from Argus Chemicals (Vernio, Italy) and DMAAs<sup>V</sup> ((CH<sub>3</sub>)<sub>2</sub>AsO(OH)) from Strem Chemicals (Kehl, Germany). Argon of 4.6 quality and Helium of 5.0 quality (both Air Liquide, Düsseldorf, Germany) were used for ICP-MS and GC, respectively.

#### 4.3.2. Description of the compost sample

For testing the applicability of the carbon isotope analysis to complex matrices, a compost material from a laboratory composting experiment series was investigated.<sup>[21]</sup> In brief, 1 kg dried lucerne hay was amended with sodium arsenate dissolved in 1 L tap water and composted for 15 days in temperature isolated vessels. At the end of the experiment, the compost contained 24 mg<sub>As</sub>/kg<sub>wet weight</sub>, of which 36% was converted to TMAAsO and 2% to dimethylarsenate by biomethylation.

The compost had a relative humidity of 82%. As only wet material was processed, all following weight specifications refer to the wet weight. The compost was cryogrinding using a Freezer Mill 6850 (Spex CertiPrep, Metuchen, USA) in order to improve the sample homogeneity.

#### 4.3.3. HG-P&T-hcGC procedure

For hydride generation and subsequent heart-cut gaschromatography, a self-developed semi-automated system was used (Figure 4-1; left part), which is a further refinement of a previously described system.<sup>[21]</sup> The system consists of a home-built derivatization unit and low temperature GC with packed column (ID: 4 mm, length: 40 cm, stationary phase 1.15 g of 10% SP-2100 on 80/100 mesh Supelcoport (Sigma-Aldrich, St. Louis, US), which was wrapped with 2.1 m resistance wire (3.9  $\Omega$ /m; Block, Werden, Germany). The system allows computer-controlled derivatization agent addition, time-programmed heating of the GC-column, adjustment of purge gas flows as well as switching of valve positions. A 100-mL three-neck round-bottomed flask was used as reaction vessel; a homogeneous mixture was attained by magnetic stirring. The heart-cut was realised by two automated switching valves (4-port and 6-port, both VICI AG (Schenkon, Switzerland). The transfer line to ICP-MS, GC-MS or GC-IRMS (length: 100 cm) as well as internal transfer line between valves and column (total length: 20 cm) were made of sulfinert coated steel capillaries (OD: 1/16" ID: 1.02 mm, Restek, Corp., Bellefonte, PA, US) heated to a temperature of 100 °C. Helium purge gas flow was controlled by a rotameter (Kobold, Hofheim, Germany), carrier gas flows were adjusted by two mass flow controllers (Bronkhorst, Schenkon, Netherlands).

For hydride generation, the sample was dissolved in 40 mL citric acid/citrate buffer and purged by 400 mL min<sup>-1</sup> He for 120 s for oxygen removal. Then, 10 ml 1 M NaBH<sub>4</sub> and 5 mL 2 M HCl were continuously added *via* automated piston pumps with ceramic head (REGLO-CPF Ismatec, Wertheim, Germany) within 300 s. The volatile derivatives were continuously purged out of the reaction solution by 400 mL min<sup>-1</sup> and cryofocussed on the column immersed in liquid nitrogen. Breakthrough during the cryofocussing, as monitored by ICP-MS, was not observed. After derivatization, the purge flow is maintained for additional 2 min in order to assure completeness of purging. At the beginning of the GC run the dewar with liquid nitrogen was removed. The column was warmed by ambient air for 300 s to 20 °C and then heated to 180 °C

with a linear ramp within 290 s. A column flow rate of 20 mL min<sup>-1</sup> was used in all experiments.

For the optimization of chromatography and determination of heart-cut times, the HG-P&T-hcGC was coupled to element-selective online detection by ICP-MS (7500a, Agilent Technologies, Yokogama, Japan). By using a T-piece introduced between the plasma torch and the nebulizer, the GC-efflux was added to the wet aerosol of the nebulizer, which was used for continuous addition of internal standards (10 µg L<sup>-1</sup> Li, Ga, Y, Rb, Rh, Ce, Tl, 100 µg L<sup>-1</sup> In, in 0.65% HNO<sub>3</sub>). 0.1 g of compost containing 1.56 µg TMA<sub>2</sub>O (0.86 µg<sub>As</sub>, 0.41 µg<sub>C</sub>) were analyzed both without heart-cut and with heart-cut between 210-300 s.

#### 4.3.4. Control of the purity of the heart-cut fractions by HG-P&T-hcGC-GC-MS

To control the purity of the compost heart-cut fraction, the HG-P&T-hcGC-system was coupled to a 6890 N GC equipped with a DB-5 capillary column (28 m x 0.25 mm x 0.25 µm) with electron impact mass spectrometric detection (5973 N, all Agilent Technologies, Santa Clara, US). The heart-cut-fraction between 210-300 s of 0.1 g of compost containing 1.56 µg TMA<sub>2</sub>O (0.86 µg<sub>As</sub>, 0.41 µg<sub>C</sub>) was transferred to the liner (ID: 1/8") packed with 10% SP-2100 on 80/100 mesh Supelcoport (Sigma-Aldrich, St. Louis, US) cooled to -100 °C. At the beginning of the GC-MS run the injector was heated to 200 °C. A split ratio of 1:10 and a column flow of 2.5 ml He/min were used. After 3 min at 35 °C, the oven was heated with 30 °C min<sup>-1</sup> to 180 °C and with 100 °C min<sup>-1</sup> to 250 °C held for 3 min. The mass range m/z 33-300 was monitored.

#### 4.3.5. HG-P&T-hcGC-GC-IRMS procedure

For compound-specific δ<sup>13</sup>C-analysis, the HG-P&T-hcGC was coupled to GC-IRMS as illustrated in Figure 4-1. The coupling was realized with a cannula at the end of the heated HG-P&T-hcGC transfer line which penetrated the PTV injector septum (Optic 3, ATAS GL, Eindhoven, Netherlands) of the gas chromatograph (Trace GC Ultra, Thermo Electron Corporation, Bremen, Germany). HG-P&T-hcGC parameters were used as indicated above. The heart-cut fraction between 210-300 s was cryofocussed on-column (15 m x 0.25 mm x 0.25 µm, Rxi-5, Restek Corp., Bellefonte, US) at a temperature of -120 °C. After 7 min, the cryofocussing unit was heated to 200 °C (15 °C s<sup>-1</sup>) and the oven was held at 30 °C for 2 min. Then, the

temperature was raised at a gradient of  $10\text{ }^{\circ}\text{C min}^{-1}$  to  $200\text{ }^{\circ}\text{C}$ . Helium 5.0 (Air Liquide, Oberhausen, Germany) at a constant flow of  $1\text{ mL min}^{-1}$  was used as carrier gas. After capillary chromatographic separation and subsequent combustion *via* a GC-Combustion III Interface (Thermo Electron Corporation, Bremen, Germany) at a temperature of  $960\text{ }^{\circ}\text{C}$  with a NiO/Pt/CuO catalyst. Carbon isotope ratio was then detected by measuring the oxidation product  $\text{CO}_2$  with a MAT 253 (Thermo Electron Corporation) isotope mass spectrometer.

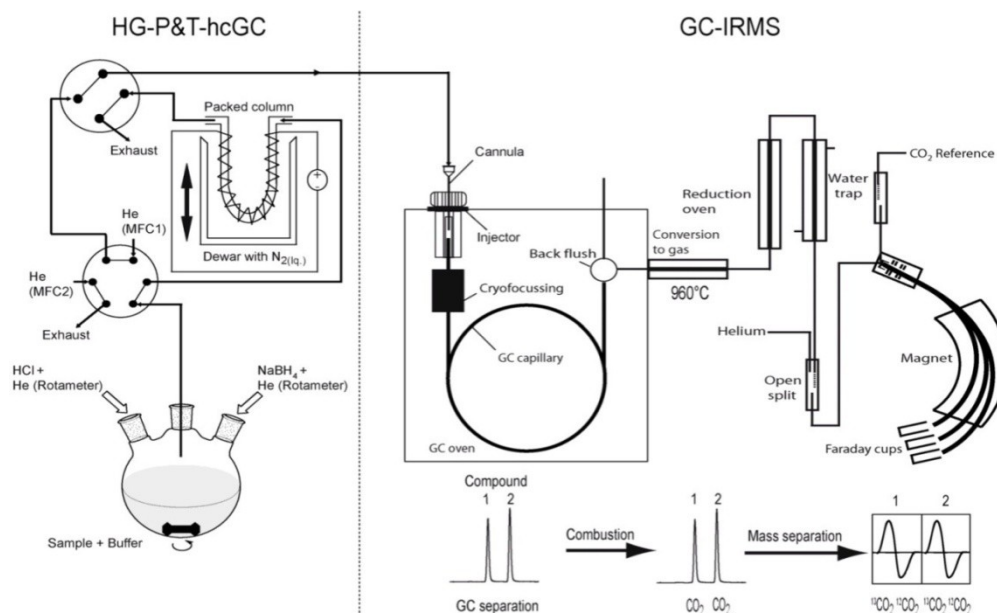


**Figure 4-1.** Schematic overview of the HG-P&T-hcGC-GC-IRMS method. On the left side, the hydride generation, the P&T and the cryofocussing on the packed GC column is shown. On the right side, the GC-IRMS method is illustrated.

Helium of 5.0 quality (Air Liquide, Oberhausen, Germany) was used as carrier gas for the GC-IRMS as well as working gas for the GC combustion interface and the LC-Isolink interface (Thermo Electron Corporation, Bremen).

The isotopic signatures of all compounds were measured relative to  $\text{CO}_2$ , which was calibrated relative to Vienna Pee Dee Belemnite (VPDB). Reoxidation of the combustion oven was carried out regularly after 20 measurements. Data analysis was conducted with the software Isodat 2.5 (Thermo Electron Corporation) and Origin 7.0 (OriginLab, Northampton, US).

#### 4.3.6. Flow-injection analysis-IRMS

Determination of bulk isotopic value for a TMAOs standard was performed by flow-injection analysis (FIA)-IRMS using a Spectra P100 HPLC pump coupled to a DeltaV Advantage isotope ratio mass spectrometer by a LC ISOLINK interface (all Thermo Electron Corporation, Bremen, Germany). As mobile phase for the FIA-IRMS measurements as well as for preparation of solutions and samples, deionized water from the house water purification system was used, which was additionally distilled three times using a distillation unit (Westdeutsche Quarzschmelze, Geesthacht, Germany). 10  $\mu\text{L}$  of an aqueous solution of TMAOs (1  $\mu\text{g}_{\text{As}}$ , 0.47  $\mu\text{g}_{\text{C}}$ ) were analyzed. A flow-rate of 300  $\mu\text{L min}^{-1}$  was used for the mobile phase (water). Oxidation of TMAOs to  $\text{CO}_2$  as achieved using an oxidation reactor heated to 99 °C after addition of 50  $\mu\text{L min}^{-1}$  of orthophosphoric acid (1.5 M) (99%, Fluka, Buchs, Switzerland) and 50  $\mu\text{L min}^{-1}$  sodium peroxodisulfate (100 g  $\text{L}^{-1}$ ) ( $\geq 99\%$ , Fluka, Buchs, Switzerland). After oxidation, the resulting  $\text{CO}_2$  was separated from the liquid phase by a membrane and dried by using two Nafion membranes.  $\text{CO}_2$  was introduced into the Delta V isotope ratio mass spectrometer *via* an open split. For a detailed discussion of LC-IRMS interface we refer to the literature<sup>[5]</sup> and Figure 4-5.

#### 4.3.7. Elemental Analyzer-IRMS measurement of the compost sample

The bulk  $\delta^{13}\text{C}$  value of the compost sample was determined by using an elemental analyzer (EA) (NC2500, Thermoquest, San Jose, CA) coupled to an IRMS Delta XL IRMS (Thermo, Bremen). A USGS 24 standard ( $\delta^{13}\text{C} = -16.00 \text{ ‰}$ , relative to VPDB) was used for calibration of the system. Prior to the measurement, the compost sample was freeze-dried. A bulk  $\delta^{13}\text{C}$  value of  $-29.49 \text{ ‰}$  with a reproducibility of  $\pm 0.01 \text{ ‰}$  and a carbon content of  $44.7\% \pm 5\%$  were determined.

### 4.4. RESULTS AND DISCUSSION

#### 4.4.1. Optimization of matrix separation by HG-P&T-hcGC-ICP-MS

To separate TMAOs from the organic compost matrix, we applied hydride generation and subsequent enrichment of the volatile derivative TMAs by P&T. In order to exclude the introduction of  $\text{CO}_2$  and water into the GC-IRMS system, heart-cut gas chromatography was used for matrix separation. For this purpose, a packed column was preferred, as such columns are less prone to blockage and allow higher purge

flow rates and thus better purging efficiency. Furthermore, packed columns allow simple realization of low-temperature gaschromatography for separation of low-boiling analytes. One problem encountered was that packed columns are operated at higher carrier gas flow rates than capillary columns ( $1 \text{ mL min}^{-1}$  in the GC-IRMS system). In order to couple both systems, it was necessary to split the efflux of the packed GC column, which caused an undesirable loss in sensitivity. In order to minimize this loss, the lowest carrier gas flow necessary for satisfying separation of matrix components had to be determined. Chromatographic optimization and determination of heart-cut points was conducted for the compost sample by online-monitoring of both  $^{13}\text{C}$ - and  $^{75}\text{As}$ -mass traces by ICP-MS.

A flow rate of  $20 \text{ mL min}^{-1}$  proved to be an acceptable compromise yielding a satisfying separation of TMAs from volatile matrix compounds (Figure 4-2a). Baseline separation of di- and trimethylarsine was achieved. The element-specific  $^{13}\text{C}$ -ICP-MS mass trace allowed the monitoring of carbon-containing compounds eluting from the column (Figure 4-2b). While the  $^{75}\text{As}$ - and the  $^{13}\text{C}$ -mass traces of TMAs show the identical retention times, the  $^{75}\text{As}$ -ICP-MS is four orders of magnitude more sensitive in comparison to the  $^{13}\text{C}$ -signal due to the low abundance of the carbon isotope and the lower ionization efficiency of carbon. In comparison to the carbon signal of TMAs, the signal of  $\text{CO}_2$  is more than three orders of magnitude more intensive. Subsequently, the timing of the heart-cut was optimized. In Figure 4-2c&d, a HG-P&T-hcGC-ICP-MS run is shown with the final cut points at 210 and 300 s.

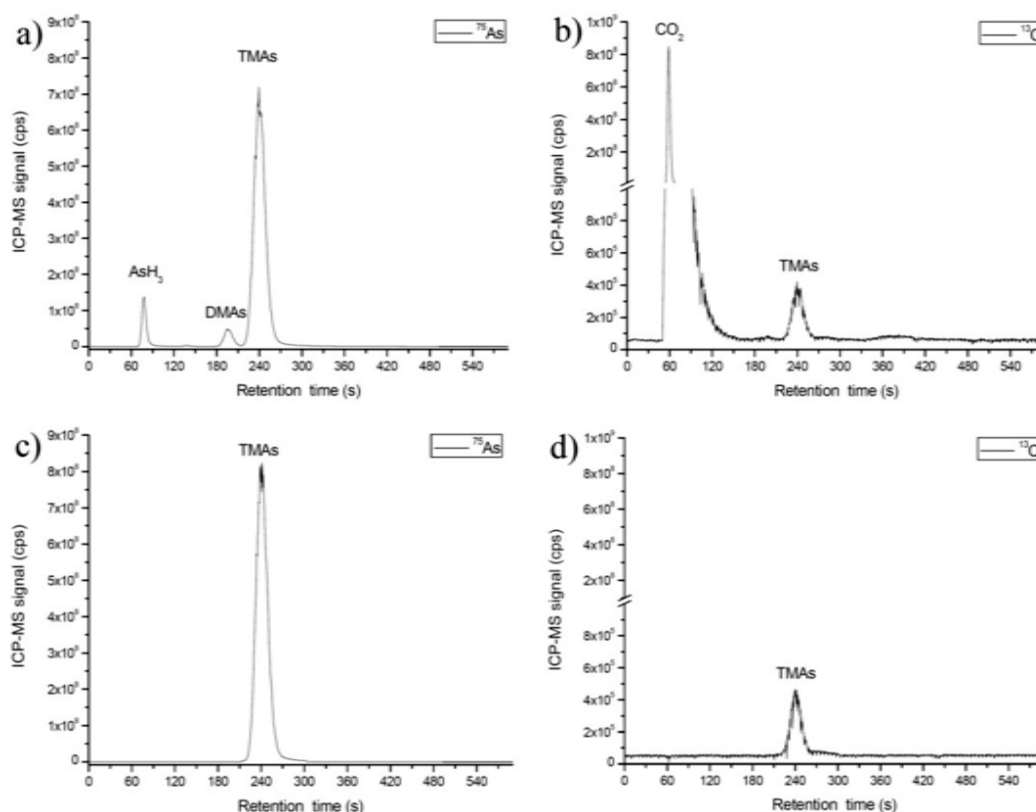


**Figure 4-2.**  $^{13}\text{C}$  and  $^{75}\text{As}$  traces obtained by HG-P&T-hcGC-ICP-MS of 0.1 g compost containing  $1.56 \mu\text{g}$  TMAsO ( $0.86 \mu\text{g}_{\text{As}}$ ,  $0.41 \mu\text{g}_{\text{C}}$ ); Chromatograms a) and b) show the  $^{75}\text{As}$  and  $^{13}\text{C}$  traces without heart-cut and in the chromatograms c) and d) a heart-cut at 210-300 s was applied for successful separation of volatile matrix components from the target compound TMAs.

#### 4.4.2. Control of purity of heart-cut fraction by GC-MS

While ICP-MS has the advantage of species-independent monitoring of carbon-containing compounds, the  $^{13}\text{C}$ -ICP-MS trace has a comparatively low sensitivity. Furthermore, molecule selective detection by GC-MS allows the identification of co-eluting organic trace compounds as well as the verification of the identity of TMAs derivatives. Thus, comparative measurements of the HG-P&T-hcGC fraction were conducted using GC-MS. Therefore, the HG-P&T-hcGC fraction of the standard as well as the compost was cryofocussed, separated on a capillary column and the total ion current in the mass range  $m/z$  33-300 was monitored (Figure 4-3).

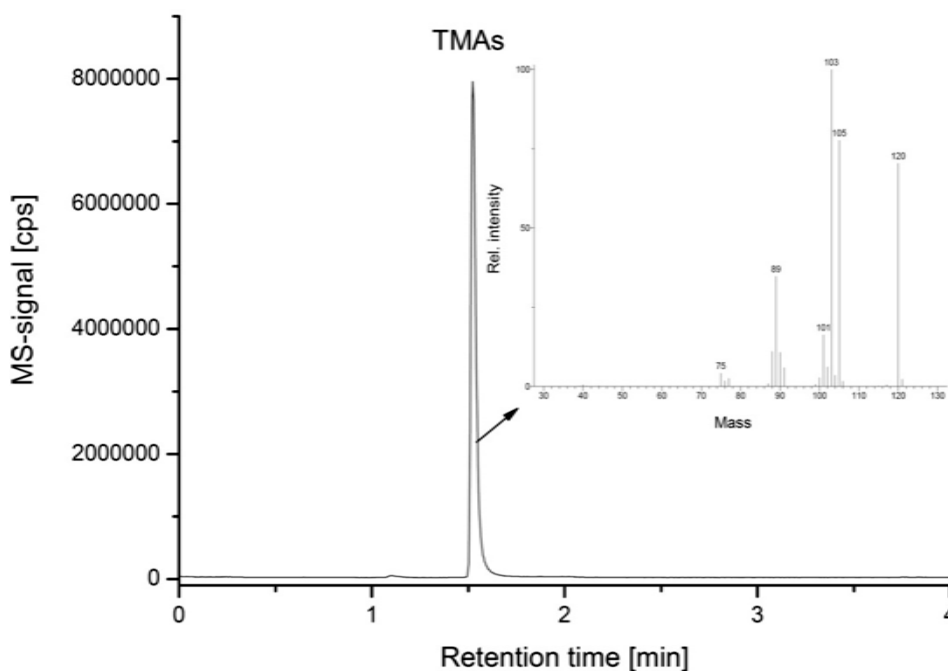


**Figure 4-3.** Chromatogram, obtained by HG-P&T-hcGC-GC-MS of 0.1 g<sub>wet weight</sub> compost containing 1.56  $\mu\text{g}$  TMAOs (0.86  $\mu\text{g}_{\text{As}}$ , 0.41  $\mu\text{g}_{\text{C}}$ ) with heart-cut at 210-300 s. The inserted mass spectrum shows that no other volatile matrix compounds interfere with the TMAOs peak and a clean heart cut of the TMAOs was achieved.

The chromatogram showed that the heart-cut fraction derived from the compost sample contained only TMAOs. The mass spectrum of TMAOs derived from the compost sample was identical to the one from the standard (Figure 4-4) and was consistent over the entire peak range, thereby a co-elution of organic matrix compounds can be excluded.

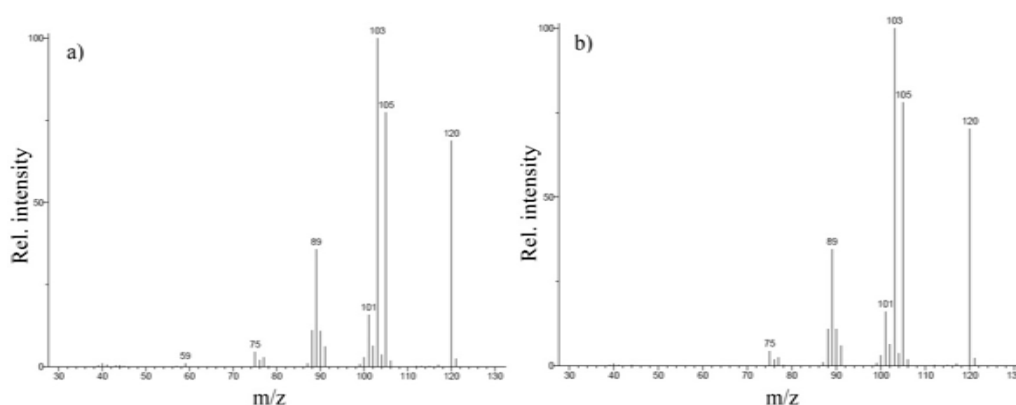


**Figure 4-4.** Comparison of mass spectrum of TMAs measured by HG-P&T-hcGC-GC-MS in a) TMAO standard b) compost sample

#### 4.4.3. HG-P&T-hcGC-GC-IRMS for carbon isotope ratio analysis of TMAO

Prior to the HG-P&T-hcGC-GC-IRMS measurements, the bulk  $\delta^{13}\text{C}$ -value of TMAO standard was measured *via* FIA-IRMS. A mean bulk value of  $-57.67\text{‰}$  was determined with an excellent standard deviation of  $\pm 0.08\text{‰}$  ( $n=4$ ). In Figure 4-5 a FIA-IRMS measurement including the method description is presented.

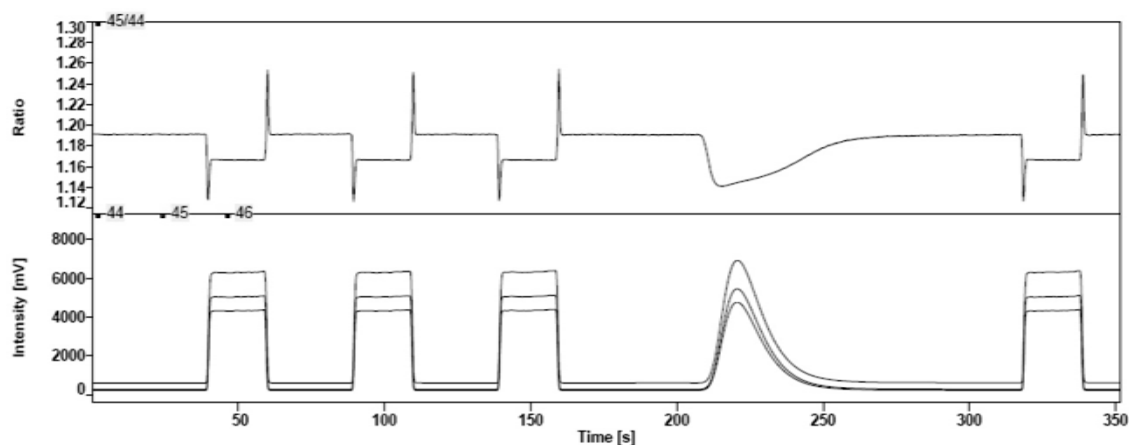


**Figure 4-5.** The lower part shows a FIA-IRMS measurement of  $1.81\ \mu\text{g}$  TMAO-standard ( $1\ \mu\text{g}_{\text{As}}$ ,  $0.47\ \mu\text{g}_{\text{C}}$ ). This concentration was chosen to balance the signal intensity of the sample to the signal intensity of the reference standards as it is used in  $\delta^{13}\text{C}$  bulk analysis by Elemental Analyzer-IRMS. In the upper part, the isotopic swing expressing the ratios of mass 45 ( $^{13}\text{CO}_2$  and  $^{12}\text{C}^{17}\text{O}^{16}\text{O}$ ) to mass 44 ( $^{12}\text{CO}_2$ ) is shown. The first three and the last flat topped peaks correspond to the reference  $\text{CO}_2$  gas. The second reference gas peak was used for calculation of  $\delta^{13}\text{C}$ -values.

Following the optimization of matrix separation using HG-P&T-hcGC-ICP-MS as well as control of peak purity by HG-P&T-hcGC-GC-MS, the carbon isotope ratio analysis of TMAsO was determined by coupling the HG-P&T-hcGC system to GC-IRMS. Due to the different column flow rates of the packed and capillary column ( $20 \text{ mL min}^{-1}$  and  $1 \text{ mL min}^{-1}$ , resp.), a split ratio of 1:20 had to be used. Typical HG-P&T-hcGC-GC-IRMS chromatograms of a TMAsO standard as well as a TMAsO-containing compost sample are presented in Figure 4-6. GC-IRMS measurement confirmed that removal of matrix components was complete, as TMAs was the only peak detected by GC-IRMS in both the standard and the compost.

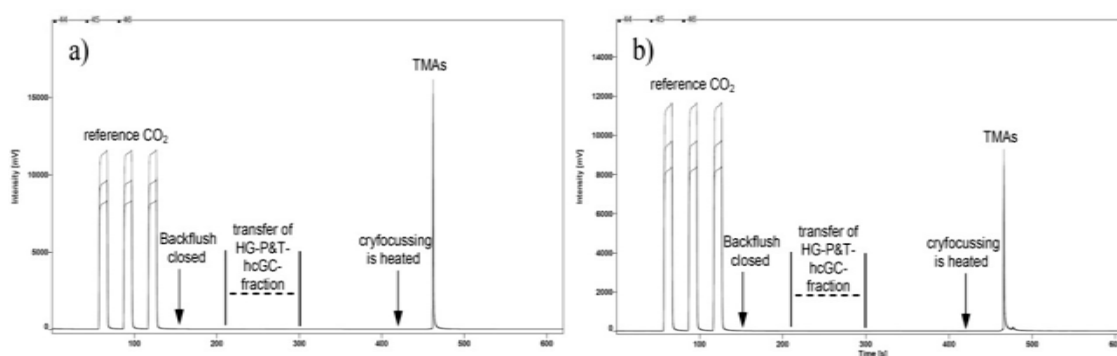


**Figure 4-6.** C-IRMS-chromatogram after hydride generation and matrix separation by HG-P&T-hcGC-GC of a)  $5.44 \mu\text{g}$  TMAsO-standard ( $3 \mu\text{g}_{\text{As}}$ ,  $1.41 \mu\text{g}_{\text{C}}$ ) and b)  $0.31 \text{ g}$  compost containing  $4.83 \mu\text{g}$  TMAsO ( $2.66 \mu\text{g}_{\text{As}}$ ,  $1.26 \mu\text{g}_{\text{C}}$ ). The transfer windows for the heart cut fraction and the heating point of the cryo trap as well as the closure of the back flush are indicated in the chromatograms.

Prior to the start of heart-cut fraction transfer to the cryo trap, the analytical column was connected with the combustion oven by setting open split in and backflush off in order to monitor break-through during the cryofocussing step of the GC-IRMS system. No break-through of TMAs was observed during the measurements.

Subsequently, different amounts of TMAsO standard ranging from  $1.8\text{--}9.1 \mu\text{g}$  were analyzed by HG-P&T-hcGC-GC-IRMS (Figure 4-7), because an amount-dependent variability of  $\delta^{13}\text{C}$  values has been reported for GC-IRMS.<sup>[1, 26-27]</sup> For HG-P&T-hcGC-GC-IRMS analysis of the TMAsO standard, the mean  $\delta^{13}\text{C}$  value of the four highest

concentration levels was  $-57.59\text{‰}$ , which is in excellent agreement with the bulk value determined by FIA-IRMS ( $\Delta\delta^{13}\text{C}_{\text{method value-bulk value}} = -0.08\text{‰}$ ). The high accuracy of the HG-P&T-hcGC-GC-IRMS method demonstrates that no fractionation occurs during derivatization, enrichment and matrix separation. Within this concentration range, reproducibility of  $\delta^{13}\text{C}$  was  $\pm 0.31\text{‰}$  ( $n=12$ ), which is below the typical range of total uncertainty ( $\pm 0.5\text{‰}$ ) reported for GC-IRMS.<sup>[1]</sup> For lower levels of TMAso, higher  $\delta^{13}\text{C}$ -values were observed. Similar observations have been reported by Schmitt *et al.*<sup>[26]</sup> and Sherwood Lollar *et al.*<sup>[1]</sup> As measurements were conducted in randomized order, detector drift effects can be ruled out. Furthermore, signal intensity of all TMAso levels were within the linear range of the IRMS.

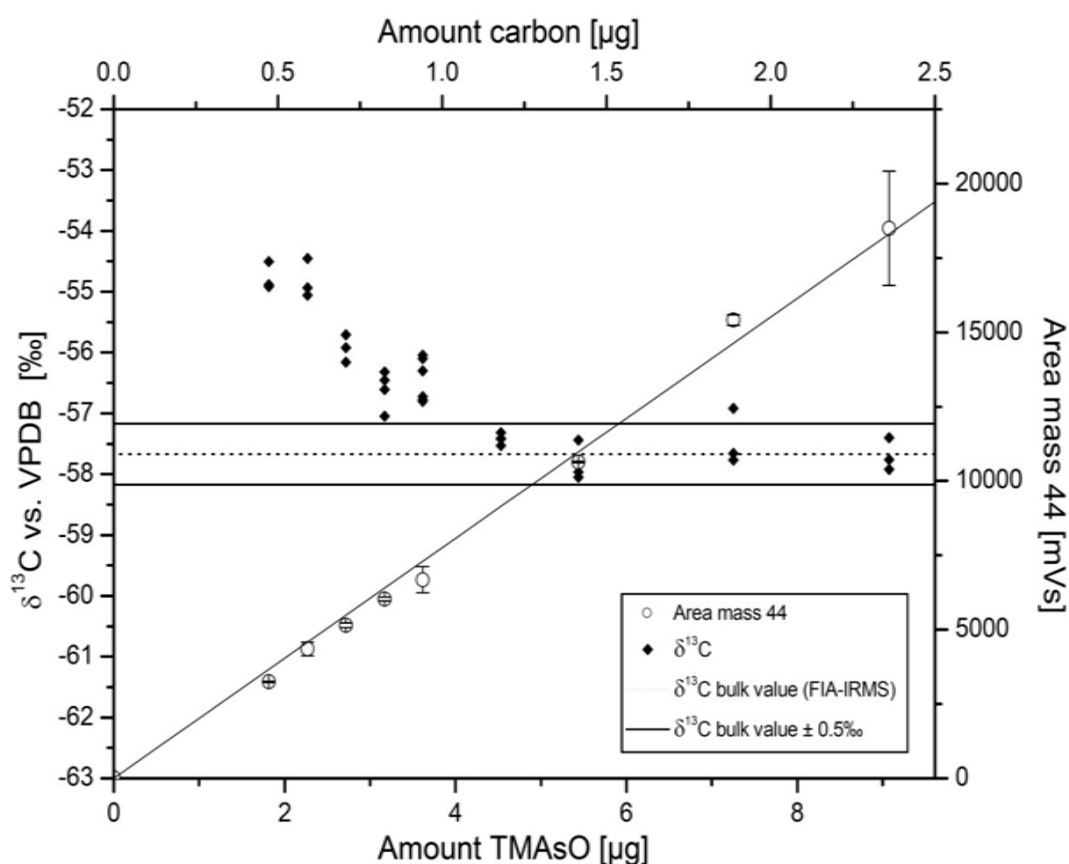


**Figure 4-7.** Determination of the method detection limit for TMAso of the HG-P&T-GC-GC-IRMS method.  $\delta^{13}\text{C}$  values are represented by diamonds, open squares indicate the area of mass 44. The horizontal dotted line represents the mean  $\delta^{13}\text{C}$  bulk TMAso value determined by FIA-IRMS. The solid lines around the mean value represent a  $\pm 0.5\text{‰}$  interval that includes the total uncertainty of isotope analysis incorporating both reproducibility and accuracy.

Based on the  $\pm 0.5$  ‰ criteria for the total uncertainty of GC-IRMS,<sup>[1]</sup> the method detection limit was determined as the lowest TMA<sub>SO</sub> level, for which the  $\delta^{13}\text{C}$  values was within the  $\pm 0.5$  ‰ interval of the bulk value. Thus, a detection limit of  $4.5 \mu\text{g}_{\text{TMA}_{\text{SO}}}$  ( $1.2 \mu\text{g}_{\text{C}}$ ) was determined. According to Sessions,<sup>[3]</sup> in GC-IRMS 0.1-5 nmol carbon is required on-column for a precise determination of the  $\delta^{13}\text{C}$ -value. Taking into account the split ratio of 1:20, an absolute detection limit of the method of  $225 \text{ ng}_{\text{TMA}_{\text{SO}}}$  respectively  $60 \text{ ng}_{\text{C}}$  ( $5 \text{ nmol}_{\text{C}}$ ) was achieved, which is at the upper end of the range indicated by Sessions.

In addition to the isotope ratio determination, the GC-IRMS showed a satisfying linear correlation between the amounts of TMA<sub>SO</sub> derivatized and the area of mass 44 (correlation coefficient  $r = 0.9983$ ). The good correlation offers the feasibility for quantitative determination of TMA<sub>SO</sub> sample concentrations by HG-P&T-hcGC-GC-IRMS, which can be used for the determination of enrichment factors using the Rayleigh equation.

Applicability of the HG-P&T-hcGC-GC-IRMS method on complex matrices was demonstrated by 5-fold analysis of the  $\delta^{13}\text{C}$  value of biogenic TMA<sub>SO</sub> in a compost sample (Figure 4-6b). The biogenic TMA<sub>SO</sub> showed a very low  $\delta^{13}\text{C}$ -value of  $-48.38 \pm 0.41$  ‰. In contrast, the bulk carbon isotope value of the compost determined by EA-IRMS was  $-29.49 \pm 0.01$  ‰. The fractionation between the carbon source (bulk compost) and the organometal(loid) compound can originate from the enzymatic incorporation of the methyl group into methyl donors like methylcobalamin as well as the final transfer to the metal(loid). However, an elucidation of the underlying reaction mechanisms will require the investigation of kinetic isotope effects of the individual reaction steps.

#### 4.5. CONCLUSION

In this work we developed a method for the determination of  $^{13}\text{C}/^{12}\text{C}$  isotopic ratios of organometal(loid) compounds formed by biomethylation in complex matrices. The precision, accuracy as well as the detection limit of this method are suitable for isotope analysis of environmental organometal(loid) samples. The applicability of the HG-P&T-hcGC-GC-IRMS method to real samples has been demonstrated for TMA<sub>SO</sub> in a complex lucerne hay matrix. As the precision of the analytical method is much higher than the observed shift between carbon isotopic pattern of the organometal(loid) compound compared to the bulk value of the compost matrix,

carbon isotope analysis is a feasible tool for investigation of fractionation processes during biomethylation.

Though the developed method is already sensitive enough for studies investigating samples containing high levels of organometal(loid)s, several method parameters have been identified that indicate the potential to substantially improve the overall method performance. First, an optimization of the capillary chromatography is necessary. Because of the high volatility of the partly permethylated element species the use of capillary columns with larger film thickness or the use of cooled GC ovens is preferable. The improvement of the chromatography for low-boiling species will allow to extend the analyzable species spectrum, as methylated Ge-, As, Sn-, Sb-, Te- and Hg-compounds can be derivatised by hydride generation.<sup>[21]</sup>

A substantial increase in the detection limit is expected by an optimization of the sample introduction as well as matrix removal, in particular by lowering the split ratio of 1:20. In the current hcGC-GC-coupling, this could be achieved by using of packed columns with smaller inner diameters. Alternatively, established methods for the removal of CO<sub>2</sub> and water, e.g. increased trapping temperatures or use of Nafion<sup>®</sup> dryers could be used, but their effect on isotopic fractionation has to be investigated carefully. Due to the effective concentration and matrix separation by hydride generation, sample volumes of up to 1 L can be used,<sup>[28]</sup> thereby allowing sufficient sensitivity of the overall method for the investigation of the biomethylation at typical environmental levels.

The use of carbon isotope analysis for methylated metal(loid) compounds is a promising tool for tracing the origin of the organometal(loid) compound complementary to isotope analysis of the metal(loid) by GC-MC-ICP-MS. Depending on the educts and the synthesis route used, anthropogenic organometal(loid) compounds will significantly vary in their respective isotopic patterns.

More interestingly, isotope analysis can be used for elucidation of different mechanistic pathways. In particular, for investigation of the methyl group transfer process during biomethylation of metal(loid)s, carbon isotope analysis can give valuable insights into reaction mechanism. Further information can be obtained by assessing the hydrogen isotope fractionation by using dual isotope plots as shown by Elsner *et al.*<sup>[11]</sup> Overall, the newly developed method offers a wide range of interesting possibilities for further investigations.

#### 4.6. REFERENCES

- [1] T. A. Abrajano, B. Sherwood Lollar, *Org. Geochem.* **1999**, 30, V.
- [2] D. E. Matthews, J. M. Hayes, *Anal. Chem.* **1978**, 50, 1465.
- [3] A. L. Sessions, *J. Sep. Sci.* **2006**, 29, 1946.
- [4] J.-P. Godin, L.-B. Fay, G. Hopfgartner, *Mass Spectrom. Rev.* **2007**, 26, 751.
- [5] M. Krummen, A. W. Hilker, D. Juchelka, A. Duhr, H. J. Schluter, R. Pesch, *Rapid Commun. Mass Spectrom.* **2004**, 18, 2260.
- [6] T. C. Schmidt, L. Zwank, M. Elsner, M. Berg, R. U. Meckenstock, S. B. Haderlein, *Anal. Bioanal. Chem.* **2004**, 378, 283.
- [7] G. F. Slater, *Environ. Forensics* **2003**, 4, 13.
- [8] J. M. Hayes, K. H. Freeman, B. N. Popp, C. H. Hoham, *Org. Geochem.* **1990**, 16, 1115.
- [9] R. U. Meckenstock, B. Morasch, C. Griebler, H. H. Richnow, *J. Contam. Hydrol.* **2004**, 75, 215.
- [10] L. Melander, W. H. Saunders, *Reaction rates of isotopic molecules*, John Wiley, New York, **1980**.
- [11] M. Elsner, L. Zwank, D. Hunkeler, R. P. Schwarzenbach, *Environmental Science and Technology* **2005**, 39, 6896.
- [12] J. S. Thayer, *Appl. Organomet. Chem.* **2002**, 16, 677.
- [13] F. Challenger, *Chem.Rev.* **1945**, 36, 315.
- [14] D. W. Boening, *Chemosphere* **2000**, 40, 1335.
- [15] M. Styblo, Z. Drobna, I. Jaspers, S. Lin, D. J. Thomas, *Environ. Health Perspect.* **2002**, 110, 767.
- [16] D. J. Thomas, J. X. Li, S. B. Waters, W. B. Xing, B. M. Adair, Z. Drobna, V. Devesa, M. Styblo, *Exp. Biol. Med.* **2007**, 232, 3.
- [17] M. Dzurko, D. Foucher, H. Hintelmann, *Anal. Bioanal. Chem.* **2008**, manuscript in press.
- [18] E. M. Krupp, C. Pecheyran, S. Meffan-Main, O. F. X. Donard, *Fresenius' J. Anal. Chem.* **2001**, 370, 573.
- [19] S. Wehmeier, R. Ellam, J. Feldmann, *J. Anal. At. Spectrom.* **2003**, 18, 1001.
- [20] M. Blessing, M. A. Jochmann, T. C. Schmidt, *Anal. Bioanal. Chem.* **2008**, 390, 591.
- [21] R. A. Diaz-Bone, M. Hitzke, *J. Anal. At. Spectrom.* **2008**, 23, 861.

- 
- [22] O. Rouxel, J. Ludden, Y. Fouquet, *Chem. Geol.* **2003**, *200*, 25.
- [23] T. M. Johnson, *Chem. Geol.* **2004**, *204*, 201.
- [24] J. Feldmann, L. Naels, K. Haas, *J. Anal. At. Spectrom.* **2001**, *16*, 1040.
- [25] A. Merijanlian, R. Zingaro, *Inorg.Chem.5* **1966**, *5*, 187.
- [26] J. Schmitt, B. Glaser, W. Zech, *Rapid Commun. Mass Spectrom.* **2003**, *17*, 970.
- [27] M. A. Jochmann, M. Blessing, S. B. Haderlein, T. C. Schmidt, *Rapid Commun. Mass Spectrom.* **2006**, *20*, 3639.
- [28] C. M. Tseng, D. Amouroux, I. D. Brindle, O. F. X. Donard, *J. Environ. Monit.* **2000**, *2*, 603.

**Chapter 5. Position specific isotope analysis of the methyl group carbon in methylcobalamin for the investigation of biomethylation processes and mechanistic investigation of the abiotic methyl transfer from CH<sub>3</sub>Cob to arsenic induced by glutathione**

*Redrafted from “O. Wuerfel, M. Greule, F. Keppler, M. A. Jochmann, T. C. Schmidt, Position Specific Isotope Analysis of the Methyl Group Carbon in Methylcobalamin for the Investigation of Biomethylation Processes, Anal. Bioanal. Chem. (submitted)”*

**5.1. ABSTRACT**

In the environment, the methylation of metal(loid)s is a widespread phenomenon and occurs by abiotic as well as enzymatically catalyzed transfer of a methyl group. While S-adenosyl methionine (SAM) is the main methyl-donor in mammals, methylcobalamin (CH<sub>3</sub>Cob) can be the methyl-donor for the methylation of metal(loid)s by anaerobic microorganisms. As the methylation enhances both biomobility as well as mostly the toxicity of the precursory metal(loid)s, the full comprehension of the underlying reaction mechanism is of high importance. Different reaction mechanisms for abiotic as well as enzyme-catalyzed transfer of the methyl group have been proposed for arsenic, but not really proven yet. Here, carbon isotope analysis can foster our understanding of these processes, as the extent of the isotopic fractionation allows to differentiate between different types of reaction, such as concerted (S<sub>N</sub>2) or stepwise nucleophilic substitution (S<sub>N</sub>1) as well as to determine the origin of the methyl group. For the determination of the kinetic isotope effect the initial isotopic value of the transferred methyl group has to be determined.

To that end, we used hydroiodic acid for abstraction of the methyl group from CH<sub>3</sub>Cob or SAM and subsequent analysis of the formed methyl iodide by gas chromatography isotope ratio mass spectrometry (GC-IRMS). The correctness of position-specific  $\delta^{13}\text{C}$  value of CH<sub>3</sub>Cob was consolidated by using three further independent techniques involving photolytic cleavage with different additives or thermolytic cleavage of the methyl-cobalt bonding and subsequent measurement of the formed methane by GC-IRMS.

Furthermore, we extended a recently developed method for the determination of carbon isotope ratios of organometal(loid)s in complex matrices using hydride

generation for volatilization and matrix separation before heart-cut gaschromatography and IRMS to the analysis of the low boiling partly methylated arsenicals, which are formed in the course of arsenic methylation.

Finally, we demonstrated the applicability of this methodology by investigation of carbon fractionation due to the methyl transfer from  $\text{CH}_3\text{Cob}$  to arsenic induced by glutathione. The obtained kinetic isotope effect ( $KIE= 1.051$ ) points to a concerted mechanism.

## 5.2. INTRODUCTION

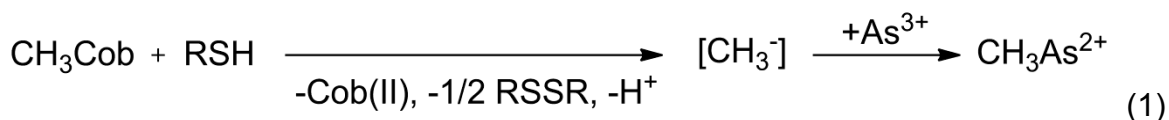
The methylation of a wide of range of metal(loid)s has been shown in the environment.<sup>[1]</sup> Among these metal(loid)s, arsenic is of high toxicological relevance, as it is a widespread ground water contaminant in large parts of the world. Ingestion can lead to many diseases affecting the gastro intestinal tract, respiration tract, skin, liver, cardiovascular system, hematopoietic system, and nervous system.<sup>[2]</sup> As the methylation of metal(loid)s influences both toxicity as well as mobility to a large extent,<sup>[3]</sup> the investigation of these processes is of high importance. Initially, the methylation of arsenic had been considered as a detoxification step,<sup>[4]</sup> but the partly methylated arsenic species seem to be responsible for adverse health effects<sup>[2]</sup> and in cell studies  $\text{MMA}^{\text{III}}$  ( $\text{CH}_3\text{As}(\text{OH})_2$ ) and  $\text{DMA}^{\text{III}}$  ( $(\text{CH}_3)_2\text{AsI}$ ) was shown to be more or at least as toxic as inorganic  $\text{As}^{\text{III}}$ .<sup>[5-6]</sup>

There are mainly two important methyl donors, S-adenosyl methionine (SAM) and methylcobalamin ( $\text{CH}_3\text{Cob}$ ). While SAM is the main methyl-donor in many bacteria and mammals,  $\text{CH}_3\text{Cob}$  can be the methyl-donor for the methylation of metal(loid)s by anaerobic microorganisms. For the methylation of arsenic by SAM, which is catalyzed by a microbial arsenite methyltransferase  $\text{ArsM}^{\text{[7]}}$  or mammal analogues such as Cyt 19,<sup>[8-9]</sup> two contradicting reaction pathways were suggested - either with<sup>[10-11]</sup> or without a change of the oxidation state of arsenic.<sup>[9]</sup>

In the case of  $\text{CH}_3\text{Cob}$ , there are three different possibilities of transferring the methyl group depending on the reaction conditions and the metal(loid) itself,<sup>[12]</sup> either as carbanion, carbocation or as a methyl radical. Beside enzyme-catalyzed methyl transfer from SAM<sup>[1, 9, 13]</sup> or at least enzyme-mediated methyl transfer induced by  $\text{Cob}(\text{I})$ ,<sup>[14]</sup> the non-enzymatical methylation by  $\text{CH}_3\text{Cob}$  has been demonstrated for arsenic in presence of thiols. In this case, three different reaction mechanisms,

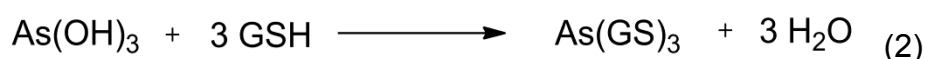
including formation of a crypto carbanion,<sup>[15]</sup> a concerted group exchange<sup>[16]</sup> or a methyl radical transfer<sup>[17]</sup> have been suggested.

Schrauzer proposed the formation of an crypto carbanion, followed by arsenic methylation:<sup>[15]</sup>

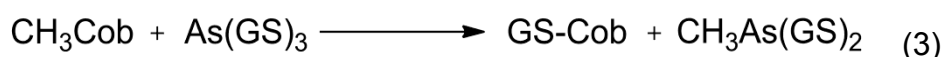


However, the reaction conditions make it unlikely that the reaction proceed via this pathway, as a carbanion is not stable in the solution.

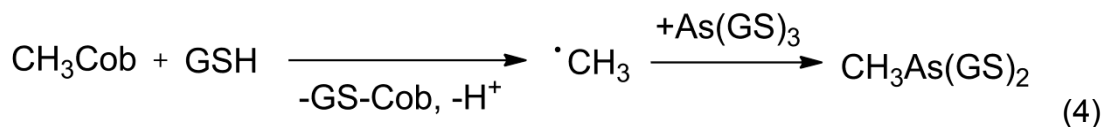
Zakharian and Aposhian showed the methylation of arsenic in presence of GSH. They proposed the formation of a glutathione-arsenic complex (equation 2) followed by nucleophilic attack of the arsenic-GSH complex on  $\text{CH}_3\text{Cob}$ .<sup>[16]</sup>



Hayawa *et al.* showed the formation of the  $\text{As(GS)}_3$  complex and drafted a concerted group exchange mechanism according to equation (3).<sup>[9]</sup>



Finally, Nakamura *et al.* assumed a radical mechanism (equation 4). By transaxial coordination of  $\text{CH}_3\text{Cob}$  a Co-GSH complex and a methyl radical is formed, which reacts with  $\text{As(GS)}_3$ .<sup>[17]</sup>



For the elucidation of reaction mechanisms, compound specific isotope analysis (CSIA) is a valuable tool, as the observation of the carbon isotopic fractionation during the methyl transfer allows the differentiation between different types of reaction.<sup>[18]</sup> For CSIA, a separation of single compounds is needed, which can be

achieved by gaschromatography (GC).<sup>[19-20]</sup> In the case of carbon, after separation follows a catalytic oxidation to CO<sub>2</sub> and subsequent analysis of the isotope ratios by an isotope ratio mass spectrometer (IRMS).

The isotopic fractionation originates from different reaction rates ( $k_{light}$ ,  $k_{heavy}$ ) of molecules containing the lighter and molecules containing the heavier isotope (isotopologues) due to their different physicochemical properties. The lighter isotopologue has a lower zero-point energy than the more stable heavier one leading to different activation energies for a reaction, where bonds are broken and new ones are formed. This activation energy varies dependent on the different types of reaction, due to different molecular geometry during the transition state.<sup>[18]</sup> The relation between the reaction rates yields the kinetic isotope effect ( $KIE$ ) (equation 5).

$$KIE = \frac{k_{light}}{k_{heavy}} \quad (5)$$

Collected data showed that the  $KIE$  for a concerted reaction (S<sub>N</sub>2) with a symmetric transition state is in the range of 1.03-1.08 and for a stepwise reaction (S<sub>N</sub>1) in the range of 1-1.03.<sup>[21]</sup> For the determination of the  $KIE$  the ratio  $R$  of the heavy to the light isotope according to equation 6 regarding to carbon is determined for a sample by IRMS.

$$R = \frac{^{13}\text{C}}{^{12}\text{C}} \quad (6)$$

Due to the small differences of the isotopic ratios resulting in small values, the delta notation is used. The delta value for <sup>13</sup>C is defined as following:

$$\delta^{13}\text{C} = \frac{R_{sample} - R_{VPDB}}{R_{VPDB}} \quad (7)$$

$R_{sample}$  represents the ratio of the light to the heavy isotope of the sample.  $R_{VPDB}$  is the ratio of the internal standard Vienne PeeDee Belemnite (VPDB) which is used for referencing.

The isotopic fractionation between a reactant and a product can be described according to equation 8 using the fractionation factor  $\alpha$  which is related to the  $KIE$  and the enrichment factor  $\epsilon$  that is used, because  $\alpha$  is close to 1.

$$\alpha = \frac{\delta^{13}\text{C}_{\text{product}+1}}{\delta^{13}\text{C}_{\text{reactant}+1}} = \frac{1}{KIE} = \epsilon + 1 \quad (8)$$

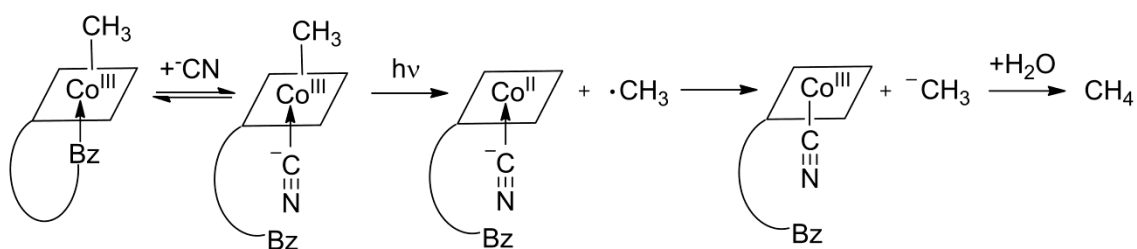
For irreversible reactions in a closed system, the enrichment factor  $\epsilon$  is related to the reactant at time  $t$  and  $t=0$  (initial value) according to the Raleigh equation (equation 9), with  $f$  as the remaining fraction of the reactant.

$$\epsilon \times \ln f = \ln \frac{\delta_{\text{reactant},t+1}}{\delta_{\text{reactant},0+1}} \quad (9)$$

The aim of this work was the determination and validation of the initial  $\delta^{13}\text{C}$  value of the methyl group of methylcobalamin, which is needed for the determination of the kinetic isotope effect in the methylation of metal(loid)s. Since site-specific natural isotope fractionation nuclear magnetic resonance spectroscopy (SNIF-NMR) requires high sample amounts and solubility for an acceptable signal to noise ratio, such as a 50 % solution (w/v) for vanillin<sup>[22]</sup> and it is very complicated or even impossible to apply to complex compounds like  $\text{CH}_3\text{Cob}$ , a method for abstraction of the methyl group and subsequent measurement of the methyl derivative was needed. The requirements were to ensure that no fractionation occurs during this abstraction reaction as well as to exclude a contamination with other sources of carbon.

Several promising possibilities for abstraction of the methyl group of methylcobalamin have already been described in the literature.<sup>[23-26]</sup> The anaerobic photolysis or thermolysis yield methane and ethane.<sup>[23]</sup> In the case of thermolysis, a time dependency of the methane to ethane ratio was observed. As more methane is formed during onset of the reaction this indicates a preference for the abstraction of hydrogen before a radical dimerization becomes significant.<sup>[23]</sup> For photolysis, experiments with deuterated  $\text{CH}_3\text{Cob}$  revealed that 95 % of the formed ethane originates from dimerization and the 5 % left are formed by ligand methyl group abstraction.<sup>[23]</sup> The formation of ethane as byproduct during photolysis can be suppressed by addition of an alcohol, such as isopropyl alcohol, which can act as

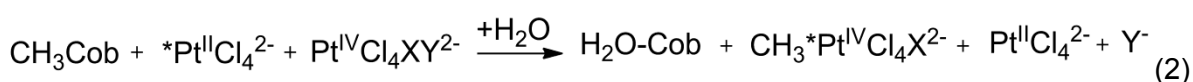
hydrogen donor.<sup>[23, 27]</sup> The methyl radical formed by homolytic cleavage of the carbon-cobalt bond abstracts hydrogen of isopropyl alcohol in the alpha position. This was verified by the finding of pinacol in an extract of an anaerobically photolyzed solution of methylcobalamin in isopropyl alcohol.<sup>[27]</sup> In addition, cyanide increases the electron density of cobalt by displacing the 5,6-dimethylbenzimidazole ligand and thus favors the reduction of the methyl radicals to carbanions according to equation 1,<sup>[23]</sup> which should result in exclusive methane formation.



Bz=benzimidazole

(1)

As an alternative to these approaches, platinum (II/IV) couples can be used for quantitative abstraction of the methyl group from  $\text{CH}_3\text{Cob}$  (equation 2). In the course of the reaction a trinuclear complex is formed and platinum undergoes a redox switch.<sup>[28]</sup> By subsequent extraction of the cobalamin with phenol followed by lyophilization a methylhexachloro platinate can be isolated<sup>[24]</sup> as main reaction product.



All the former abstraction techniques have been used in the presented work for the determination of the initial isotopic signature of methylcobalamin. The reaction products are measurable using GC-IRMS and flow injection analysis (FIA)-IRMS or elemental analyzer (EA)-IRMS, respectively. Furthermore, as the reaction of methylcobalamin and iodide has been demonstrated,<sup>[25]</sup> we tested a method basing on the Zeisel method, which is actually used for the abstraction of methoxy groups.<sup>[29]</sup> Hydroiodic acid (HI) is used for abstraction of the methyl group from  $\text{CH}_3\text{Cob}$  or SAM yielding methyl iodide which is subsequently analyzed by GC-IRMS. For the determination of  $\delta^{13}\text{C}$  values of plant methoxyl groups, Keppler *et al.*<sup>[30]</sup> employed a technique that was a modification of the Zeisel method. This technique was improved

and validated by Greule *et al.*<sup>[31]</sup> using methoxyl-rich plant components, such as vanillin, lignin, wood and pectin. The analytical precision obtained, expressed as the average standard deviation for these compounds, was found to be better than 0.13 ‰.

As the methylation of arsenic is a stepwise process, we additionally extended a recently developed method, which uses selective derivatization of non-volatile organometal(loid)s by hydride generation (HG) for matrix separation followed by purge and trap (P&T) enrichment, heart-cut gaschromatography (hcGC-GC) and subsequent analysis by isotopic ratio mass spectrometry (IRMS)<sup>[32]</sup> to the analysis of partly methylated arsenic species to allow future studies on the methylation of arsenic.

To demonstrate the applicability of this methodology to the investigation of methylation processes, we exemplarily investigated the fractionation of the methyl group carbon of methylcobalamin while the methyl transfer to arsenic induced by glutathione (GSH).

### 5.3. EXPERIMENTAL SECTION

For all experiments deionized water (Seralpur Pro 90 CN system, Elga Berkefeld GmbH, Celle, Germany) has been used. In the case of anaerobic experiments the water has been freed from oxygen by bubbling with nitrogen. All chemicals had analytical grade or better, if not stated otherwise.

#### 5.3.1. Position specific determination of the methyl group of CH<sub>3</sub>Cob using photolytic or thermolytic cleavage

For photolytic methyl group abstraction, 100 µL of 6.4 µM CH<sub>3</sub>Cob (Sigma-Aldrich, St. Louis, MO, USA) were mixed with 900 µL isopropyl alcohol (VWR International BVBA, Leuven, Belgium) under dim red light in an anaerobic glove box (2% H<sub>2</sub>/98% N<sub>2</sub>).

Alternatively, 100 mM KCN (Merck, Darmstadt, Germany) and 100 mM NaOH (VWR, Leuven, Netherlands) were added to 200 µL of 6.4 µM CH<sub>3</sub>Cob. Vials (2 mL, clear) were airtight sealed using 1.3 mm PTFE/silicon septa and placed 10.5 cm in front of a 200 W standard light bulb for 65 h or for 120 min in front of a 100 W UV-lamp (254 nm) in the case of the mixture containing CH<sub>3</sub>Cob and KCN.

Thermolytic cleavage was achieved by heating 200  $\mu\text{L}$  of 6.4  $\mu\text{M}$   $\text{CH}_3\text{Cob}$  in vials which were encased in pressure vessels at 250°C for 150 min. As the pressure produced by vaporization of the water would lead to bursting of silicon septa, an equivalent amount of water was added to the pressure vessels compensating the inner pressure of the vial. 300-500  $\mu\text{L}$  headspace each were sampled for GC-IRMS using a gas-tight syringe. For determination of the methane yield, different aliquots of 2% methane (purity 2.5, Messer Griesheim, Bad Soden, Germany) in He (purity 5.0, Air Liquide, Oberhausen, Germany) were injected into the GC-IRMS system for calibration (Figure 5-1).

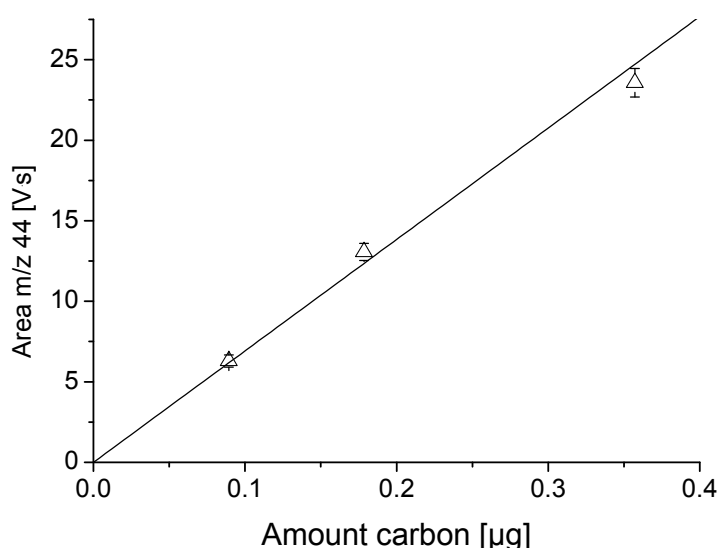


**Figure 5-1.** GC-IRMS calibration slope for  $\text{CH}_4$

A 30 m Q-bond column, 0.32 mm inner diameter, 10  $\mu\text{M}$  film thickness (Restek GmbH, Bad Homburg, Germany) was used for separation. The flow of the helium 5.0 carrier gas (Air Liquide, Oberhausen, Germany) was set to 1.6  $\text{mL min}^{-1}$  and split flow to 32  $\text{mL min}^{-1}$ . The oven was held at 30°C for 5 min and then raised with a rate of 30°C  $\text{min}^{-1}$  to a final temperature of 120°C. After separation and subsequent combustion *via* a GC-Combustion III Interface (Thermo Fisher Scientific, Bremen, Germany), carbon isotope ratios of the oxidation product  $\text{CO}_2$  were measured with a MAT 253 isotope mass spectrometer (Thermo Fisher Scientific, Bremen, Germany) and measured relative to  $\text{CO}_2$ , which was calibrated relative to Vienna Pee Dee Belemnite (VPDB).

### 5.3.2. Position specific determination of the methyl group of CH<sub>3</sub>Cob using platinum(II)/platinum(IV)

2 mL of 5 mM of K<sub>2</sub>PtCl<sub>6</sub>, K<sub>2</sub>PtCl<sub>4</sub>, (both, Alfa Aesar GmbH, Karlsruhe, Germany) and CH<sub>3</sub>Cob in 10 mM HCl (Fischer Scientific, Schwerte, Germany) in a 20 mL vial, which was wrapped with alumina foil, were allowed to react for 24 h. The completeness of the reaction was controlled by UV/Vis spectroscopy as a conversion of the spectrum from methylcobalamin to aquocobalamin (Specord 200, Analytic Jena, Jena, Germany).

Without a preliminary separation by liquid chromatography aquocobalamin would significantly falsify the  $\delta^{13}\text{C}$  measured *via* FIA-IRMS. Thus, for extraction of the formed aquocobalamin 3 x 1 mL phenol (Sigma-Aldrich, St. Louis, USA) were used. Again, this was checked using UV/Vis spectroscopy. After 24 h of lyophilization in the dark (ALPHA 1-4 MARTIN CHRIST Gefriertrocknungsanlagen GmbH, Osterode, Germany), the residue was diluted in 1 mL water. 10  $\mu\text{L}$  of the aqueous solution were analyzed by FIA-IRMS using a HPLC pump (Spectra P100) coupled to a Delta V Advantage isotope ratio mass spectrometer by a LC Isolink interface (all Thermo Fisher Scientific, Bremen, Germany). Water with a flow of 300  $\mu\text{L min}^{-1}$  was used as mobile phase. The oxidation of the methyl-platinum complex to CO<sub>2</sub> was achieved by addition of 1.5 M orthophosphoric acid (Fluka, Buchs, Switzerland) sodium peroxodisulfate (100 g L<sup>-1</sup>) (Fluka, Buchs, Switzerland) with a flow rate of 50  $\mu\text{L min}^{-1}$  and passing an oxidation reactor heated to 99°C. The resulting CO<sub>2</sub> was separated from the liquid phase by a membrane, dried by two Nafion membranes, introduced into a Delta V mass spectrometer (Thermo Fisher Scientific, Bremen, Germany) via an open split and measured relative to CO<sub>2</sub>, which was calibrated against VPDB.

### 5.3.3. Position specific determination of the methyl group of CH<sub>3</sub>Cob using HI

About 10-15 mg CH<sub>3</sub>Cob or 3-6 mg SAM (both Sigma-Aldrich, St. Louis, MO, USA) were placed in 1.5 mL glass vials and 0.5 mL 55-58% hydriodic acid (Fluka, Buchs, Switzerland) were added. Then, the vials were sealed with crimp caps with 0.9 mm PTFE-lined butyl rubber septa and heated in an oven for 30 min at a temperature of 130°C. For the measurement of the methyl iodide standard (Seelze, Germany or Gillingham, UK), vials were first sealed and then 1  $\mu\text{L}$  liquid methyl iodide was injected through the septum of each using a GC syringe (1  $\mu\text{L}$ , Hamilton Bonaduz

AG, Bonaduz, Switzerland). Following an equilibration period of 30 min, 20-90  $\mu\text{L}$  of the headspace (depending on the sample amount) was injected into the GC-IRMS system by the GC autosampler using a gas-tight syringe. For the measurement of the methyl iodide standard (Sigma-Aldrich, Munich, Germany), vials were first sealed and then 1  $\mu\text{L}$  liquid methyl iodide was injected through the septum of each using a GC syringe (10  $\mu\text{L}$ , Hamilton Bonaduz AG, Bonaduz, Switzerland). Subsequently, 5  $\mu\text{L}$  of headspace from the standard vial were injected into the GC-IRMS system.

For determination of position-specific carbon isotope ratios, a HP 6890N gas chromatograph (Agilent, Santa Clara, CA, USA) equipped with an A200S autosampler (CTC Analytics, Zwingen, Switzerland) was coupled to a Delta<sup>PLUS</sup>XL isotope ratio mass spectrometer (ThermoQuest Finnigan, Bremen, Germany) using a GC Combustion III Interface (ThermoQuest Finnigan) with a Cu/Ni/Pt catalyst (activated by oxygen) at 960°C. A 30m ZB-5ms (0.25 mm i.d., 1.0  $\mu\text{m}$  film thickness; Phenomenex, Torrance, CA, USA) capillary column was used with an injector temperature of 200°C. Helium at a constant flow of 1.8  $\text{mL min}^{-1}$  was used as the carrier gas. Split ratio was set to 10:1. Oven temperature was held at 30°C for 3.8 min. Then, the temperature was raised at a gradient of 30°C  $\text{min}^{-1}$  to 100°C. The isotope signatures were measured relative to a high purity  $\text{CO}_2$  reference working gas (carbon dioxide 4.5, Messer Griesheim, Frankfurt, Germany).  $\text{CH}_3\text{Cob}$  or SAM samples were usually analyzed 5 times and all  $\delta^{13}\text{C}$  values were normalized relative to VPDB using a  $\text{CH}_3\text{I}$  standard. The  $\delta^{13}\text{C}$  value of  $\text{CH}_3\text{I}$  was calibrated against international reference substances (IAEA-CH-6, IAEA-CH-7, NBS-22) using an offline EA-IRMS (Iso-Analytical Ltd, Sandbach, UK). The calibrated  $\delta^{13}\text{C}$  value in ‰ vs. VPDB for  $\text{CH}_3\text{I}$  was  $-69.27 \pm 0.05$  ‰ ( $n=15$ ,  $1\sigma$ ).  $\text{CH}_3\text{I}$  standard measurements were made after every fifth sample injection.<sup>[31]</sup>

#### 5.3.4. Modifications of the hydride generation method

Basically, the same hydride generation setup and separation technique as previously described was used.<sup>[32]</sup> In accordance to a study by Diaz-Bone,<sup>[33]</sup> we used a gradient for high efficient hydride generation. In brief, now 10 mL of 1 M  $\text{NaBH}_4$  (Alfa Aesar, Karlsruhe, Germany) stabilized with 0.1 M  $\text{NaOH}$  (Carl Roth GmbH, Karlsruhe, Germany) and 10 mL of 2 M  $\text{HCl}$  (trace analysis grade, Fischer Scientific, Schwerte, Germany) were added within 480 s to the liquid sample diluted in 40 mL of 40 mM citrate buffer at pH 7 (prepared from citric acid (Fluka, Buchs, Switzerland)

and trisodiumcitrate dihydrate (Merck, Darmstadt, Germany)). To expel volatile arsenicals, the solution was purged with a helium flow of 230 mL min<sup>-1</sup> (400 mL min<sup>-1</sup> before) during the addition of chemicals and for additional 120 s after this. The purge flow rate was reduced to prevent freezing of the column as we increased the total purge time due to a prolonged addition of chemicals. Additionally, we changed the GC program for the packed column (ID: 4 mm, length: 40 cm, stationary phase 1.15 g of 10% SP-2100 on 80/100 mesh Supelcoport (Sigma-Aldrich, St. Louis, US), which was wrapped with 2.1 m resistance wire (3.9 Ω m<sup>-1</sup>; Block, Werden, Germany). After removal of the dewar with liquid nitrogen, the column was warmed by ambient air for 150 s and then heated to 180°C with a linear ramp within 570 s. Furthermore, the flow rate for packed column gas chromatography was lowered to 10 mL min<sup>-1</sup> for all experiments.

#### 5.3.5. Validation of the heartcut-window using HG-P&T-hcGC-GC-EI-MS detection

The heart-cut window was validated by HG-P&T-hcGC-GC coupled to electron ionization mass spectrometry (EI-MS). The coupling was realized with a cannula at the end of the heated HG-P&T-hcGC transfer line which penetrated the standard GC split/splitless injector (Trace GC Ultra, Thermo Electron Corporation, Bremen, Germany).

The heart-cut fraction of the packed GC (see above) between 120-300 s was cryofocussed on a pre-column (Optic 3, ATAS GL, Eindhoven, Netherlands) of the GC-MS system (Trace GC Ultra, Thermo Electron Corporation, Bremen, Germany). A cryofocussing temperature of -165°C was used. After 7 min, the temperature of the cryofocussing was raised with a rate of 15°C s<sup>-1</sup> to a temperature of 200°C. For separation a 60 m VMS column with 0.32 mm i.d. and 1.8 μm film thickness (Restek Corp., Bellefonte, US) with a helium flow of 1 mL min<sup>-1</sup> was used. The inlet temperature was set to 120°C. The oven temperature of 35°C was held for 12 min and afterwards raised with a rate of 15°C min<sup>-1</sup> to an end temperature of 155°C.

#### 5.3.6. Extended method for determination of carbon isotope ratios of organometal(loid)s in complex matrices

For analysis of carbon isotope ratios of organometal(loid)s, the heart-cut fraction between 120 s to 450 s was transferred to the GC-IRMS system after hydride generation (see above). GC-IRMS setting was as follows: For capillary separation, a

30 m Optima 1 thick-film column (0.32 i.d., 10 µm film thickness, Macherey-Nagel, Düren, Germany) was used. The carrier flow was set to 1 mL min<sup>-1</sup>. The cryofocussing temperature was set to -165°C. After 8 min, the cryofocussing was heated with a rate of 30°C s<sup>-1</sup>. Oven temperature was held at 45°C for 18 min and then raised with a rate of 5°C min<sup>-1</sup> to 75°C and afterwards with 30°C to 165°C, then hold for 1 minute.

For determination of the method detection limits, different amounts of arsenic species were analyzed using aliquots of a standard stock solution containing MMA<sup>V</sup> (CH<sub>3</sub>AsO(ONa)<sub>2</sub>, Argus Chemicals, Vernio, Italy), DMA<sup>V</sup> ((CH<sub>3</sub>)<sub>2</sub>AsO(OH)), Strem Chemicals, Kehl, Germany), TMAO ((CH<sub>3</sub>)<sub>3</sub>AsO)), which was synthesized by oxidation of trimethylarsine (Strem Chemicals, Kehl, Germany) with hydrogen peroxide in diethyl ether.<sup>[34]</sup> A MMA<sup>V</sup>:DMA<sup>V</sup>:TMAO ratio of 6:3:2 mg L<sup>-1</sup> arsenic content was chosen resulting in a similar response in IRMS for all methylated arsenicals due to the same content of carbon. At least triplicates of all concentration levels were measured.

#### 5.3.7. Elemental analysis (EA-IRMS) measurement of the arsenic standard compounds

The bulk δ<sup>13</sup>C values of arsenic standard compounds, which were used for calibration were determined by using an elemental analyzer (EA) (NC2500, Thermoquest, San Jose, CA) coupled to a MAT 253 (Thermo Fisher Scientific, Bremen, Germany) isotope ratio mass spectrometer. A NBS 22 standard (δ<sup>13</sup>C = -30.03 ‰, relative to VPDB) was used for calibration of the system.

#### 5.3.8. Abiotic methylation of arsenic by methylcobalamin in presence of GSH

For abiotic methylation experiments, 2.5 mL of 500 µM CH<sub>3</sub>Cob, 25 mM reduced GSH (C<sub>10</sub>H<sub>17</sub>N<sub>3</sub>O<sub>6</sub>S, Sigma-Aldrich, St. Louis, US), and 170 µM AsNaO<sub>2</sub> (Fluka, Buchs, Switzerland) in 50 mM phosphate Buffer (K<sub>2</sub>HPO<sub>4</sub>+KH<sub>2</sub>PO<sub>4</sub>, both Merck, Darmstadt, Germany), adjusted to a pH of 7.2, were incubated at 37°C for 0-12 days. For strict anaerobic conditions, the solutions were prepared in 20 mL Vials wrapped with alumina foil and sealed airtight with screw caps with septa in an anaerobic glove box (2% H<sub>2</sub>/98% Ar) under dim red light. After incubation, the abiotic methylation assays were frozen to -20°C until the measurement. Aliquots of 2 mL were measured with

the extended method for determination of the carbon isotopic ratios in complex matrices.

## 5.4. RESULTS AND DISCUSSION

### 5.4.1. Position-specific determination of the methyl-group of methylcobalamin

In order to investigate and compare methylation processes, it is necessary to determine the isotopic signature of the methyl group of methylcobalamin. Because of the high importance of this value for the calculation and future investigations, we used five independent approaches.

At first, the use of platinum (II) and platinum (IV) for complete abstraction of the methyl group followed by a phenol extraction of the aquocobalamin followed by lyophilization of the platinum complexes similar to Fanchiang *et al.*<sup>[23]</sup> and subsequent analysis of the methyl platinum complex by FIA-IRMS was tested. After incubation for 24 h, the completeness of demethylation of CH<sub>3</sub>Cob by the platinum (II/IV) couple was controlled by UV/Vis spectroscopy. As expected, aquocobalamin was formed from methylcobalamin (Figure 5-2A). After extraction with phenol, the aquocobalamin could be completely removed as indicated by a second UV/Vis measurement (Figure 1-2B). However, the  $\delta^{13}\text{C}$  value obtained by subsequent measurement of the methyl-platinum complex ( $\delta^{13}\text{C} = -39.3 \pm 0.4 \text{ ‰}$ ) by FIA-IRMS after lyophilization (Figure 5-3) was significantly different from the ones obtained by the other methods (see below). This probably was caused by an incomplete separation of solvated phenol by lyophilization (solubility in water of 0.5 M at 20°C, boiling point 182°C) which results in a significant falsification of the measured  $\delta^{13}\text{C}$  values.

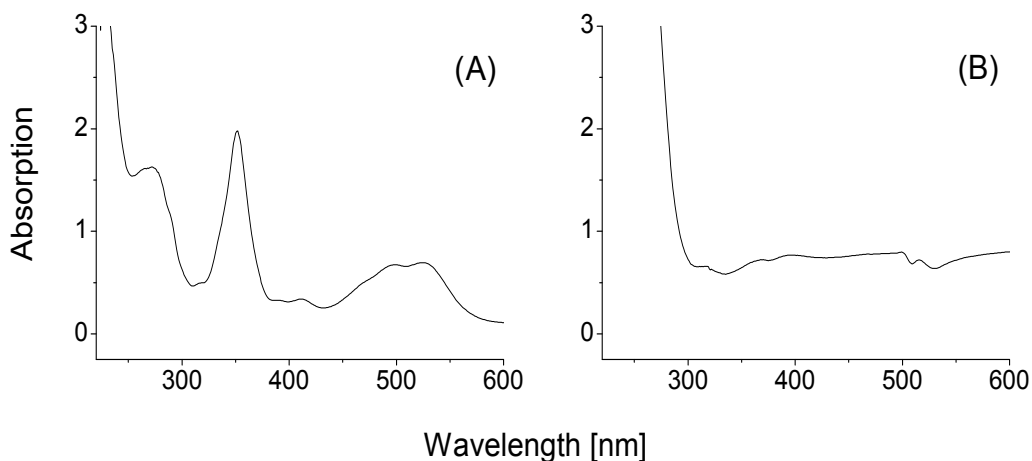


**Figure 5-2.** Control of the completeness of the conversion of  $\text{CH}_3\text{Cob}$  to aquocobalamin using  $\text{Pt}^{\text{II}}$  and  $\text{Pt}^{\text{IV}}$  (A) and removal of aquocobalamin after phenol extraction (B) by UV/Vis spectroscopy. The characteristic wavelength of aquocobalamin is 350 nm. As this absorption band in (A) shows no shoulder at about 340 nm originating from remaining  $\text{CH}_3\text{Cob}$ , the conversion seems to be quantitative. Solutions were diluted to a “theoretical” cobalamin concentration of 100  $\mu\text{M}$  before measurement.

This problem could possibly be solved by a LC-separation of the Pt-complex and the still remaining phenol, before the analysis by IRMS. However, such an approach was not pursued due to a potential isotope fractionation in a further transformation of the complex. For the same reaction with  $^{14}\text{C}$ -labeled  $\text{CH}_3\text{Cob}$  a complete demethylation of  $\text{CH}_3\text{Cob}$  was shown, but a significant loss of the label upon lyophilization or chromatography was observed by Taylor and Hanna.<sup>[34]</sup>

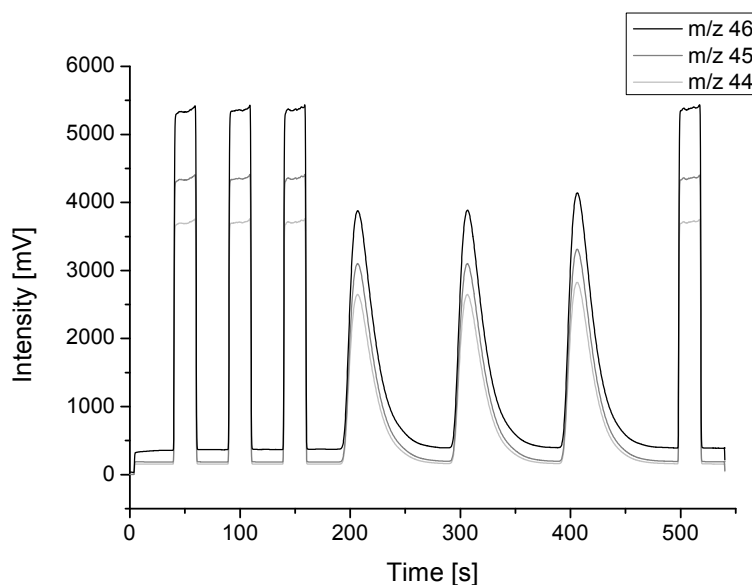


**Figure 5-3.** FIA-IRMS measurement of the methyl-platinum complex after phenol extraction and lyophilization. The first three and the last flat topped peak correspond to the reference CO<sub>2</sub> gas.

The second approach used the photolytic abstraction of the methyl group. The reaction was carried out in 90% isopropyl alcohol as hydrogen donor to prevent formation of ethane or other side products. Although no formation of other products were observed (Figure 5-4) the methane yield was only  $37 \pm 3\%$  after 65 h irradiation by a light bulb. Prolonging the time of photolysis for additional 24 h showed no significant increase of the methane yield. A  $\delta^{13}\text{C}$  value of  $-127.2 \pm 0.4 \text{ ‰}$  was determined by GC-IRMS analysis ( $n=4$ ). An incomplete oxidation of the CH<sub>4</sub> in the oxidation reactor can be excluded, as we found the same areas of m/z 44 obtained by CH<sub>4</sub> and CO<sub>2</sub> standards at the same concentration and observed no peak at the retention time of CH<sub>4</sub> at m/z 15 ( $^{+}\text{CH}_3$ ).

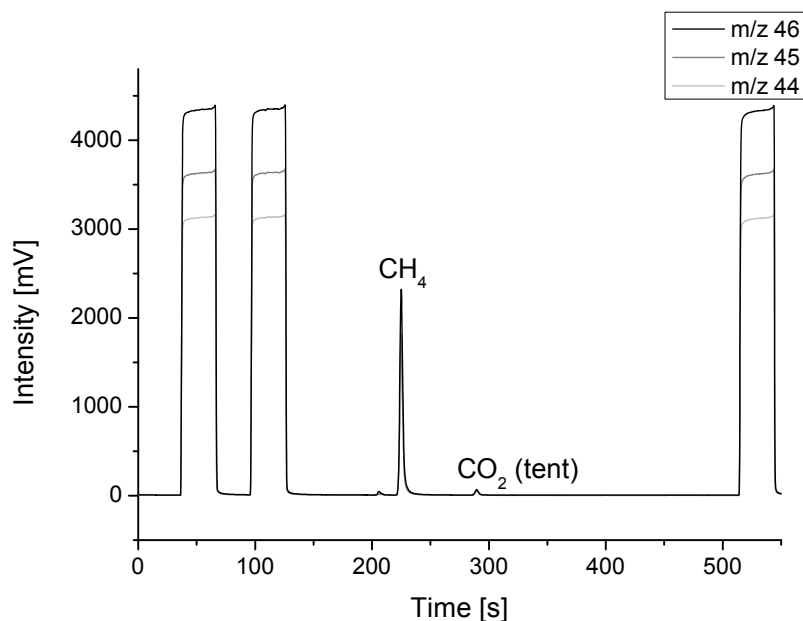


**Figure 5-4.** GC-IRMS measurement of methane formed by photolytic abstraction of the methyl group from CH<sub>3</sub>Cob. The first two and the last flat topped peak correspond to the reference CO<sub>2</sub> gas. The second reference gas peak was used for calculation of  $\delta^{13}\text{C}$ -values. The CO<sub>2</sub> peak is detected due to CO<sub>2</sub> traces in the atmosphere of the anaerobic glove box.

In the third technique, instead of isopropyl alcohol, cyanide and NaOH were added to aqueous CH<sub>3</sub>Cob solution to prevent formation of side products. Afterwards, the reaction mixture was irradiated with a fixed wavelength of 254 nm for 120 min. The recorded UV/Vis spectrum indicated the nearly complete conversion of CH<sub>3</sub>Cob to cyanocobalamin as the spectrum is almost identical to that recorded for cyanocobalamin at an equal concentration under alkaline conditions and with additional cyanide added (Figure 4) However, analysis *via* GC-IRMS revealed a methane yield of only  $26.9 \pm 0.1\%$  and a  $\delta^{13}\text{C}$  value of  $-124.4 \pm 1.4\text{‰}$ , which is near to the value obtained before.

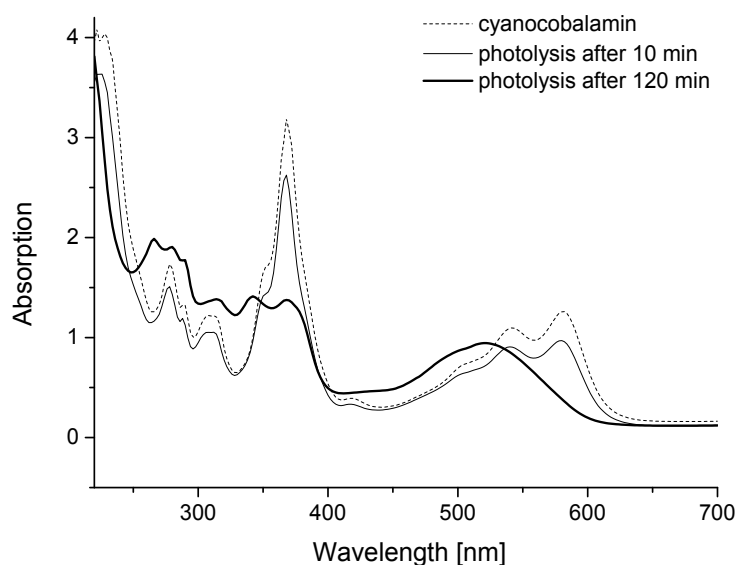


**Figure 5-5.** UV/Vis analyses after photolysis of CH<sub>3</sub>Cob at 254 nm for 10 and 120 min in presence of 100 mM cyanide and 100 mM NaOH (diluted to a cobalamin concentration of 100 μM) in comparison to 100 μM cyanocobalamin in presence of 100 mM cyanide at *pH* 13. The photolysis led to a decrease at the characteristic absorption wavelength for CH<sub>3</sub>Cob at 520 nm and an increase at 368 nm, which is the characteristic absorption wavelength for cyanocobalamin.

The fourth approach involved the abstraction of the methyl group with HI and subsequent measurement of the produced methyl iodide using GC-IRMS. The measured delta values showed a good reproducibility ( $n=6$ ) and low standard deviation ( $\delta^{13}\text{C} = -118.6 \pm 0.2 \text{ ‰}$ ). The conversion of methylcobalamin seems to be quantitative, since prolonging the reaction time did not change the observed  $\delta^{13}\text{C}$  value. The difference of about 7 and 9 ‰ in comparison to the  $\delta^{13}\text{C}$  value obtained using photolysis is probably caused by the incomplete photolytic conversion of CH<sub>3</sub>Cob to methane or by “loss” of methyl groups due to unpreventable side reactions of the methyl radicals despite the presence of cyanide or isopropyl alcohol. Nevertheless, the values are of the correct order of magnitude and corroborate the  $\delta^{13}\text{C}$  obtained by the HI technique. With the HI technique, we also analyzed SAM ( $\delta^{13}\text{C} = -20.6 \pm 0.3 \text{ ‰}$ ).

As a fifth method a thermolysis of an aqueous CH<sub>3</sub>Cob solution was carried out. Despite a very low conversion of CH<sub>3</sub>Cob to methane ( $8.3 \pm 1.6\%$ ) the  $\delta^{13}\text{C}$  value

measured by GC-IRMS ( $-118.7 \pm 2.5 \text{ ‰}$ ) was in very good agreement to that one obtained by abstraction with HI. We decided not to extend the reaction time as this could lead to unwanted formation of ethane. As the HI-technique showed the lowest standard deviation and matches the value of thermolysis, we refer to this value for our following methylation experiment.

#### 5.4.2. Extension of the HG-P&T-hcGC-GC-IRMS for the determination of organometal(loid) compounds in complex matrices

We recently developed a method for the investigation of the carbon isotopic values of organometal(loid)s in complex matrices, which uses selective derivatization of non-volatile organometal(loid)s by hydride generation (HG) for matrix separation followed by purge and trap (P&T) enrichment, heart-cut gaschromatography (hcGC-GC) and subsequent analysis by isotopic ratio mass spectrometry (IRMS).<sup>[31]</sup>

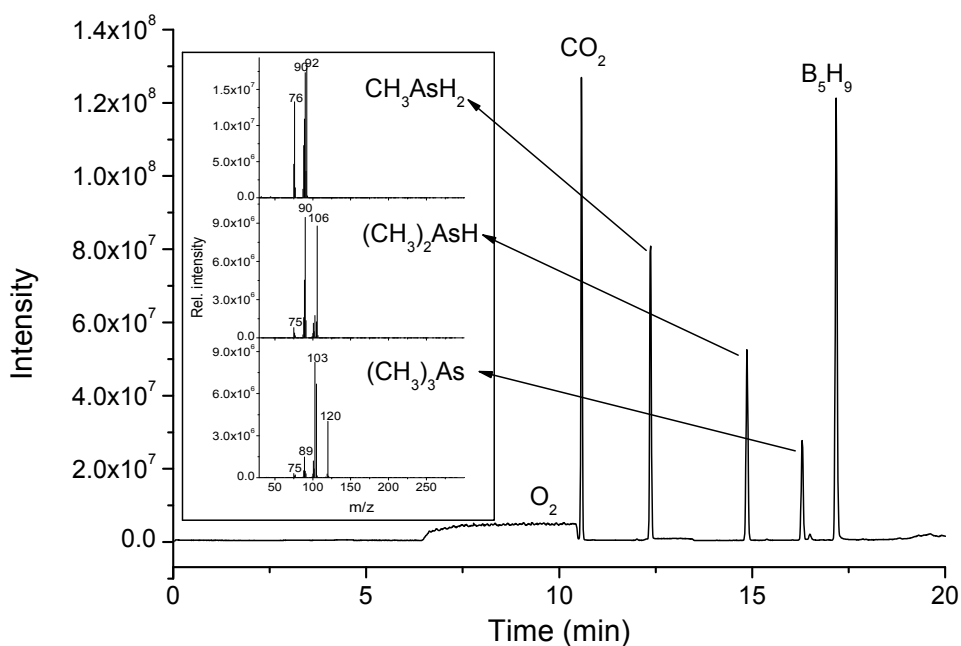
To extend the method which was applied for TMAO to the analysis of MMA and DMA as well as to lower the detection limits by optimization of the hcGC-GC transfer, we applied some changes.

The completeness of the derivatization of the partly methylated arsenicals was ensured by realizing a pH gradient according to Diaz-Bone and Hitzke.<sup>[32]</sup>

Additionally, we changed the injector type from a programmed temperature vaporization (PTV) inlet to the standard split/splitless one resulting in a slightly different split flow rate: The total flow rate is measured using the split/splitless injector, while the PTV measures the internal flow resulting in an increase of the split flow rate due to the external carrier gas flow rate. In addition, we lowered the split flow rate of the capillary GC from 20 to 10 mL min<sup>-1</sup> disregarding a good chromatographic resolution between the arsenic species, but still allowing the removal of most of the CO<sub>2</sub> and water formed by the exothermic hydride generation.

The use of a column with a higher film-thickness increases the capacity as well as chromatographic separation of low boiling arsenic compounds.

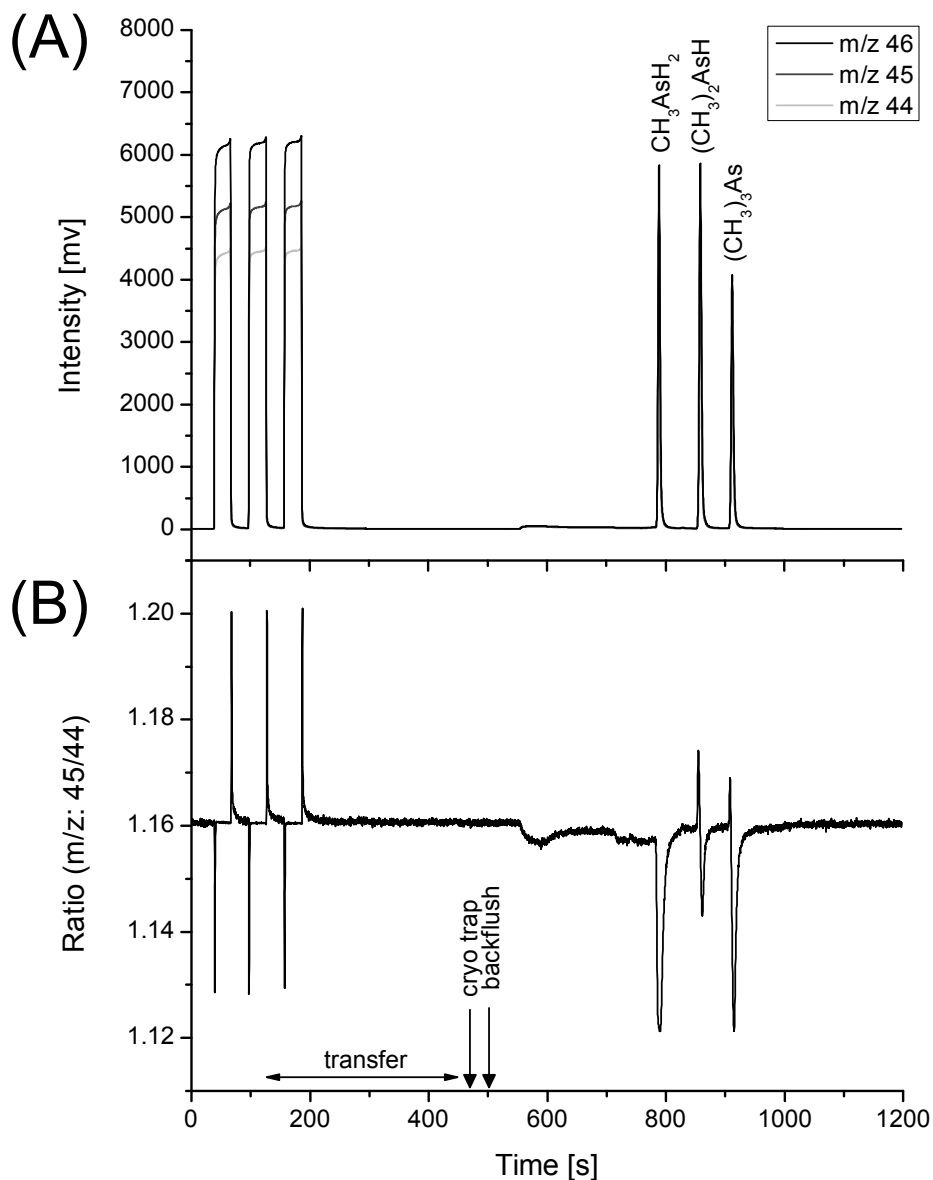
To validate the heart-cut window as well as to control the purity of the arsenic standards, a HG-P&T-hcGC-GC-EI-MS measurement of an arsenic standard mixture was conducted (see Figure 5-6). All of the three arsenic species were transferred within the selected time range of 120-300 s and no coeluting compounds were observed.



**Figure 5-6.** Validation of the heart-cut window. A HG-P&T-hcGC-GC-EI-MS measurement of  $0.3 \mu\text{g}_{\text{As}}$  MMA<sup>V</sup>,  $0.15 \mu\text{g}_{\text{As}}$  DMA<sup>V</sup> and  $0.1 \mu\text{g}_{\text{As}}$  TMAO is presented.

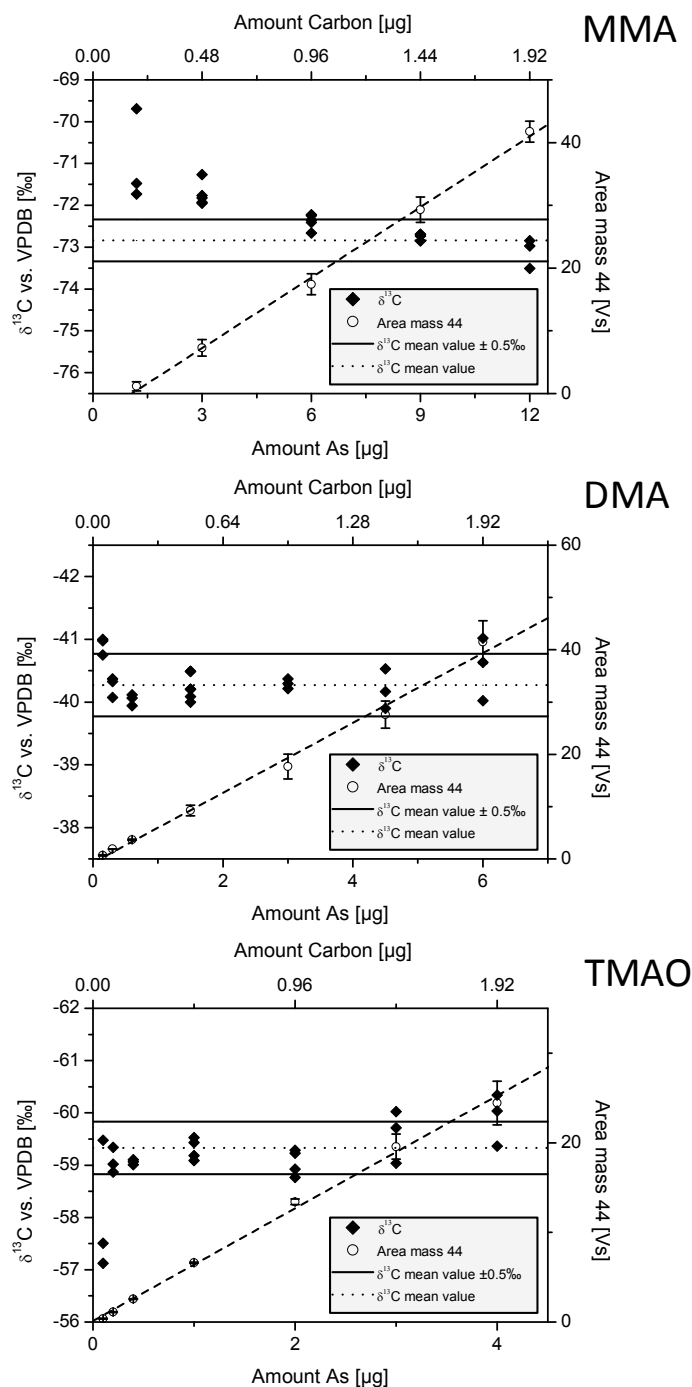
However, for the coupling to the GC-IRMS system the heart-cut window was extended to 120–450 s to ensure a complete transfer of all arsenicals.

Figure 5-7 shows a sample GC-IRMS chromatogram and the corresponding isotope ratio of  $m/z$  45 to 44. By the use of a thick-film column the low boiling arsenicals showed an excellent baseline separation and no coeluting compounds which is essential for the correct determination of the isotope ratios. The low  $\delta^{13}\text{C}$  value obtained for MMA ( $-72.84 \pm 0.36 \text{‰}$ ) results in absence of an observable upswing of the ratio of  $m/z$  45 to 44.



**Figure 5-7.** Typical chromatogram of an arsenic standard containing  $6 \mu\text{g}_{\text{As}}$   $\text{MMA}^{\text{V}}$ ,  $3 \mu\text{g}_{\text{As}}$   $\text{DMA}^{\text{V}}$ , and  $2 \mu\text{g}_{\text{As}}$  TMAO obtained by HG-P&T-hcGC-GC-IRMS (A) and corresponding ratio of m/z 44 and 45 (B). The transfer windows for the heart cut fraction and the heating point of the cryo trap as well as the closure of the back flush are indicated in the chromatograms.

For determination of the method detection limit, we analyzed different amounts of arsenic species (Figure 5-8).



**Figure 5-8.** Determination of the method detection limit for MMA, DMA and TMAO of the HG-P&T-hcGC-GC-IRMS method.  $\delta^{13}\text{C}$  values are represented by diamonds, open circles indicate the area of  $m/z$  44. The horizontal dotted line represents the mean  $\delta^{13}\text{C}$  value of the concentration levels possessing a standard deviation less than 0.5 ‰ and a moving mean, which doesn't change more than 0.5 ‰. The solid lines around the mean value represent a  $\pm 0.5$  ‰ interval around the mean that includes the total uncertainty of isotope analysis incorporating both precision and accuracy.

To exclude memory effects, we measured the standards in a randomized order regarding the concentration. We observed an amount-dependent drift of the delta values. Thus, detection limits were determined according to Jochmann *et al.*<sup>[35]</sup> It is defined as the lowest concentration at which the standard deviation of the  $\delta^{13}\text{C}$  value was below 0.5 ‰ and the mean  $\delta^{13}\text{C}$  value was within a 0.5 ‰ interval around the moving mean of all higher concentrated samples. In comparison to the previous technique, the method detection limit for TMAO was lowered by a factor of 7, more precisely from 4.5  $\mu\text{g}$  (2.48  $\mu\text{g}_{\text{As}}$ , 1.19  $\mu\text{g}_{\text{C}}$ ) to 0.36  $\mu\text{g}$  (0.2  $\mu\text{g}_{\text{As}}$ , 0.1  $\mu\text{g}_{\text{C}}$ ). For the partly methylated arsenicals MMAs and DMAs the detection limits were 14.7  $\mu\text{g}$  (6  $\mu\text{g}_{\text{As}}$ , 0.96  $\mu\text{g}_{\text{C}}$ ) and 0.5  $\mu\text{g}$  (0.3  $\mu\text{g}_{\text{As}}$ , 0.1  $\mu\text{g}_{\text{C}}$ ), respectively.

The calibration curve showed a sufficient linearity of the m/z 44 signal for quantification ( $R^2 \geq 0.98$ ) within the linear range of the GC-IRMS instrument. However, we observed for MMA that the intercept of the calibration curve fit is not zero. Reasons could be adsorption effects or a minimal breakthrough of MMA despite of the cryofocussing temperature was set to  $-165^\circ\text{C}$ , as it is the compound with the lowest boiling point.

For determination of a possible isotopic fractionation in the course of the complete HG-P&T-hcGC-GC-IRMS method, the bulk values of the standard compounds were analyzed using elemental analysis (EA)-IRMS for referencing. We observed a small offset between the EA-values and HG-P&T-hcGC-GC-IRMS in the range of 0.15-1.44 ‰ (Table 5-1). In the case of DMA<sup>V</sup> and TMAO, the offset is below 0.5 ‰ and thus lower than the respective standard deviation. The higher offset for MMA<sup>V</sup> is probably caused by a small breakthrough indicated by the calibration intercept or due to incomplete conversion to  $\text{CO}_2$ . To take this into account all following values for MMA<sup>V</sup> determined by HG-P&T-hcGC-GC-IRMS are corrected by this offset.

**Table 5-1.** Comparison of  $\delta^{13}\text{C}$  values obtained by EA-IRMS and HG-P&T-hcGC-GC-IRMS

	EA-IRMS	HG-P&T-hcGC-GC-IRMS	Offset in ‰
	$\delta^{13}\text{C}$ in ‰	$\delta^{13}\text{C}$ in ‰	
MMA <sup>V</sup>	$-71.4 \pm 0.33$	$-72.84 \pm 0.36$	$-1.44 \pm 0.69$
DMAs <sup>V</sup>	$-40.42 \pm 0.10$	$-40.27 \pm 0.17$	$0.15 \pm 0.27$
TMA <sub>5</sub> O	$-58.91 \pm 0.26$	$-59.33 \pm 0.35$	$-0.42 \pm 0.61$

### 5.4.3. Investigation of the carbon fractionation due to the abiotic methyl group transfer from methylcobalamin to arsenic induced by GSH

With the developed methodology, we investigated the abiotic methylation of arsenic by methylcobalamin presence of glutathione (GSH). In Figure 5-9, a sample HG-PT-hcGC-GC-IRMS chromatogram of an abiotic methylation assay is presented. The main transformation product was MMA, but we also observed the formation of small amounts of DMA (<1%). Beside MMA and DMA, we identified methanethiol (boiling point=6°C) *via* HG-GC-EI-MS. Methanethiol is probably a degradation product of glutathione due to the HG.

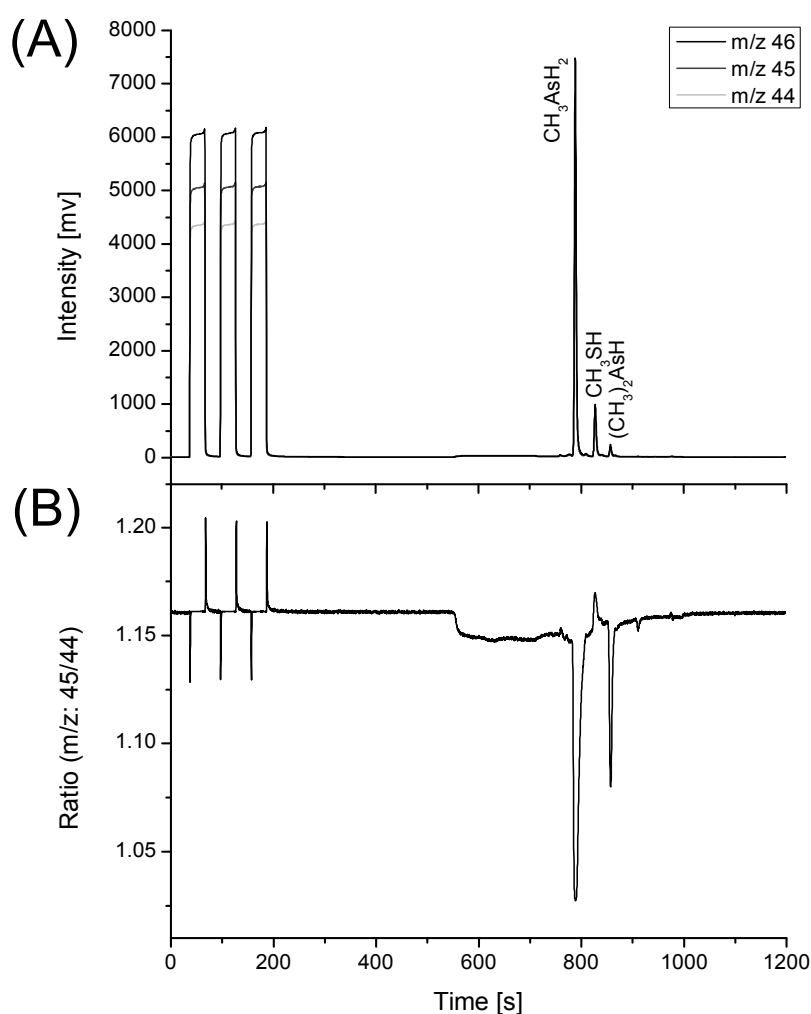


**Figure 5-9.** HG-P&T-hcGC-GC-IRMS chromatogram obtained for 2 mL of an abiotic methylation assay (A) and corresponding ratio of m/z 44 and 45 (B).

It was shown (Chapter 1) that the reaction seems to reach a plateau before 48 h. An increase of the incubation time did not lead to a higher methylation yield. To ensure

this, we varied the reaction time of the abiotic methylation assays from 0 to 12 days. Furthermore, it is addressed to control the stability of the formed MMA in solution regarding the isotopic composition as the reaction vessels had to be stored at  $-20^{\circ}\text{C}$  until the measurement. Additionally, a further reaction of MMA to DMA had to be excluded.

We observed no significant change of the MMA concentration within 12 days. As expected, assays frozen at  $-20^{\circ}\text{C}$  without previous incubation showed no methylated arsenicals (Figure 5-10). Since the methylation efficiency of all other assays was nearly the same, the reaction must reach a plateau before 24 h. A total methylation yield of  $19.9 \pm 2.2\%$  was observed and thus the obtained  $\delta^{13}\text{C}$ -values of MMA showed no significant variation for the different reaction times ( $-160.48 \pm 1.67 \text{‰}$ ;  $n=25$ ) and regarding the parallel reaction vessels a satisfying reproducibility.

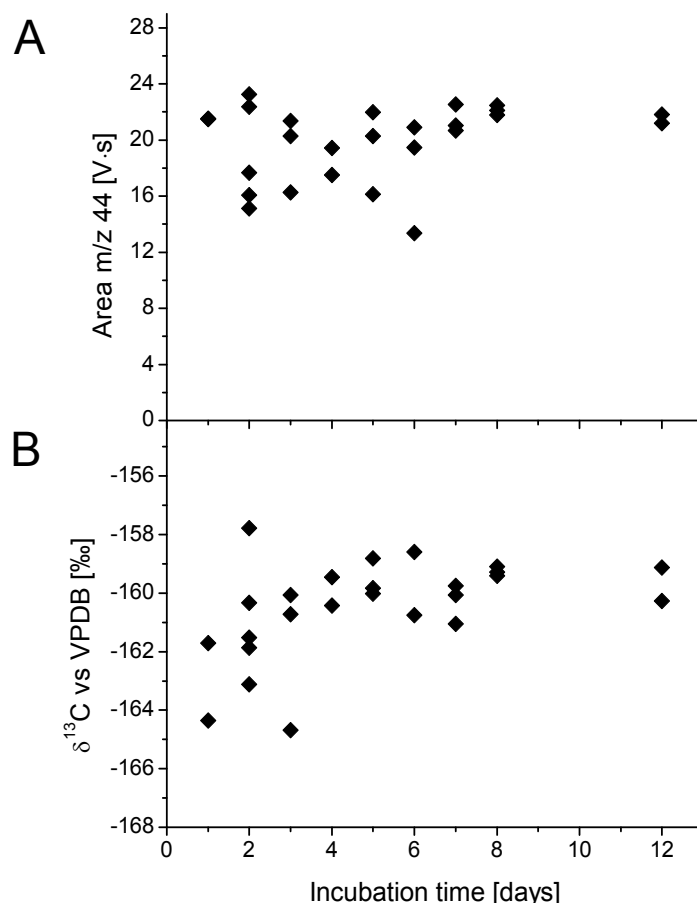


**Figure 5-10.** HG-P&T-hcGC-GC-IRMS data of the abiotic methylation of arsenic in presence of GSH. (A) shows the area of m/z 44 in relation to the incubation time and (B) the corresponding  $\delta^{13}\text{C}$  values.

In comparison to the studies under aerobic conditions of Zakharian *et al.*<sup>[16]</sup> and of Hall *et al.*<sup>[37]</sup>, which used smaller CH<sub>3</sub>Cob to arsenic ratios ( $\leq 1$ ), the methylation yield was tenfold higher. However, the methylation efficiency of this study is in good agreement to Nakamura *et al.*,<sup>[17]</sup> despite they used aerobic conditions, 24 h incubation time, a 1.8-fold higher CH<sub>3</sub>Cob:arsenic ratio, and a 5 times higher GSH to CH<sub>3</sub>Cob ratio.

Due to the CH<sub>3</sub>Cob to arsenic ratio of about 3:1 and the low methylation efficiency, the carbon pool can be regarded as infinite. Furthermore, the formed MMA should be stable and there should be no significant demethylation. In addition, the small amount of formed DMA is negligible and possesses the same isotopic composition. Hence, we can assume an irreversible reaction in an open system with product accumulation. For this system, equation 8 applies for the enriched product and the initial value (-118.6 ‰) yielding directly the kinetic isotope effect ( $KIE = 1.051$ ). The applicability of the assumption of an open system was verified by applying the Rayleigh equation (equation 9) to calculate a possible change of the  $\delta^{13}\text{C}$  of the reactant during the reaction, with the remaining fraction of 0.93, using the  $\epsilon$  derived from the obtained  $KIE$  ( $\epsilon = -48.2$  ‰), and setting  $\delta^{13}\text{C}_{\text{reactant}, 0} = -118.6$  ‰. As the calculated change of the isotopic composition of the reactant is below 3 ‰, the assumption seems to be correct regarding the big differences in the delta value of the accumulated product and the initial value.

In comparison to the literature values of  $KIE$ 's,<sup>[21]</sup> the extent of fractionation points towards a concerted reaction ( $S_N2$ -type). This rather is in agreement to the concerted reaction mechanism drafted by Hayakawa *et al.*<sup>[9]</sup> However, a radical reaction according to the proposal of Nakamura *et al.*<sup>[17]</sup> cannot be excluded due to the lack of reliable literature values for radical reactions.

## 5.5. CONCLUSION

We presented different methods to determine carbon isotopic signature of the methyl group of the important methyl-donor methylcobalamin.

Table 5-2 shows a summary of the  $\delta^{13}\text{C}$  for the methyl group carbon obtained for the different abstraction techniques.

**Table 5-2.** Summary of  $\delta^{13}\text{C}$  values obtained for the different abstraction techniques

<b>Abstraction technique</b>	<b><math>\delta^{13}\text{C}</math> in ‰</b>
HI	$-118.6 \pm 0.2$
Thermolysis	$-118.7 \pm 2.5$
Photolysis + KCN	$-124.4 \pm 1.4$
Photolysis + isopropyl alcohol	$-127.2 \pm 0.4$
Pt <sup>II</sup> /Pt <sup>IV</sup>	$(-39.3 \pm 0.4)^{\text{a}}$

<sup>a</sup> contaminated by phenol

Out of these, the abstraction technique using HI showed the lowest standard deviation as well as good reproducibility and was also demonstrated for SAM as important methyl-donor in many bacteria and mammals. As the measured  $\delta^{13}\text{C}$  for  $\text{CH}_3\text{Cob}$  was exactly the same as the one obtained by thermolysis and two further independent methods involving photolysis indicated a value in a similar range, we can conclude that this value is correct.

In addition, we extended the recently HG-P&T-hcGC-GC-IRMS method to the partly methylated arsenicals and moreover lowered the method detection limits for TMAO.

The applicability of these techniques was shown by the investigation of the abiotic methylation of arsenic in presence of GSH. Here, a very large carbon fractionation of the transferred methyl group was observed. A kinetic isotope effect of 1.051 for the whole reaction was observed pointing to a concerted reaction mechanism.

Overall, this methodology provides new possibilities for the investigation of biomethylation processes. Together with computer based predictions of the isotopic fractionation for certain types of reaction, a refined mechanistic process understanding may be achieved.

### 5.6. REFERENCES

- [1] J. S. Thayer, *Appl. Organomet. Chem.* **2002**, *16*, 677.
- [2] B. K. Mandal, K. T. Suzuki, *Talanta* **2002**, *58*, 201.
- [3] J. S. Thayer, *Abstr. Pap. Am. Chem. Soc.* **1988**, *195*, 79.
- [4] T. Sakurai, *Journal of Health Science* **2003**, *49*, 171.
- [5] J. S. Petrick, F. Ayala-Fierro, W. R. Cullen, D. E. Carter, H. V. Aposhian, *Toxicol. Appl. Pharmacol.* **2000**, *163*, 203.
- [6] M. Styblo, L. M. Del Razo, L. Vega, D. R. Germolec, E. L. LeCluyse, G. A. Hamilton, W. Reed, C. Wang, W. R. Cullen, D. J. Thomas, *Arch. Toxicol.* **2000**, *74*, 289.
- [7] J. Qin, B. P. Rosen, Y. Zhang, G. J. Wang, S. Franke, C. Rensing, *Proc. Natl. Acad. Sci. U. S. A.* **2006**, *103*, 2075.
- [8] S. Lin, Q. Shi, F. B. Nix, M. Styblo, M. A. Beck, K. M. Herbin-Davis, L. L. Hall, J. B. Simeonsson, D. J. Thomas, *J. Biol. Chem.* **2002**, *277*, 10795.
- [9] T. Hayakawa, Y. Kobayashi, X. Cui, S. Hirano, *Arch. Toxicol.* **2005**, *79*, 183.
- [10] R. Bentley, T. G. Chasteen, *Microbiol. Mol. Biol. Rev.* **2002**, *66*, 250.
- [11] T. G. Chasteen, R. Bentley, *Chem. Rev.* **2003**, *103*, 1.
- [12] W. Ridley, L. Dizikes, J. Wood, *Science* **1977**, *197*, 329.
- [13] F. Challenger, *Chemical Reviews* **1945**, *36*, 315.
- [14] F. Thomas, R. A. Diaz-Bone, O. Wuerfel, B. Huber, K. Weidenbach, R. A. Schmitz, R. Hensel, *Appl. Environ. Microbiol.* **2011**, *77*, 8669.
- [15] G. N. Schrauzer, J. A. Seck, R. J. Holland, T. M. Beckham, E. M. Rubin, J. W. Sibert, *Bioinorg. Chem.* **1973**, *2*, 93.
- [16] R. A. Zakharyan, H. V. Aposhian, *Toxicol. and Appl. Pharmacol.* **1999**, *154*, 287.
- [17] K. Nakamura, Y. Hisaeda, L. Pan, H. Yamauchi, *J. Organomet. Chem.* **2009**, *694*, 916.
- [18] M. Elsner, *J. Environ. Monit.* **2010**, *12*, 2005.

- [19] D. E. Matthews, J. M. Hayes, *Anal. Chem.* **1978**, *50*, 1465.
- [20] A. L. Sessions, *J. of Sep. Sci.* **2006**, *29*, 1946.
- [21] M. Elsner, L. Zwank, D. Hunkeler, R. P. Schwarzenbach, *Environ. Sci. Technol.* **2005**, *39*, 6896.
- [22] E. Caytan, E. P. Botosoa, V. Silvestre, R. J. Robins, S. Akoka, G. S. Remaud, *Anal. Chem.* **2007**, *79*, 8266.
- [23] G. N. Schrauzer, J. W. Sibert, R. J. Windgassen, *J. Am. Chem. Soc.* **1968**, *90*, 6681.
- [24] Y. T. Fanchiang, J. J. Pignatello, J. M. Wood, *Organometallics* **1983**, *2*, 1748.
- [25] S. L. Manley, *Mar. Chem.* **1994**, *46*, 361.
- [26] D. Dolphin, A. W. Johnson, R. Rodrigo, *J. Chem. Soc. (Resumed)* **1964**.
- [27] R. H. Yamada, S. Shimizu, S. Fukui, *Biochim. Biophys. Acta* **1966**, *124*, 195.
- [28] Y. T. Fanchiang, J. J. Pignatello, J. M. Wood, *Organometallics* **1983**, *2*, 1752.
- [29] S. Zeisel, *Monatshefte für Chemie / Chemical Monthly* **1886**, *7*, 406.
- [30] F. Keppler, R. M. Kalin, D. B. Harper, W. C. McRoberts, J. T. G. Hamilton, *Biogeosciences* **2004**, *1*, 123.
- [31] M. Greule, A. Mosandl, J. T. G. Hamilton, F. Keppler, *Rapid Commun. Mass Spectrom.* **2009**, *23*, 1710.
- [32] O. Wuerfel, R. A. Diaz-Bone, M. Stephan, M. A. Jochmann, *Anal. Chem.* **2009**, *81*, 4312.
- [33] R. A. Diaz-Bone, M. Hitzke, *J. Anal. At. Spectrom.* **2008**, *23*, 861.
- [34] Merijani, A., R. A. Zingaro, *Inorg. Chem.* **1966**, *5*, 187.
- [35] R. T. Taylor, M. L. Hanna, *Bioinorg. Chem.* **1976**, *6*, 281.
- [36] M. A. Jochmann, M. Blessing, S. B. Haderlein, T. C. Schmidt, *Rapid Commun. Mass Spectrom.* **2006**, *20*, 3639.
- [37] M. N. Hall, X. Liu, V. Slavkovich, V. Ilievski, Z. Mi, S. Alam, P. Factor-Litvak, H. Ahsan, J. H. Graziano, M. V. Gamble, *Environ. Health Perspect.* **2009**, *117*.

## **Chapter 6. General Conclusion and Outlook**

### **6.1. GENERAL CONCLUSION**

The purpose of this thesis was to foster the understanding of the methylation processes of the group 15 and 16 metal(loid)s As, Sb, Te, Se and Bi by methylcobalamin by the development and usage of different new approaches and analytical techniques.

In **Chapter 2**, the role of cob(I)alamin for methylation of group 15 and group 16 elements metal(loid)s by methanoarchaea was reinvestigated by the use of UV/Vis spectroscopy and P&T-GC-ICP-MS. It was demonstrated that Cob(I), formed by enzymatic demethylation of CH<sub>3</sub>Cob, is the causative agent during methylation and is capable to non-enzymatically induce the methyl transfer from CH<sub>3</sub>Cob to metal(loid)s. The reaction is enzyme-mediated, but not directly enzyme-catalyzed. Therefore, it has to be regarded as side reaction of methanogenesis. Further studies revealed, that the glutathione and coenzyme M also have the capability to produce organometal(loid)s in presence of methylcobalamin and thus different biogenic “reducing agents” also might contribute to the methylation of metal(loid)s *in vivo* in dependency on their availability.

In **Chapter 3**, a new oxidation-state specific hydride generation technique was developed for arsenic speciation and applied to the investigation of the reaction mechanism of metal(loid) methylation by CH<sub>3</sub>Cob and Cob(I). The method was validated and showed low redox miss finding rates, good reproducibility and detection limits. With the use of this technique and by applying different arsenic species, which are metabolites in the alternate Challenger mechanism to MtaA-assays, it could be demonstrated that the reduction mechanism is non-oxidative and the pentavalent arsenicals have to be regarded rather as side products than as intermediates in the methylation mechanism. Furthermore, a series of detailed UV/Vis and P&T-GC-ICP-MS studies on the methylation of arsenic and other group 15 and 16 elements using CH<sub>3</sub>Cob and electrochemically produced Cob(I) was conducted and underlined this finding. In addition, the data indicated that the metal(loid)s antimony, selenium, tellurium, and bismuth are methylated in a similar way, even though in the case of Se and Te an additional reduction step is required upon methylation to form volatile species. A concerted nucleophilic substitution

reaction after formation of a reduced methylcobalamin is likely, but also a caged radical mechanism for the methyl transfer to the metal(loid)s cannot be excluded. For the hydride generation, the formation of hydridocobalamin as an intermediate that transfers a hydride ion directly to the metal(loid)s is likely.

For an elucidation of the reaction mechanisms proposed for arsenic methylation, the investigation of the change in the isotopic signature in the course of a reaction can be a promising tool. Thus, the first method for the determination the carbon isotopic values of organometal(loid)s in complex matrices was developed in **Chapter 4** which was carefully validated. The applicability to an environmental sample was shown by analyzing biogenically formed trimethylarsine oxide in a compost sample.

As a prerequisite for the investigation of the occurring kinetic isotope effect due to the methyl transfer, the initial isotopic value, which is the isotopic signature of the methyl group from the methyl donor methylcobalamin, had to be determined. Therefore, in **Chapter 5** five different independent approaches were used, because of the high importance of this  $\delta^{13}\text{C}$ . For the position-specific determination of the methyl group carbon, the abstraction of the methyl group with HI, photolysis in presence of isopropyl alcohol or KCN, thermolytic cleavage, and the reaction with platinum (II/IV) couples were applied. The reaction products were subsequent measured by GC-IRMS or by FIA-IRMS in the case of Pt.

The abstraction technique using HI showed the lowest standard deviation as well as good reproducibility and was also demonstrated for SAM as important methyl-donor in many bacteria and mammals. The accuracy of the  $\delta^{13}\text{C}$  can be assumed as methane produced by thermolysis from  $\text{CH}_3\text{Cob}$  yielded exactly the same  $\delta^{13}\text{C}$  and the  $\delta^{13}\text{C}$  obtained by both photolysis techniques were in the same range.

Finally, the in chapter 4 developed IRMS method was extended and optimized to the analysis of monomethylarsine and dimethylarsine. Furthermore, it was possible to lower the detection limits for trimethylarsine oxide.

With this methodology the abiotic methylation of arsenic by methylcobalamin in presence of glutathione was investigated. The determined *KIE* points to a concerted reaction mechanism.

The developed IRMS techniques are promising tools for further studies on the biomethylation of metal(loid). In the following, some ideas are given.

## 6.2. OUTLOOK

For further investigations on the biomethylation of metal(loid)s in the environment, the developed and extended method for the determination of the carbon isotopic values of metal(loid) compounds in complex matrices holds tremendous potential.

After the determination of the *KIE* during the methylation of arsenic by methylcobalamin in presence of GSH, the next step could be the investigation of the *KIE* replacing GSH by Cob(I). In connection with a computer based modeling of the reaction and calculation of the *KIE*, a complete elucidation of the proposed reaction mechanisms for Cob(I) might be possible. In addition, the reaction mechanism of the SAM dependent methylation might be elucidated in the same way.

In addition, a comparison of the obtained *KIE* of the other “bioreducing agents” would allow to ascertain whether the underlying reaction mechanism is similar to GSH or Cob(I). Furthermore, if there are differences between the *KIE* of different bioreducing agents, the relative contribution of these to the methylation of an amended metal(loid) might be investigated.

Another interesting field for future investigations is the *KIE* due to the methyl group transfer by microorganisms *in vivo*. As the isotopic signature of the methylated metal(loid) produced by microorganisms depends on initial carbon source as well as the methylation process, this could allow a differentiation between certain microorganisms of a complex microbiocenosis, if a specific microorganism produces a specific isotopic fractionation as a fingerprint. This is at least expected for species using different substrates with differing initial value for methanogenesis. In this way, the relative contribution of a specific bacterial species to the methylation of a metal(loid) might be obtained by mixing calculation.

Finally, the method allows an easy differentiation of biogenically formed metal(loid) species and anthropogenic ones in the environment by their different isotopic compositions.

**Chapter 7. Appendix****7.1. ABBREVIATIONS**

As <sup>III</sup>	arsenite
As <sup>V</sup>	arsenate
CH <sub>3</sub> Cob	methylcobalamin
Cob(I)	cob(I)alamin
Cob(II)	cob(II)alamin
Cob(III)	aquocobalamin
CoM	coenzyme M (2-mercaptoethanesulfonic acid)
CSIA	compound-specific stable isotope analysis
DMA	dimethylarsine
DMAs <sup>III</sup>	dimethylarsinous acid
DMAs <sup>V</sup>	dimethylarsenic acid
DTE	dithioerythritol
E <sub>0</sub>	standard reduction potential at <i>pH</i> 7
EI	electron impact
FIA	flow injection analysis
GC	gaschromatography
GSH	glutathione
h	hour(s)
hcGC	heart-cut gaschromatography
HEPES	4-(2-hydroxyethyl)-1-piperazineethanesulfonic acid
HG	hydride generation
HPLC	high performance liquid chromatography
ICP	inductively coupled plasma
IRMS	isotope ratio mass spectrometry
<i>KIEHG</i>	hydride generationkinetic isotope effect
L	liter
LC <sub>50</sub>	mean lethal concentration
LD <sub>50</sub>	mean lethal dose
m	meter(s)
M	molar
MC	multi-collector
MeSe <sup>IV</sup>	methaneseleninic acid
min	minute(s)

MMA	monomethylarsine
MMA <sup>s</sup>	monomethylarsinous acid
MMA <sup>v</sup>	monomethylarsenic acid
MS	mass spectrometry
P&T	purge and trap
PTFE	polytetrafluoroethylene
s	second(s)
SAM	S-adenosyl methionine
SD	standard deviation
S <sub>N</sub> 1	stepwise nucleophilic substitution
S <sub>N</sub> 2	concerted nucleophilic substitution
THF	tetrahydrofolate
TiCit	titanium citrate
TMAO	trimethylarsine oxide
TMA <sub>s</sub>	trimethylarsine
TRIS	tris(hydroxymethyl)aminomethane
UV/Vis	ultraviolet-visible
VPDB	Vienna Pee-Dee Belemnite
Ω	Ohm

## 7.2. LIST OF TABLES

<b>Table 1-1.</b>	Elemental properties (combined from <sup>[1]</sup> ).....	1
<b>Table 1-2.</b>	Countries with elevated arsenic concentration found in the groundwater. (reproduced from B. Petrusovski <i>et al.</i> ) <sup>[7]</sup> .....	3
<b>Table 1-3.</b>	Acute toxicity of selected arsenic species. LD <sub>50</sub> refers to the oral administration of mice, if not indicated otherwise. ....	4
<b>Table 2-1.</b>	Quantitative data of the abiotic multi-element methylation by CH <sub>3</sub> Cob in presence of GSH. P&T-GC-ICP-MS or HG-P&T-GC-ICP-MS was conducted as indicated. In the case of P&T-GC-ICP-MS, the concentration μM refers to the total volume of the liquid phase (5 mL), while in for HG μM refers to a total headspace volume of 15 mL. The recovery of arsenic and antimony exceeding 100% is probably caused by impreciseness of the pipet and the error of quantification method for ICP-MS. <sup>[25]</sup> .....	38
<b>Table 3-1.</b>	Validation of oxidation-state specific hydride generation. Relative recovery as well as percentage of redox miss findings are indicated (n=3) For sample chromatograms refer to Figure 3-4.....	56
<b>Table 3-2.</b>	Formation of volatile and non-volatile arsenic compounds from trivalent and pentavalent arsenic reactants by MtaA containing <i>in vitro</i> assays (quantitative data). For calculation of total volatilization, all volatile species detected for each experiment were summarized first (data not shown). Means and relative standard deviations were calculated from these summarized values. Experiments were performed at least in triplicates. See Table 3-3 for a detailed quantitative list of detected species.....	57
<b>Table 3-3.</b>	Detailed quantitative list of volatile and non-volatile methylated arsenic compounds derived from trivalent and pentavalent arsenic reactants by MtaA containing <i>in vitro</i> assays as detected by headspace and HG/P&T/GC-ICP-MS analyses pmol (±%RSD). Reduced and methylated products are in boldface, reactants not transformed in the MtaA containing <i>in vitro</i> assays are in italics. Blank values derived from chemical hydride generation without addition of <i>in vitro</i> assays were subtracted. ....	60
<b>Table 3-4.</b>	Analyses of abiotic volatilization and methylation of trivalent and pentavalent arsenic reactants by CH <sub>3</sub> Cob(III) and CoM. The formation of volatile and non-volatile methylated derivatives from tri- and pentavalent arsenic reactants by <i>in vitro</i> assays containing 1 μmol CH <sub>3</sub> Cob(III) and CoM and 1 mL 50 mM HEPES pH 7 was investigated. Volatile species were analyzed by headspace P&T-GC-ICP-MS and non-volatile species by HG/P&T/GC-ICP-MS. Chemical hydride generation using NaBH <sub>4</sub> was separately performed at neutral pH 8 and during pH gradient by continuous addition of 1 M HCl in order to differentiate between trivalent and pentavalent arsenic derivatives. Reduced and methylated products are in boldface, reactants not transformed in the abiotic <i>in vitro</i> assays are in italics. Blank values derived from chemical hydride generation without addition of <i>in vitro</i> assays were subtracted. Experiments were performed at least in triplicates. For calculation of total volatilization, all volatile species detected for each experiment were summarized	

---

	first (data not shown). Means and relative standard deviations were calculated from these summarized values. ....	62
<b>Table 5-1.</b>	Comparison of $\delta^{13}\text{C}$ values obtained by EA-IRMS and HG-P&T-hcGC-GC-IRMS.....	113
<b>Table 5-2.</b>	Summary of $\delta^{13}\text{C}$ values obtained for the different abstraction techniques.....	117

### 7.3. LIST OF FIGURES

<b>Figure 1-1.</b>	Chemical structure of SAM. The transferable methyl group is highlighted.....	5
<b>Figure 1-2.</b>	Methylation mechanisms according to Challenger (A) and Hayakawa <i>et al.</i> (B).....	6
<b>Figure 1-3.</b>	Chemical structure of CH <sub>3</sub> Cob. The transferable methyl group is highlighted.....	9
<b>Figure 1-4.</b>	Simplified methylcobalamin in “base on” (left) and “base off” (right) configuration.....	9
<b>Figure 1-5.</b>	Possible ways transferring the methyl group of CH <sub>3</sub> Cob. CH <sub>3</sub> Cob is drawn simplified. R represents a ligand such as H <sub>2</sub> O or <sup>-</sup> CN which replaces the methyl group. ....	10
<b>Figure 1-6.</b>	Pourbaix diagram of cobalamin <sup>[63]</sup> .....	12
<b>Figure 1-7.</b>	Schematic overview of an ICP-MS.....	14
<b>Figure 1-8.</b>	Differences in energies of isotopologues during an unidirectional process. G is the Gibbs free energy. (modified from <sup>[78]</sup> ). ....	16
<b>Figure 1-9.</b>	Schematic view of a GC-IRMS system.....	18
<b>Figure 1-10.</b>	Origin of isotopic swing in ratio m/z: 45/44 (right) due to slight differences in the retention times of the isotopologues (left). ....	19
<b>Figure 2-1.</b>	Comparison of volatile arsenic species pattern produced by methylation assays containing purified MtaA of <i>M. mazei</i> (A) <sup>[20]</sup> and electrochemically produced Cob(I) (B) obtained by P&T-GC-ICP-MS analysis. ....	34
<b>Figure 2-2.</b>	Formation of Cob(I) due to MtaA catalyzed demethylation of CH <sub>3</sub> Cob in presence of CoM observed by UV/Vis spectrometry. A spectrum of partial (A) and nearly quantitative conversion (B) due to a variation of CoM concentration is shown. Spectra were measured in 1 min intervals for 40 min. The characteristic wavelengths of CH <sub>3</sub> Cob (520 nm) and Cob(I) (388 nm) are indicated. ....	35
<b>Figure 2-3.</b>	Reactions of arsenite with equal amounts of CH <sub>3</sub> Cob and Cob(I) produced by MtaA-catalyzed transfer from CH <sub>3</sub> Cob to CoM (A), excess of Cob(I) produced by MtaA-catalyzed transfer from CH <sub>3</sub> Cob to CoM (B); equal amounts of electrochemically produced Cob(I) and CH <sub>3</sub> Cob (C), and electrochemically produced Cob(I) only (D). Assays were analyzed by UV/VIS (I) and P&T-GC-ICP-MS (II). The characteristic wavelengths of Cob(I) (388 nm) and Cob(II) (312, 478 nm) are indicated in (I). ....	36
<b>Figure 2-4.</b>	Dependency of abiotic methylation of arsenic by methylcobalamin in presence of GSH on pH, reaction time, concentration as well as on the temperature. Assays have been analyzed by HG-P&T-GC-ICP-MS. If not indicated otherwise, a GSH concentration of 25 mM and an incubation temperature of 37°C, and pH 7 were used. MMA: CH <sub>3</sub> AsH <sub>2</sub> ; DMA: (CH <sub>3</sub> ) <sub>2</sub> AsH <sub>2</sub> ; TMA: (CH <sub>3</sub> ) <sub>3</sub> As.....	41
<b>Figure 2-5.</b>	Comparison of methylation efficiency of arsenic by CH <sub>3</sub> Cob in presence of CoM, TiCit, and Cob(I), as well of photomethylation. Concentration and incubation time was varied as indicated. Assays have been analyzed by HG-P&T-GC-ICP-MS. Thus, the methylation yield for Cob(I) regards HS as well as HG. MMA: CH <sub>3</sub> AsH <sub>2</sub> ; DMA: (CH <sub>3</sub> ) <sub>2</sub> AsH <sub>2</sub> ; TMA: (CH <sub>3</sub> ) <sub>3</sub> As.....	42

- Figure 3-1.** Overview on possible methylation and reduction pathways. Mechanism proposed for the reaction of arsenite with  $\text{CH}_3\text{Cob(III)}$  and  $\text{Cob(I)}$  is indicated in **bold**. ..... 49
- Figure 3-2.** Schematic view of oxidation state specific HG/P&T/GC-ICP-MS system. .... 51
- Figure 3-3.** Simulated pH-course during the two-step oxidation-state-specific HG. For measurement of the pH-course the consumption of protons due to the derivatization using  $\text{NaBH}_4$  was simulated by addition of  $\text{NaOH}$  instead of  $\text{NaBH}_4$  to prevent damage of pH-electrode by  $\text{NaBH}_4$  and no sample was added to the buffer-solution. .... 55
- Figure 3-4.** Sample chromatograms for oxidation-state-specific HG/P&T/GC-ICP-MS. The chromatograms A and B show a two-step oxidation-state-specific HG/P&T/GC-ICP-MS analysis of a standard mixture containing  $\text{MMAs}^{\text{III}}$ ,  $\text{DMAs}^{\text{III}}$ ,  $\text{TMAOs}$  for method validation (for simulated pH-course, refer to Figure 3-3). For C and D a mixture of  $\text{As}^{\text{V}}$ ,  $\text{MMAs}^{\text{V}}$ ,  $\text{DMAs}^{\text{V}}$  was used (for quantitative data, refer to Table 3-1). The peaks are labeled with the corresponding starting compounds before derivatization. .... 56
- Figure 3-5.** Investigation of conversion of different arsenic reactants by MtaA containing *in vitro* assays. Trivalent and pentavalent non-volatile arsenicals were analyzed by oxidation-state-specific HG/P&T/GC-ICP-MS after measurement of headspace of the reaction vessels using P&T/GC-ICP-MS. The peaks are labeled with the corresponding starting compounds before derivatization with  $\text{NaBH}_4$ . For the arsenic reactants white font on black background is used. See Figure 3-6 for comparison with arsenic standards. As\_u: unidentified volatile arsenical. .... 58
- Figure 3-6.** Measurement of trivalent and pentavalent reactants (white font on black background) *via* oxidation-state-specific HG/P&T/GC-ICP-MS. The peaks are labeled with the corresponding starting compounds before derivatization with  $\text{NaBH}_4$ . .... 59
- Figure 3-7.** UV/Vis Analyses of cobalamines in the presence of various reactants. For simplification, only a spectrum for one element is displayed if there were only slight differences in absorbance. Characteristic wavelengths are 520 nm for  $\text{CH}_3\text{Cob(III)}$ , 388 nm for  $\text{Cob(I)}$  and 468 nm for  $\text{Cob(II)}$ . For comparison, see (A).  $\text{Cob(II)}$  was produced by reaction of  $\text{Cob(III)}$  and  $\text{Cob(I)}$ . .... 61
- Figure 3-8.** Hydride generation induced by  $\text{Cob(I)}$ . P&T/GC-ICP-MS chromatograms were produced under the following reaction conditions: 5 mL of 0.5 mM  $\text{CH}_3\text{Cob(III)}$  in 50 mM phosphate-buffer *pH* 7 were incubated with 0.25 mM  $\text{Cob(I)}$  and either 0.25 mM  $\text{As}^{\text{III}}$ ,  $\text{Sb}^{\text{III}}$ ,  $\text{Bi}^{\text{III}}$ ,  $\text{Se}^{\text{IV}}$  or  $\text{Te}^{\text{IV}}$  (no hydride species were produced (data not shown)) at 37 °C for 30 min prior to headspace analyses. Methylated selenium and bismuth species were properly only detected due to memory effects of the column. .... 63
- Figure 3-9.** Arsenic methylation induced by  $\text{Cob(I)}$  at *pH* 4.5 shows a different hydride to methyl ratio then at *pH* 7 (Figure 3-12). 2 mL of 0.1  $\mu\text{M}$   $\text{As}^{\text{III}}$  in 50 mM phosphate-buffer *pH* 4-5 were incubated with 0.1 mM  $\text{CH}_3\text{Cob(III)}$  and 0.1 mM  $\text{Cob(I)}$  at 37°C for 30 min prior to P&T/GC-ICP-MS measurement. .... 64

- Figure 3-10.** No significant reaction of arsine and stibine with methylcobalamin. 30 ng arsine and stibine were incubated with 0.1 mM CH<sub>3</sub>Cob(III) in 2 mL 50 mM phosphate-buffer *pH* 7 at 37 °C for 30 min prior to P&T/GC-ICP-MS measurement. .... 65
- Figure 3-11.** Transformation of methylseleninic acid induced by Cob(I). A 2 mL solution of 0.1 μM methylseleninic acid and 50 μM electrochemically produced Cob(I) was incubated in 50 mM phosphate-buffer *pH* 7 for 15 min under strict anaerobic conditions prior to P&T/GC-ICP-MS measurement. .... 66
- Figure 3-12.** Tert-butanol shows no effect on arsenic methylation induced by Cob(I). 2 mL of 0.1 μM As<sup>III</sup> in 50 mM phosphate-buffer *pH* 7 were incubated with 0.1 mM CH<sub>3</sub>Cob(III) and 0.1 mM Cob(I) in presence (A) and absence (B) of 50 mM tert-butanol at 37°C for 30 min prior to P&T/GC-ICP-MS measurement. .... 68
- Figure 3-13.** Proposed reaction schemes for multi-element methylation of trivalent metal(loid)s induced by Cob(I). Exemplarily, arsenic is shown. (1: concerted nucleophilic substitution (S<sub>N</sub>2); 2: caged radical mechanism)..... 69
- Figure 4-1.** Schematic overview of the HG-P&T-hcGC-GC-IRMS method. On the left side, the hydride generation, the P&T and the cryofocussing on the packed GC column is shown. On the right side, the GC-IRMS method is illustrated. .... 80
- Figure 4-2.** <sup>13</sup>C and <sup>75</sup>As traces obtained by HG-P&T-hcGC-ICP-MS of 0.1 g compost containing 1.56 μg TMAsO (0.86 μg<sub>As</sub>, 0.41 μg<sub>C</sub>); Chromatograms a) and b) show the <sup>75</sup>As and <sup>13</sup>C traces without heart-cut and in the chromatograms c) and d) a heart-cut at 210-300 s was applied for successful separation of volatile matrix components from the target compound TMAs. .... 83
- Figure 4-3.** Chromatogram, obtained by HG-P&T-hcGC-GC-MS of 0.1 g<sub>wet weight</sub> compost containing 1.56 μg TMAsO (0.86 μg<sub>As</sub>, 0.41 μg<sub>C</sub>) with heart-cut at 210-300 s. The inserted mass spectrum shows that no other volatile matrix compounds interfere with the TMAs peak and a clean heart cut of the TMAs was achieved. .... 84
- Figure 4-4.** Comparison of mass spectrum of TMAs measured by HG-P&T-hcGC-GC-MS in a) TMAsO standard b) compost sample ..... 85
- Figure 4-5.** The lower part shows a FIA-IRMS measurement of 1.81 μg TMAsO-standard (1 μg<sub>As</sub>, 0.47 μg<sub>C</sub>) This concentration was chosen to balance the signal intensity of the sample to the signal intensity of the reference standards as it is used in δ<sup>13</sup>C bulk analysis by Elemental Analyzer- IRMS. In the upper part, the isotopic swing expressing the ratios of mass 45 (<sup>13</sup>CO<sub>2</sub> and <sup>12</sup>C<sup>17</sup>O<sup>16</sup>O ) to mass 44 (<sup>12</sup>CO<sub>2</sub>) is shown. The first three and the last flat topped peaks correspond to the reference CO<sub>2</sub> gas. The second reference gas peak was used for calculation of δ<sup>13</sup>C-values. .... 85
- Figure 4-6.** C-IRMS-chromatogram after hydride generation and matrix separation by HG-P&T-hcGC-GC of a) 5.44 μg TMAsO-standard (3 μg<sub>As</sub>, 1.41 μg<sub>C</sub>) and b) 0.31 g compost containing 4.83 μg TMAsO (2.66 μg<sub>As</sub>, 1.26 μg<sub>C</sub>). The transfer windows for the heart cut fraction and the heating point of the cryo trap as well as the closure of the back flush are indicated in the chromatograms. .... 86

- Figure 4-7.** Determination of the method detection limit for TMA<sub>5</sub>O of the HG-P&T-GC-GC-IRMS method.  $\delta^{13}\text{C}$  values are represented by diamonds, open squares indicate the area of mass 44. The horizontal dotted line represents the mean  $\delta^{13}\text{C}$  bulk TMA<sub>5</sub>O value determined by FIA-IRMS. The solid lines around the mean value represent a  $\pm 0.5$  ‰ interval that includes the total uncertainty of isotope analysis incorporating both reproducibility and accuracy. .... 87
- Figure 5-1.** GC-IRMS calibration slope for CH<sub>4</sub> ..... 99
- Figure 5-2.** Control of the completeness of the conversion of CH<sub>3</sub>Cob to aquocobalamin using Pt<sup>II</sup> and Pt<sup>IV</sup> (A) and removal of aquocobalamin after phenol extraction (B) by UV/Vis spectroscopy. The characteristic wavelength of aquocobalamin is 350 nm. As this absorption band in (A) shows no shoulder at about 340 nm originating from remaining CH<sub>3</sub>Cob, the conversion seems to be quantitative. Solutions were diluted to a “theoretical” cobalamin concentration of 100  $\mu\text{M}$  before measurement. .... 105
- Figure 5-3.** FIA-IRMS measurement of the methyl-platinum complex after phenol extraction and lyophilization. The first three and the last flat topped peak correspond to the reference CO<sub>2</sub> gas. .... 106
- Figure 5-4.** GC-IRMS measurement of methane formed by photolytic abstraction of the methyl group from CH<sub>3</sub>Cob. The first two and the last flat topped peak correspond to the reference CO<sub>2</sub> gas. The second reference gas peak was used for calculation of  $\delta^{13}\text{C}$ -values. The CO<sub>2</sub> peak is detected due to CO<sub>2</sub> traces in the atmosphere of the anaerobic glove box. .... 107
- Figure 5-5.** UV/Vis analyses after photolysis of CH<sub>3</sub>Cob at 254 nm for 10 and 120 min in presence of 100 mM cyanide and 100 mM NaOH (diluted to a cobalamin concentration of 100  $\mu\text{M}$ ) in comparison to 100  $\mu\text{M}$  cyanocobalamin in presence of 100 mM cyanide at *pH* 13. The photolysis led to a decrease at the characteristic absorption wavelength for CH<sub>3</sub>Cob at 520 nm and an increase at 368 nm which is the characteristic absorption wavelength for cyanocobalamin. .... 108
- Figure 5-6.** Validation of the heart-cut window. A HG-P&T-hcGC-GC-EI-MS measurement of 0.3  $\mu\text{g}_{\text{As}}$  MMA<sup>V</sup>, 0.15  $\mu\text{g}_{\text{As}}$  DMA<sup>V</sup> and 0.1  $\mu\text{g}_{\text{As}}$  TMAO is presented. .... 110
- Figure 5-7.** Typical chromatogram of an arsenic standard containing 6  $\mu\text{g}_{\text{As}}$  MMA<sup>V</sup>, 3  $\mu\text{g}_{\text{As}}$  DMA<sup>V</sup>, and 2  $\mu\text{g}_{\text{As}}$  TMAO obtained by HG-P&T-hcGC-GC-IRMS (A) and corresponding ratio of *m/z* 44 and 45 (B). The transfer windows for the heart cut fraction and the heating point of the cryo trap as well as the closure of the back flush are indicated in the chromatograms. .... 111
- Figure 5-8.** Determination of the method detection limit for MMA, DMA and TMAO of the HG-P&T-hcGC-GC-IRMS method.  $\delta^{13}\text{C}$  values are represented by diamonds, open circles indicate the area of *m/z* 44. The horizontal dotted line represents the mean  $\delta^{13}\text{C}$  value of the concentration levels possessing a standard deviation less than 0.5 ‰ and a moving mean, which doesn't change more than 0.5 ‰. The solid lines around the mean value represent a  $\pm 0.5$  ‰ interval around the mean that includes the total uncertainty of isotope analysis incorporating both precision and accuracy. .... 112

- Figure 5-9.** HG-P&T-hcGC-GC-IRMS chromatogram obtained for 2 mL of an abiotic methylation assay (A) and corresponding ratio of m/z 44 and 45 (B). ..... 114
- Figure 5-10.** HG-P&T-hcGC-GC-IRMS data of the abiotic methylation of arsenic in presence of GSH. (A) shows the area of m/z 44 in relation to the incubation time and (B) the corresponding  $\delta^{13}\text{C}$  values..... 115

#### 7.4. ORIGIN 8.5 SCRIPT FOR SEMI-AUTOMATED EVALUATION OF GC-ICP-MS MEASUREMENTS

For time resolved GC-ICP-MS measurements using the inter-element inter-aggregate calibration developed by Feldmann *et al.* for quantification, an automated peak integration based on Origin 8.5 (OriginLab Corporation, Northampton, USA) was developed using the Origin programming language LabTalk. This routine is designed for the import of multiple .csv or .txt files by the Origin import wizard and yields a summary of the peaks area of all specified elements and the corresponding internal standards. Before usage an integration theme has to be created.

```
//declaration of variables
stringarray elemente;
stringarray standards;
stringarray integration;
int ab, ac, ae, ff, gg, hh, ii, jj, kk;
string aktiv;
double xanfang=1;
double xende=1;
string ins, result, str, ind, inst, beg, end, isarea;
int tt, pp, ar, ix1, ix2, xx, qq, rr, cn, uu;

//Please enter the elements, internal standards and integration theme:
//element 1
elemente.Add("As75");
standards.Add("Ga71");
integration.Add("Auto_10sig");
//element 2
elemente.Add("Se77");
standards.Add("Ga71");
integration.Add("Auto_10sig");
//element 3
elemente.Add("Sb121");
standards.Add("In113");
integration.Add("Auto_10sig");
```

```
//element 4
elemente.Add("Te125");
standards.Add("In113");
integration.Add("Auto_10sig");
//Element 5
elemente.Add("Bi209");
standards.Add("TI205");
integration.Add("Auto_10sig");

//calculation of the areas of the internal standards for the single elements:
%L=%H;
newsheet name:=Multi col:=1;
loop (ab,1,elemente.getsize())
{
if (ab==1){
ac=4;
}
else {
ac=ac+11;}
page.active=2;
wks.ncols=wks.ncols+2;
page.active=1;
if (ColNum(%(elemente.GetAt(ab)$)) > 0)
{
{
@NOE = 0;
vErr = 1;
page.active=1;
pa          iy:=(1,$(ColNum(%(elemente.GetAt(ab)$))))          smode:=1
theme:=%(integration.GetAt(ab)$);
if (page.active>1){
ae=ae+1;
aktiv$=[%H]Integration_Result$(ae)!;
page.active=2;
```

```
wrcopy iw:=%(aktiv$) c1:=1 c2:=8 r1:=1 r2:=20 dc1:=$(ac) dr1:=1 label:=LC
ow:=[%H]Multi!;
page.active=2;
wks.ncols=wks.ncols+1;}
else
{
page.active=2;
wks.ncols=wks.ncols+9;
}
vErr = 0;
}
@NOE = 1;
if(vErr){
page.active=2;
wks.ncols=wks.ncols+9;
}}
else
{
page.active=2;
wks.ncols=wks.ncols+9;
}
}
page.active=2;
wks.col$(1).name$=Name;
loop (ii,1,20)
{
Col(Name)[ii]$=[%L]1!wks.name$;
}
hh=1;
loop (gg, 1, elemente.getsize())
{
hh=hh+1;
wks.col$$(hh).name$=Element$(gg);
loop (jj, 1, 20)
```

```
{
Col(Element$(gg))[jj]$=elemente.GetAt$(gg)$;
}
hh=hh+1;
wks.col$( $(hh)).name$=IS$(gg);
loop (kk, 1, 20)
{
Col(IS$(gg))[kk]$=standards.GetAt$(gg)$;
}
hh=hh+1;
wks.col$( $(hh)).name$=Index$(gg);
hh=hh+1;
wks.col$( $(hh)).name$=Area$(gg);
hh=hh+1;
wks.col$( $(hh)).name$=RowIndex$(gg);
hh=hh+1;
wks.col$( $(hh)).name$=BeginningX$(gg);
hh=hh+1;
wks.col$( $(hh)).name$=EndingX$(gg);
hh=hh+1;
wks.col$( $(hh)).name$=FWHM$(gg);
hh=hh+1;
wks.col$( $(hh)).name$=Center$(gg);
hh=hh+1;
wks.col$( $(hh)).name$=Height$(gg);
hh=hh+1;
wks.col$( $(hh)).name$=ISArea$(gg);
}
loop (qq,1,elemente.getsize())
{
loop (pp,1,20)
{
ind$=Index$(qq);
inst$=IS$(qq);
```

```
beg$=BeginningX$(qq);
end$=EndingX$(qq);
isarea$=ISArea$(qq);
if (Col(%(ind$))[pp]$!="")
{
ins$=Col(%(inst$))[pp]$;
result$=[%L]1!%(ins$);
xanfang=col(%(beg$))[pp];
xende=col(%(end$))[pp];
plotxy iy:=%(result$) plot:=200;
ix1=xindex(xanfang,%c);
ix2=xindex(xende,%c);
range ab=(%c)[$(ix1): $(ix2)];
integ1 -se ab;
ar=integ1.area;
win -c Graph1;
win -a %L;
page.active=2;
COL(%(isarea$))[PP]=ar;
}
else
{
COL(%(isarea$))[PP]="";
ar="";
pp=21;
}
}
}

//creation of the summary
page.active=2;
cn=wks.ncols;
if (exist([Summary]Results!)==0)
{
```

```
colcopy irng:=(1:$(cn)) orng:=[Summary]Results! data:=1
  format:=1 lname:=1 units:=1 comments:=1;
win -a Summary;
hh=1;
wks.col$( $(hh)).name$=Name;
hh=hh+1;
loop (gg,1,elemente.getsize())
{
wks.col$( $(hh)).name$=Element$(gg);
hh=hh+1;
wks.col$( $(hh)).name$=IS$(gg);
hh=hh+1;
wks.col$( $(hh)).name$=Index$(gg);
hh=hh+1;
wks.col$( $(hh)).name$=Area$(gg);
hh=hh+1;
wks.col$( $(hh)).name$=RowIndex$(gg);
hh=hh+1;
wks.col$( $(hh)).name$=BeginningX$(gg);
hh=hh+1;
wks.col$( $(hh)).name$=EndingX$(gg);
hh=hh+1;
wks.col$( $(hh)).name$=FWHM$(gg);
hh=hh+1;
wks.col$( $(hh)).name$=Center$(gg);
hh=hh+1;
wks.col$( $(hh)).name$=Height$(gg);
hh=hh+1;
wks.col$( $(hh)).name$=ISArea$(gg);
hh=hh+1;
}
}
else {
win -a Summary;
```

```
uu=wks.maxRows+1;
wrcopy iw:=[%L]Multi! c1:=1 c2:=$(cn) r1:=1 r2:=20 dc1:=1 dr1:=$(uu) name:=0
ow:=[Summary]Results!;}
if (exist(Book1==2){
win -c Book1;};
```

### 7.5. CONVERTER FOR ELAN 6000 ICP-MS DATA BASED ON MICROSOFT WORD (.XL to .CSV)

For the use of the script above with the data originating from an ELAN 6000 ICP-MS, which actually is not designed for time resolved analysis, a conversion of the .XL-files to .csv-files and addition of the time scale are necessary. For this purpose, the following VBA script was created for the usage with Microsoft WORD. The macro adds the missing time data values, which are calculated from the acquisition time you are requested to enter. Furthermore, unwanted line breaks are removed. Please note that you have to open a single .XL-file and that all files in this folder will be converted and saved in the comma separated value (.CSV) format.

```
Sub Convert()
Dim i As Long
Dim h As Integer
Dim g As Double
Dim Zahl1 As String
Dim Eingabe As String
Dim Wert As Double
Dim Pfad As String
Dim Datei As String
Wert = 0
Start:
Eingabe = InputBox("Bitte Replicate Time eingeben!", "XL to TXT-Converter -
Dateien im Verzeichnis by OW")
If StrPtr(Eingabe) = 0 Then
MsgBox "Abbruch"
GoTo Ende
```

```
End If
If Eingabe = "" Then
MsgBox "Es wurde nichts eingegeben"
GoTo Start
End If
If Not IsNumeric(Eingabe) Then
MsgBox "Nur Zahlen eingeben!"
GoTo Start
End If
Eingabe = Replace(Eingabe, ".", ",")
MsgBox "Es wurde "" & Eingabe & "" eingegeben"
Wert = CDbI(Eingabe)
Pfad = ActiveDocument.Path & "\*.xl"
Datei = Dir(Pfad, vbDirectory)
While Datei <> ""
Documents.Open FileName:=Datei
For h = 0 To 10000
g = (h + 1) * Wert
Zahl1 = CStr(g)
Zahl1 = Replace(Zahl1, ",", ".")
    Selection.Find.ClearFormatting
    Selection.Find.Replacement.ClearFormatting
    With Selection.Find
        .Text = "^p" + CStr(0) + ",,"
        .Replacement.Text = "^p" + Zahl1 + ",,"
        .Forward = True
        .Wrap = wdFindContinue
        .Format = False
        .MatchCase = False
        .MatchWholeWord = False
        .MatchWildcards = False
        .MatchSoundsLike = False
        .MatchAllWordForms = False
    End With

```

```
Selection.Find.Execute
With Selection
  If .Find.Forward = True Then
    .Collapse Direction:=wdCollapseStart
  Else
    .Collapse Direction:=wdCollapseEnd
  End If
  .Find.Execute Replace:=wdReplaceOne
End With
If Selection.Find.Found = False Then h = 10000
Next h
Selection.Find.ClearFormatting
Selection.Find.Replacement.ClearFormatting
With Selection.Find
  .Text = "^p^p"
  .Replacement.Text = "^p"
  .Forward = True
  .Wrap = wdFindContinue
  .Format = False
  .MatchCase = False
  .MatchWholeWord = False
  .MatchWildcards = False
  .MatchSoundsLike = False
  .MatchAllWordForms = False
End With
Selection.Find.Execute Replace:=wdReplaceAll
ChangeFileOpenDirectory _
  ActiveDocument.Path
ActiveDocument.SaveAs          FileName:=Left(ActiveDocument.Name,
(Len(ActiveDocument.Name)) - 3), _
  FileFormat:=wdFormatText, LockComments:=False, Password:="", _
  AddToRecentFiles:=True,          WritePassword:="",
ReadOnlyRecommended:=False, _
```

---

```
EmbedTrueTypeFonts:=False,          SaveNativePictureFormat:=False,
SaveFormsData _
:=False,          SaveAsAOCELetter:=False,          Encoding:=1252,
InsertLineBreaks:=False _
, AllowSubstitutions:=False, LineEnding:=wdCRLF
ActiveDocument.Close
Datei = Dir()
Wend
Ende:
End Sub
```

7.6. CV

The CV is not included in the online version for privacy protection.



---

**List of scientific publications**

---

**a. Peer-reviewed international journals**

1. **O. Wuerfel**, M. Greule, F. Keppler, M. A. Jochmann, T. C. Schmidt:  
Position Specific Isotope Analysis of the Methyl Group Carbon in Methylcobalamin for the Investigation of Biomethylation Processes  
*Anal. Bioanal. Chem.* (submitted)
2. **O. Wuerfel**, F. Thomas, M. Schulte, R.A. Diaz-Bone, R. Hensel:  
Mechanism of multi-metal(loid) methylation and hydride generation by methylcobalamin and Cob(I)alamin – A side reaction of methanogenesis  
*Appl. Organomet. Chem.*, **26** (2012), 94-101  
DOI: 10.1002/aoc.2821
3. F. Thomas, R.A. Diaz-Bone, **O. Wuerfel**, B. Huber, K. Weidenbach, R.A. Schmitz, R. Hensel:  
Connection between multimetal(loid) methylation in methanoarchaea and central central intermediates of methanogenesis  
*Appl. Environ. Microbiol.*, **77**, (2011), 8669-8675  
DOI: 10.1128/AEM.06406-11
4. **O. Wuerfel**, R. A. Diaz-Bone, M. Stephan, M. A. Jochmann:  
Determination of  $^{13}\text{C}/^{12}\text{C}$  isotopic ratios of biogenic organometal(loid) compounds in complex matrices  
*Anal. Chem.* **81** (2009), 4312–4319  
DOI: 10.1021/ac8027307
5. R.A. Diaz-Bone, M. Hollmann, **O. Wuerfel**, D. Pieper:  
Analysis of volatile arsenic compounds formed by intestinal microorganisms: Rapid identification of new metabolic products by use of simultaneous EI-MS and ICP-MS detection after gas chromatographic separation  
*J. Anal. At. Spectrom.* **24** (2009), 808 – 814  
DOI: 10.1039/B822968F

**b. Oral presentations**

1. **O. Wuerfel**, R.A. Diaz-Bone, M.A. Jochmann, T.C. Schmidt:  
 $^{13}\text{C}/^{12}\text{C}$  isotopic ratios of biogenic organometal(loid) compounds – Tools and prospects  
Bremen, GDCh-Wissenschaftsforum der Chemie, Session Element- und Speziationsanalytik, September 7, 2011
2. R.A. Diaz-Bone, **O. Würfel**, M.A. Jochmann, F. Thomas, R. Hensel, T.C. Schmidt: Investigation of the biochemical process of metal(loid) methylation by analysis of  $^{13}\text{C}/^{12}\text{C}$  carbon isotope fractionation  
Bruges, Benelux Association for Stable Isotope Scientists (BASIS) Annual Meeting, March 18, 2011
3. **O. Wuerfel**, R.A. Diaz-Bone, M.A. Jochmann, T.C. Schmidt:  
Determination of  $^{13}\text{C}/^{12}\text{C}$  isotopic ratios of biogenic organometal(loid) compounds in complex matrices – A promising tool for investigation of carbon isotope fractionation during methylation of metal(loid)s by methylcobalamin  
Hohenroda, 21. Doktorandenseminar des AK Separation Science, January 10, 2011

4. **O. Wuerfel**, R.A. Diaz-Bone, M.A. Jochmann, T.C. Schmidt:  
Determination of  $^{13}\text{C}/^{12}\text{C}$  isotopic ratios of biogenic organometal(loid) compounds in complex matrices – A promising tool for investigation of carbon isotope fractionation during methylation of metal(loid)s by methylcobalamin  
Amsterdam, The Fifth International Symposium on Isotopomers, June 23, 2010

### c. Poster presentations

1. R.A. Diaz-Bone, **O. Wuerfel**, M.A. Jochmann, A. Dybala-Defratyka, F. Thomas, R. Hensel, T.C. Schmidt:  
Determination of  $^{13}\text{C}/^{12}\text{C}$  Isotopic Ratios of Biogenic Organometal(loid) Compounds - A Promising Tool for Investigation of Carbon Isotope Fractionation during Methylation of Metal(loid)s  
Zürich, ANAKON, May 22-25, 2011 (Poster)
2. R.A. Diaz-Bone., F. Thomas, **O. Würfel**, R. Hensel:  
Biomethylation of metal(loid)s in anaerobic habitats: A novel multi-metal(loid) methylation mechanism directly coupled to methanogenesis  
Karlsruhe, Annual Conference of the Association of General and Applied Microbiology (VAAM), April 3-6, 2011 (Poster)
3. R.A. Diaz-Bone, H. Hollmann, **O. Wuerfel**, D. Pieper:  
Identification of volatile metal(loid) compounds formed by intestinal microorganisms by use of simultaneous EI-MS and ICP-MS detection after gas chromatographic separation  
Hannover, Annual Conference of the Association of General and Applied Microbiology (VAAM), March 28-31, 2010 (Poster)
4. F. Thomas, **O. Wuerfel**, B. Huber, R.A. Diaz-Bone, R. Hensel:  
Biomethylation and volatilization of metal(loid)s - Capability of corrinoid-dependent methyltransferases from *Methanosarcina mazei* to volatilise a broad range of metal(loid)s  
Hannover, Annual Conference of the Association of General and Applied Microbiology (VAAM), March 28-31, 2010 (Poster)
5. **O. Wuerfel**, R.A. Diaz-Bone, M. Stephan, M.A. Jochmann:  
Determination of  $^{13}\text{C}/^{12}\text{C}$  isotopic ratios of biogenic organometal(loid) compounds in complex matrices  
Mainz, Workshop on Progress in Analytical Methodologies for Trace Metal Speciation (TraceSpec), September 15-18, 2009 (Poster)
6. R.A. Diaz-Bone, H. Hollmann, **O. Wuerfel**, D. Pieper:  
Identification of volatile metal(loid) compounds formed by intestinal microorganisms by use of simultaneous EI-MS and ICP-MS detection after gas chromatographic separation  
Mainz, 12th Workshop on Progress in Analytical Methodologies for Trace Metal Speciation (TraceSpec), September 15-18, 2009 (Poster)
7. F. Thomas, **O. Wuerfel**, B. Huber, R.A. Diaz-Bone, R. Hensel:  
Towards microbial methylation of metals and metalloids. Capability of corrinoid-dependent methyltransferases from *Methanosarcina mazei* to volatilise metal(loid)s  
Mainz, 12th Workshop on Progress in Analytical Methodologies for Trace Metal Speciation (TraceSpec), September 15-18, 2009 (Poster)

8. **O. Wuerfel**, R.A. Diaz-Bone, M. Stephan, M.A. Jochmann:  
Determination of  $^{13}\text{C}/^{12}\text{C}$  isotopic ratios of biogenic organometal(loid) compounds  
in complex matrices  
Bremen, 18th IMSC Conference, August 30-September 4, 2009 (Poster)
9. **O. Wuerfel**, R.A. Diaz-Bone, M. Stephan, M.A. Jochmann:  
Entwicklung einer Methode zur Bestimmung der natürlichen  
Kohlenstoffisotopenverteilung von biogenen metall(oid)organischen Verbindungen  
Berlin, Anakon, March 17-20, 2009 (Poster)
10. **O. Wuerfel**, R.A. Diaz-Bone, M. Stephan, M.A. Jochmann:  
Determination of  $^{13}\text{C}/^{12}\text{C}$  isotopic ratios of biogenic organometal(loid) compounds  
in complex matrices  
Essen, 11. JCF-Frühjahrssymposium, March 11-14, 2009 (Poster)
11. R.A. Diaz-Bone, **O. Wuerfel**, M. Stephan, M.A. Jochmann:  
Determination of  $^{13}\text{C}/^{12}\text{C}$  isotopic ratios of biogenic organometal(loid) compounds  
in complex matrices  
Bochum, Annual Conference of the Association of General and Applied  
Microbiology (VAAM), March 8-11, 2009 (Poster)

### 7.7. DECLARATION

Hereby, I declare that all the results and data included in this dissertation were obtained from my independent work. All sources and auxiliary materials used by me in this dissertation were cited completely.

Essen, 25.09.2012